THE IMMUNOLOGICAL CONSEQUENCES OF OBESITY ON PRIMARY AND SECONDARY IMMUNE DEFENSES TO THE 2009 PANDEMIC H1N1 INFLUENZA VIRUS

J. Justin Milner

A dissertation submitted to the faculty of the University of North Carolina at Chapel Hill in partial fulfillment of the requirements for the degree of Doctor of Philosophy in the Department of Nutrition in the Gillings School of Global Public Health.

Chapel Hill
2014

Approved by:

Melinda A. Beck

Patricia A. Sheridan

Liza Makowski

P. Kay Lund

Ilona Jaspers

ABSTRACT

J. JUSTIN MILNER: The Immunological Consequences of Obesity on Primary and Secondary Immune Defenses to the 2009 Pandemic H1N1 Influenza Virus.
(Under the direction of Melinda A. Beck)

Obese individuals are more susceptible to hospitalization and death from infection with the 2009 pandemic H1N1 influenza virus (pH1N1). Greater pH1N1 severity in the obese is a global public health concern given the persistent threat of influenza outbreaks and the current obesity epidemic. In this dissertation, the consequences of obesity on pH1N1 immunity were investigated in mice to uncover mechanisms by which obesity enhances pH1N1 illness. During a primary pH1N1 infection, 80% of obese mice died compared with 40% of lean, low fat diet fed mice and no mortality in lean, chow fed mice. Further, a genetic model of obesity was generated in which leptin signaling was conditionally disrupted in hypothalamic neurons to confirm that obesity, independent of diet, enhances pH1N1 mortality. Both diet- and genetic-induced obese mice exhibited greater lung damage during infection, likely due to fewer lung regulatory T cells and impaired regulatory T cell function. We extended our analysis to include a secondary heterologous pH1N1 infection model. Obese mice had fewer cross-reactive, non-neutralizing pH1N1 antibodies, overactive $CD8^+$ effector memory T cell responses and greater lung damage in this model.

During the primary pH1N1 infection, obese mice had greater serum and bronchoalveolar lavage leptin concentrations compared with lean mice. Given that leptin regulates T cell function, we then determined if conditional disruption of leptin signaling in T cells ameliorates

obesity-induced pH1N1 mortality. However, obese mice lacking leptin signaling in T cells were not protected from pH1N1 mortality compared with control, obese mice. The pathophysiological complications of obesity are diverse and complex. Therefore, we also extended our analysis to include ^{1}H NMR-based metabolic profiling of urine, feces, serum, lungs, bronchoalveolar lavage fluid, mesenteric white adipose tissue, and livers to obtain a more comprehensive examination of infection responses in obese mice. We uncovered a number of metabolites and metabolic signatures uniquely altered in obese mice that, ultimately, may facilitate early prediction of influenza infection outcomes and help to identify mechanisms for impaired. In summary, novel immunologic and metabolic techniques were integrated in this dissertation to establish that obesity enhances greater lung damage during primary and secondary pH1N1 infections in mice.

To my mom, dad, and sister: thank you for all
your love and support along the way.

ACKNOWLEDGEMENTS

I would like to acknowledge my dissertation committee for their incredible guidance and support: Melinda A. Beck (chair), Patricia A. Sheridan, Liza Makowski, P. Kay Lund and Ilona Jaspers. During my graduate studies, Dr. Beck provided me with the perfect balance of guidance and independence that has allowed me to develop to my maximum potential as a researcher and independent thinker. Her unwavering support has encouraged me to take risks and pursue difficult research questions, which ultimately has given me the confidence that I can be successful in approaching and solving any research question. Additionally, she has been a great mentor in terms of demonstrating that integrity, hard work and fun are critical components of being a successful scientist. Additionally, I would like to acknowledge previous and past members of the Beck lab for all of their help, especially Erik A. Karlsson and Patricia A. Sheridan. I would also like to thank all my professors over the years for all their dedication, hard work and help, especially Liza Makowski and Rosalind Coleman. I am also grateful to the extremely helpful staff members of the Department of Nutrition, including Joanne Lee.

I would like to acknowledge the funding sources that made this research possible: NIH ROI AI078090 to Melinda A. Beck and NIK DK056350 to the University of North Carolina Nutrition Obesity Research Center.

Lastly, but most importantly, I would like to thank my family and friends for all their support throughout the years.

TABLE OF CONTENTS

LIST OF TABLES x

LIST OF FIGURES xii

LIST OF ABBREVIATIONS xiiii

CHAPTER I: OVERVIEW AND SPECIFIC AIMS 1

Overview 1

Specific Aims 3

CHAPTER II: BACKGROUND AND SIGNIFICANCE 4

Introduction 4

The obesity epidemic 4

Evidence for greater infection susceptibility in obese individuals 5

Obesity and host defense in rodents 7

Dietary considerations in mouse models of obesity 9

Obesity and influenza infection in humans and mice 11

Influenza virus biology 12

Antigenic drift, antigenic shift and highly pathogenic influenza viruses 14

The 2009 pandemic H1N1 influenza virus 16

Innate defenses to influenza virus infection in the lung 16

Adaptive immunity to influenza virus 17

Memory responses to influenza virus infection 18

Influenza virus vaccination 19

Heterologous immunity 21

Mechanisms by which obesity may impair immune cell function 22

Leptin and immunity in the obese 23

Additional considerations of the consequences of obesity on immunity 25

Metabolic profiling and infectious disease 25

CHAPTER III: DIET-INDUCED OBESE MICE EXHIBIT ALTERED HETEROLOGOUS IMMUNITY DURRING A 2009 PANDEMIC H1N1 INFECTION 27

Introduction 27

Materials and methods 30

Results 37

Discussion 45

Tables and Figures 52

CHAPTER IV: DIET- AND GENETIC-INDUCED OBESITY RESULTS IN GREATER LUNG DAMAGE AND MORTALITY DURING A PRIMARY 2009 PANDEMIC H1N1 INFLUENZA VIRUS INFECTION IN MICE 61

Introduction 61

Materials and methods 64

Results 67

Discussion 76

Tables and Figures 80

CHAPTER V: ^{1}H NMR-BASED PROFILING REVEALS DIFFERENTIAL IMMUNE-METABOLIC NETWORKS DURING INFLUENZA VIRUS INFECTION IN OBESE MICE 88

Materials and methods 90

Results 94
Discussion 98
Tables and Figures 103
CHAPTER VI: SYNTHESIS 119
Overview of research findings 119
How does obesity alter pH1N1 immunity? 121
Does hyperleptinemia underlie the consequences of obesity on pH1N1 immunity? 122
Mechanisms of greater lung damage during pH1N1 infection 124
Recommendations for future research 127
Tables and Figures 129
REFERENCES 131

LIST OF TABLES

Table 3.1 Similar levels of lung cytokine and chemokine expression during a secondary heterologous pH1N1 challenge in lean and obese mice 52

Table 4.1 BALF cytokine concentrations during a primary pH1N1 infection 80

Table 5.1 Metabolic biomarkers recovered from urine and fecal extracts during influenza infection in lean and obese mice..... 103

Table 5.2 Discriminatory metabolites between lean and obese mice at 9 days post-infection in liver, serum and white adipose tissue samples 104

Table 5.3 Lung metabolite correlation patterns with BAL T cell populations 105

Table 5.4 Lung metabolite correlation patterns with mLN T cell populations..... 106

Table 5.5 Correlation patterns between ^{1}H NMR data and BAL or mLN T cell populations 107

Table 6.1 Comparison of diets used in this dissertation 129

LIST OF FIGURES

Figure 3.1 Sublethal influenza A/PR/8/34 infection induces heterologous protection against a lethal pH1N1 challenge in lean and diet-induced obese mice 53

Figure 3.2 Obese mice exhibit delayed antibody production and impaired antibody maintenance following a sublethal PR8 infection 54

Figure 3.3 Obese mice have lower levels of cross-reactive anti-pH1N1 nucleoprotein antibodies and exhibit greater lung viral titers during a secondary pH1N1 infection 55

Figure 3.4 Obese mice exhibit a greater inflammatory and pathological response in the lungs following a secondary heterologous pH1N1 challenge 56

Figure 3.5 Exposure to PR8 elicits a rapid and robust memory $CD4^+$ T-cell response following pH1N1 infection in both lean and obese mice 57

Figure 3.6 Obese mice have enhanced cross-reactive $CD8^+$ T-cell responses at 5 dpi after a secondary heterologous pH1N1 challenge 58

Figure 3.7 Obese mice have a greater number of Tregs in the lung airways during a heterologous secondary pH1N1 challenge 59

Figure 3.8 Tregs isolated from obese mice are significantly less suppressive than Tregs isolated from lean mice 60

Figure 4.1 Diet-induced obesity results in greater pH1N1 infection mortality in mice 81

Figure 4.2 Genetically obese mice are more susceptible to pH1N1 mortality 82

Figure 4.3 Obese mice exhibit greater lung damage during pH1N1 infection 83

Figure 4.4 Obese mice did not exhibit differences in lung pathology during pH1N1 infection 84

Figure 4.5 Obese mice have fewer BAL macrophage during pH1N1 infection 85

Figure 4.6 Diet- and genetic-induced obese mice have fewer BAL Tregs at 8 dpi 86

Figure 4.7 Leptin signaling in T cells does not mediate pH1N1 mortality in obese mice 87

Figure 5.1 Summary of influenza infection and metabolic profiling model 115

Figure 5.2 Metabolic profiling can distinguish urine samples from both uninfected and infected lean and obese mice 116

Figure 5.3 Representative analysis of serum samples from infected lean and obese mice 117

Figure 5.4 Correlation analysis of lung analytes and lung and mLN T cell populations 118

Figure 6.1 Summary of heterologous infection data 130

LIST OF ABBREVIATIONS

^{1}H NMR	^{1}H Nuclear magnetic resonance
AHR	Airway hyperresponsiveness
ANOVA	Analysis of variance
BAL	Bronchoalveolar lavage
BALF	Bronchoalveolar lavage fluid
BMI	Body mass index
CCR7	Chemokine receptor 7
CD	Chow diet
ConA	Concanavalin A
COPD	Chronic obstructive pulmonary disease
CPM	Counts per minute
Cre	Cre recombinase
CVD	Cardiovascular disease
CXCL1	Chemokine (C-X-C motif) ligand 1, keritinocyte chemoattractant
DC	Dendritic cell
DIO	Diet-induced obesity
DPI	Day post-infection
ELISA	Enzyme linked immunosorbent assay
ER	Endoplasmic reticulum
FACS	Fluorescence-activated cell sorting
GzB	Granzyme B
H&E	Hematoxylin and eosin
HA	Influenza hemagglutinin
HAI	Hemagglutinin inhibition
HFD	High fat diet

ICU	Intensive care unit
IFNα	Interferon α
IFNβ	Interferon β
IL	Interleukin
IgG	Immunoglobulin G
JAK/STAT	Janus kinase/signal transducers and activators of transcription
KC	Keritinocyte chemoattractant, CXCL1
LAIV	Live attenuated influenza vaccine
Lck	Lymphocyte-specific protein tyrosine kinase
LD_{50}	Median lethal dose
LepR	Leptin receptor
$LepR^{H-/-}$	Mice with disruption of leptin receptor in hypothalamic neurons
$LepR^{H+/-}$	Heterozygous hypothalamic leptin receptor disruption mice
$LepR^{Hfl/fl}$	Hypothalamus specific fully floxed leptin receptor control mice
$LepR^{T-/-}$	T cell specific leptin receptor knockout mice
$LepR^{Tfl/fl}$	T cell specific fully floxed leptin receptor control mice
LFD	Low fat diet
M1	Influenza matrix protein 1
M2	Influenza matrix protein 2
MCP-1	Monocyte chemoattractant protein 1
MDCK	Madin-Darby Canine Kidney epithelial cells
MHCI	Major histocompatibility complex I
MHCII	Major histocompatibility complex II
mLN	Mediastinal lymph node
MOI	Multiplicity of infection
MS	Mass spectrometry
NA	Influenza neuraminidase

NK cell	Natural killer cell
NP	Influenza nucleoprotein
NS1	Influenza nonstructural protein 1
NS2	Influenza nonstructural protein 1
OD	Optical density
O-PLS-DA	Orthogonal partial least squares discriminant analysis
PA	Influenza polymerase acidic
PAMPs	Pathogen associated molecular patterns
PB1/2	Influenza polymerase basic 1/2
PBS	Phosphate buffered saline
PCA	Principal component analysis
pH1N1	2009 pandemic H1N1 influenza virus (A/Cal/04/09)
PLS-DA	Partial least squares discriminant analysis
PR8	Influenza A/Puerto Rico/8/1934 (H1N1)
PRR	Pattern recognition receptor
RANTES	Regulated on activation, normal T cell expressed and secreted
RBC	Red blood cell
RDE	Receptor destroying enzyme
RIG-I	Retinoic acid inducible gene 1
ROS	Reactive oxygen specifies
RPM	Revolutions per minute
RPMI	Roswell Park Memorial Institute medium
RSV	Respiratory syncytial virus
SEM	Standard error of the mean
SOCS-3	Suppressor of cytokine signaling 3
SPC	Surfactant protein C
STAT-3	Signal transducer and activator of transcription 3

TAG	Triacylglycerol
$TCID_{50}$	Median tissue culture infective dose
Tcm	Central memory T cell
Teff	Effector T cell
Tem	Effector memory T cell
Tfh	Follicular helper T cell
Th1	Type 1 helper T cell
Th2	Type 2 helper T cell
TIV	Trivalent influenza vaccine
TNFα	Tumor necrosis factor α
vRNA	Viral ribonucleic acid
WAT	White adipose tissue
Wk	Week
X31	Recombinant influenza virus A/X-31 (H3N2)

CHAPTER I: OVERVIEW AND SPECIFIC AIMS

Overview

Obesity, defined as a body mass index (BMI) $\geq 30 kg/m^2$, is caused by a prolonged positive energy balance (1-3). Excess adiposity increases the risk for a variety of viral and bacterial infections (2), and obese individuals were reported to be at greater risk for hospitalization and death from infection with the 2009 H1N1 pandemic strain (pH1N1) (4-7). Obesity is a global epidemic (8), and influenza epidemics and pandemics are persistent threats worldwide (9,10). Therefore, enhancing understanding of the negative impact of obesity on pH1N1 immunity is a critical global public health issue.

The mechanisms by which obesity drives greater influenza infection severity in humans are unclear. Although we have demonstrated that obese individuals have impaired cellular and humoral immune responses to influenza vaccination (11,12), there is little known regarding how obesity impacts dynamic immune responses in the lung during infection in humans. Therefore, mouse models of obesity and influenza infection are critical for elucidating potential mechanisms with the future prospect of identifying therapeutics, improving disease management and influencing vaccination approaches with the ultimate goal of limiting influenza morbidity and mortality in this at risk population.

Despite widespread transmittance, pH1N1 infection illness was surprisingly mild (13). The limited severity to the 2009 pandemic H1N1 virus was primarily mediated by pre-existing cross-reactive immunity conferred from exposure to previously circulating seasonal influenza

strains or vaccination (14). However, because obese individuals were at greater risk for pandemic H1N1 severity, we hypothesized that obesity impairs cross-reactive immune defenses to pandemic H1N1. We therefore explored this using a mouse model of obesity and heterologous immunity (Aim 1).

Obesity is associated with a chronic inflammatory state (1,2), and the majority of the pathophysiological complications of obesity are linked to excess inflammatory immune responses both locally and systemically (2). From our analysis of obesity on heterologous immunity, we found that obese mice exhibit greater lung damage during a secondary pH1N1 infection (14). We further extended our analysis to demonstrate that obesity impairs primary infection defenses to pandemic H1N1, resulting in greater lung damage and death (Aim 2).

Obesity is a multifactorial disease resulting in physiological adaptations, metabolic perturbations, hormonal changes, alterations in levels of circulating nutrients, greater oxidative stress, and changes in the gut microbiome (2). Given the complexity of this disease, it is difficult to identify one specific molecular mechanism explaining greater pH1N1 severity in the obese. Therefore, we utilized metabolic profiling to obtain a more comprehensive, global perspective of the impact of obesity on pH1N1 immunity (Aim 3). Metabolic profiling uncovered a number of distinct changes in metabolic pathways and metabolites in influenza-infected obese mice. This dissertation facilitates the establishment of metabolomics as a useful tool in characterizing influenza pathogenesis, and perhaps as a useful tool for prediction of influenza infection status and severity.

Specific Aims

Specific Aim 1: Determine if obesity impairs heterologous immunity to infection with the 2009 pandemic H1N1 virus.

Hypothesis: Obese mice will exhibit greater mortality, fewer cross-reactive memory T cells and greater lung damage during a secondary 2009 pandemic H1N1 infection.

Specific Aim 2: Determine if obesity impairs primary infection responses to the 2009 pandemic H1N1 virus, resulting in greater mortality and lung damage.

Hypothesis: Obese mice will exhibit greater mortality and lung damage during a primary infection with the 2009 pandemic H1N1 influenza virus.

Specific Aim 3: Determine if metabolic profiling of biofluids and tissues can distinguish influenza infection status in lean and obese mice and identify novel potential mechanisms for greater influenza infection severity.

Hypothesis: Metabolic profiling will uncover distinct perturbations in metabolic pathways and metabolites that allow for identification of new explanatory mechanisms for greater influenza severity in obese mice.

CHAPTER II: BACKGROUND AND SIGNIFICANCE

Introduction

In 2009, a novel influenza virus emerged causing the first pandemic of the 21st century (15). The 2009 pandemic H1N1 virus (pH1N1) caused widespread infections, and in the US alone, approximations of the number infected reach 89 million individuals (16). Although a variety of previously established risk factors increased susceptibility for severe pH1N1 outcomes, for the first time, the obese were reported to be at greater risk for hospitalization and death from influenza infection (6). Further, a recent meta-analysis demonstrated that obese individuals are at greater risk for severe seasonal influenza infections as well (17). Given that more than 500 million individuals are obese (3) and influenza outbreaks are a persistent threat, identifying mechanisms for greater influenza severity in the obese is a global public health concern.

The obesity epidemic

Globally, more than 1 in 10 individuals are considered to be obese (BMI$\geq$30kg/m^2) (3). An array of cultural, ecological, psychosocial and biochemical factors influence weight gain and obesity status (1,3). However, ultimately, obesity is caused by a prolonged positive energy balance. Excess energy consumption or insufficient energy expenditure results in triacylglycerol (TAG) deposition in adipose tissues, and overtime this causes obesity (18). The complications and risk factors associated with excess adiposity are diverse and complex and include type II

diabetes, cardiovascular disease, cancer, chronic obstructive pulmonary disease (COPD), strokes and infections (3,18). An abundance of research focuses on the negative health consequences of obesity, and interestingly, excessive inflammation and hyperactive immune responses are linked to nearly every comorbidity associated with obesity (2). Further, despite excessive inflammatory responses in the obese, excess adiposity predisposes individuals to a variety of infections (2).

Evidence for greater infection susceptibility in obese individuals

Obese patients have increased intensive care unit (ICU) length of stay (19) and are more likely to die (20-22) in the hospital. It has been reported that obesity increases infection susceptibility in clinical settings (23), and further, obesity is a well-established independent risk factor for postoperative infections (24-34). In a recent secondary analysis of a large prospective observational study including critically ill and injured patients remaining in the ICU for 48 hours or more, obesity was reported to be an independent risk factor for catheter and blood stream infections (35). In critically injured blunt trauma patients, morbid obesity (BMI≥40) was associated with increased risk of pneumonia and urinary tract infection but not with increased mortality (27).

The impact of obesity on clinical outcomes in hospitalized patients is clearly multifactorial and complex. For example, underlying disease in the obese may inhibit proper mobility in the hospital, which can increase risk for skin breakdown (36). Due to inadequate equipment or improperly trained staff, obese individuals may have prolonged visits at the hospital, thus increasing risk for acquiring nosocomial infections (23,36). Another consideration is that pharmacokinetics of antibiotics may differ in the obese, potentially affecting susceptibility to post-operative infections (37). Therefore, it is difficult to determine the direct impact of

impaired immunity on severity of nosocomial infections in obese patients, but accumulating evidence suggests a significant role.

Increased BMI is associated with greater risk for several other bacterial infections including periodontal infections (38), *Staphylococcus aureus* nasal carriage (39) and gastric infection by *Helicobacter pylori* (40). Also, a recent study reported that obesity was significantly associated with HSV1 infection, which was determined by seropositivity (41). Despite increased risk for several types of microbial infections, there is little known about how obesity may alter the pharmacokinetics of antimicrobial drugs (reviewed in (37)). Studies assessing dosing of the antibacterial drug, vancomycin, suggest that obese patients may require different dosages (42) and different dosing intervals (43) compared with non-obese individuals. An additional study of the antimicrobial drug, linezolid, reported diminished serum concentrations in the obese compared with healthy-weight volunteers receiving the same dose (44). As pointed out previously, there is greater risk of skin breakdown in obese individuals in clinical settings due to restricted mobility, improperly sized rooms/equipment and the special challenges of caring for patients undergoing or post bariatric surgery (23,36). Additionally, excess adiposity may reduce tissue perfusion and affect wound healing (36). Taken together, it is clear that obesity predisposes individuals to nosocomial infections, and that careful consideration of infection prevention and treatment is required.

In contrast to the recent surge of publications highlighting a connection between influenza severity and obesity (discussed below), there is very little known about obesity and other respiratory tract infections (45). A recent study by Akiyama et al. suggests that obesity may impact the response to respiratory syncytial virus (RSV) infection in children (46). A study from Poland reported that BMI was significantly related to susceptibility to respiratory infections in

children (47). In critically ill trauma patients, obesity or morbid obesity was associated with respiratory infections (20,29,35). Conversely, a few studies have also reported obese individuals are not at greater risk for respiratory infections (19,48). Therefore, our understanding of the effect of obesity on risk for pulmonary infection remains unclear. However, it is important to consider that obesity can complicate lung mechanics, such as restricting lung volume (49), which could potentially increase risk for pneumonia or other infections. Although the mechanisms contributing to increased susceptibility may include impaired immunity, there may be non-immune factors to consider.

Obesity and host defense in rodents

A limited number of studies have demonstrated the negative impact of excess adiposity on host defense in rodent models. The implications of these studies, in terms of obesity-related immunity impairments, are often complicated by the use of genetic models of obesity. The most commonly used genetically altered rodents for this purpose are the *ob/ob* and *db/db* mice and the rat *fa/fa* counterpart. These rodent models lacking leptin or the leptin receptor can be useful for the study of obesity-related comorbidities, as they display metabolic abnormalities characteristic of obesity such as hyperglycemia, dyslipidemia, glucocorticoid excess and hyperinsulinemia (50,51) (all of which could potentially alter immune cell homeostasis and function). However, given the vast amount of research highlighting the importance of leptin in immunity (52), a global deficiency in leptin signaling makes it difficult to tease apart the mechanisms contributing to impaired immunity and greater susceptibility to infections in these genetic models of obesity. Nonetheless, these models still provide insight into how excess adiposity may directly or indirectly alter immune cell function and host defense against infectious agents.

In general, a deficiency of leptin (*ob/ob*) or the leptin receptor (*db/db*) in mice increases susceptibility to bacterial infections and pneumonia (45). Using *ob/ob* mice, Mancuso et al. demonstrated that a complete deficiency of leptin resulted in impaired pulmonary clearance upon *Klebsiella* challenge, likely due to defective alveolar macrophage and neutrophil phagocytosis (53). Similarly, an investigation by Hsu et al. reported that *ob/ob* mice exhibited enhanced lethality and delayed clearance of *Streptococcus pneumoniae* following a pulmonary challenge (54). Interestingly, intraperitoneal injections of leptin prior to *Streptococcus* infection improved survival after the bacterial challenge, but not to the level of wild-type mice. This discrepancy in survival percentages may, in fact, be caused by the increased adiposity of the *ob/ob* mice. Other studies have reported that *ob/ob* mice exhibit greater pulmonary *Mycobactrium tuberculosis* load (55) and delayed clearance of the *Mycobacterium abcessus* (56) upon challenge.

In addition to these pulmonary infection models, mice lacking the leptin receptor were shown to be more susceptible to hind paw staphylococcal infection and exhibited a greater inflammatory response compared with wild-type mice (57). Furthermore, *db/db* and *ob/ob* mice displayed impaired resistance to hepatic *Listeria monocytogenes* infection (58). Obese Zucker rats show decreased ability to clear yeast infection upon challenge with *Candida albicans* (59).

It is clear that evidence highlighting the importance of leptin for host defense is rapidly accumulating. However, these studies do not offer insight into the mechanisms by which excess body fat (and associated metabolic abnormalities) may actually hinder host defense. Adding exogenous leptin to *ob/ob* mice is helpful in understanding the impact of other metabolic abnormalities on immune dysfunction, but exogenous administration of leptin in mice still differs from studying animals with intact leptin production and signaling. Some key considerations include indirect effects of leptin on immune responses and the fact that leptin has been shown to

have autocrine signaling capabilities on select immune cells. Although infection models in *ob/ob* or *db/db* mice provide important information on the role of leptin in host defense and immunity, these mice do not properly model non-genetically induced obesity, which constitutes the vast majority of human obesity.

Diet-induced obesity (DIO) in rodents more closely mimics human obesity compared with genetic models of obesity. DIO mice develop the prototypical comorbidities associated with obesity including hyperleptinemia, insulin resistance, white adipose tissue inflammation, low-grade systemic inflammation and greater liver TAG deposition to name a few. These DIO models are most frequently used to study metabolic perturbations associated with obesity, however, few studies have utilized these models to determine the impact of obesity on host defense. Compared with lean control mice, DIO mice have greater morbidity and mortality during either a primary or secondary influenza infection (60,61) (discussed further below). An investigation by Shamshiev et al. reported apoE$^{-/-}$ mice fed a high fat/cholesterol diet displayed impaired resistance to *Leishmania major* infection due to impaired dendritic cell function and T-helper type 1 (T_H1) cell immunity (62). Impaired T-cell activity was also reported in DIO mice transgenic for a T-cell receptor specific to a peptide derived from ovalbumuin (63). Utilization of DIO models in mice will help to better inform about the potential factors responsible for increasing infection susceptibility in obese humans.

Dietary considerations in mouse models of obesity

One complication associated with DIO models is elucidating whether the observed outcome of infection can be attributed to the complications of excess adipose tissue, the influence of the high fat diet or both. In this case, utilizing both genetic models of obesity and

DIO models in tandem may be beneficial in advancing our understanding of the impact of the diet vs. obesity status on immunity (64,65). Another important aspect of DIO studies to consider is use of a proper control diet. A purified, nutrient defined, high fat lard-based diet is commonly used for DIO models, and it is generally established that the proper control diet for lean mice is also a purified, nutrient defined low fat diet differing only in fat and carbohydrate content (66). However, chow diets are commonly used for lean control groups, which can introduce a variety of confounding variables (67,68). In addition to differences in macro and micronutrient composition between chow diets and purified high fat diets, chow diets also contain other nutrients such as phytoestrogens (plant derived chemicals with estrogenic activity), fiber and other known and unknown plant constituents (66,69). These variables could potentially confound results from DIO studies. Further, various batches of chow diets (even from the same company) are often produced with varying levels due plant components (in part driven by what plants are cheapest at the time) (69). Therefore, there is legitimate concern that experimental reproducibility is at risk when chow diets are used. With that said, there is an inherent limitation in mouse diet studies for utilizing the proper control diet, because regardless of whether or not the ingredients are purified, there will still be differences in fat content and carbohydrate content between high fat and low fat diets. Further, the standard 10% kcal fat, low fat diet, is high in sucrose, which may cause metabolic perturbations on its own (70). Now available are new low fat control diets that replace sucrose with other carbohydrates. Nonetheless, careful consideration of diet and experimental design is important in assessing the impact of obesity or diet on immunity.

Obesity and influenza infection in humans and mice

A striking number of recent studies have reported obesity to be a predictor for a worse outcome of infection with pH1N1 (71). In fact, several countries across the world have reported that obese individuals were disproportionately represented among influenza-related hospitalizations and deaths. Obesity or morbid obesity increased risk of ICU admission and even death among those infected with the pandemic strain (72-75). Those admitted to ICUs had a reportedly longer duration of mechanical ventilation, and increased time in ICUs and hospitals compared with healthy weight individuals (76). Before the advent of the 2009 pandemic season, there were no such reports investigating the relationship between obesity and influenza infection in humans. Recently, however, Kwong and colleagues published a study which explored the relationship between BMI and seasonal influenza infection using a series of Canada's cross-sectional population based health surveys (77). The surveys covered 12 influenza seasons. Analysis of the retrospective cohort demonstrated that the obese are at greater risk for respiratory hospitalizations during the seasonal flu periods. Lastly, a meta-analysis performed by Mertz et al. found that obesity was an independent risk factor for severe outcomes to seasonal influenza outbreaks as well (17).

A number of studies have demonstrated that obesity results in greater morbidity and mortality following influenza virus infection in mice (14,68,78-81). Although it is currently unclear whether obesity enhances viral replication in the lungs, it is clear that obesity modulates several aspects of the immune response (14,78,79). Both innate and adaptive arms of immunity are impaired during influenza infection as demonstrated by altered natural killer (NK) cell, dendritic cell (DC), T cell, B cell and heterologous memory responses (2). Further, obesity drives greater lung pathology and/or inflammation during influenza infection, and obese mice exhibit

impaired lung wound healing during infection (14,67,78). Of interest, it was recently demonstrated that monoclonal antibody neutralization of leptin, an adipocyte derived hormone that is chronically elevated in an obese state, during infection with pH1N1 improved infection outcome in obese mice (82). However, despite a number of publications investigating the contribution of obesity on the immune response to influenza infection, there are currently no clearly established cellular or molecular mechanisms.

Influenza virus biology

Influenza is a contagious respiratory disease caused by the influenza virus (83). There are three types of influenza viruses, A, B and C (83). Influenza A virus is responsible for the majority of infections in humans and typically results in the more severe infection illness compared with types B and C (9,83). Influenza B also commonly infects humans but induces mild illness, and influenza C can infect humans but is only associated with very minor symptoms (9,83). Influenza virus is a zoonotic, negative sense RNA virus of the Orthomyxoviridae family (83). Each influenza virion contains an envelope derived from host cells and 8 segmented RNA molecules that make up the genome of the virus (83). The encoded viral proteins include hemagluttinin (HA), neuraminidase (NA), matrix protein 1 (M1), matrix protein 2 (M2), nucleoprotein (NP), polymerase acid (PA), polymerase basic 1 and 2 (PB1/2), non-structural protein 1 (NS1), non-structural protein 2 (NS2 or NEP) and some strains also express the pro-apotoptic protein PB1-F2 (83,84). Each protein serves a distinct and specialized purpose. HA is a surface glycoprotein that binds to sialyic acid receptors on epithelial cells in the respiratory tract of humans as well as intestines in birds (83,85,86). NA cleaves sialic acid moieties to enhance viral spread from infected cells (83). HA and NA are particularly important because they are

major determinants of influenza virus infectivity and also form the basis for influenza virus subtyping (83). Thus far, 17 different HA molecules and 9 different NA molecules have been identified (87).

Influenza infection is first mediated by HA binding to cellular sialic acid receptors of an α2,6 and/or an α2,3 conformation (83,86). HA is then cleaved by cellular proteases which triggers receptor mediated endocytosis (86). The low pH of intracellular endosomes triggers a conformational change in the HA trimer that allows fusion of the endosomal membrane and the viral envelope (86). Simultaneously, the M2 protein functions as an ion channel and pumps H^+ into the virion, resulting in the disassembling of the virion and release of viral contents from the endosomal compartment into the cellular cytoplasm (83). Ribonucleoproteins containing the viral genome bound by nucleoprotein and the polymerase trimer are imported into the nucleus (83). Herein, influenza derived RNA-dependent RNA polymerases began transcribing the negative sense RNA into complimentary viral RNA, vRNA (88). The vRNA molecules are exported to the cytoplasm where they are translated by host machinery or remain in the nucleus for genome replication (88). Newly synthesized viral proteins are trafficked to the host membrane via the Golgi apparatus or enter back into the nucleus of the cell. New vRNA molecules and translated viral proteins are packaged into progeny virions at the surface of the cell (88). Finally, new virions bud from the cell, obtaining an envelope from the host membrane. Here, neuraminidase is critical for cleaving HA and sialic acid interactions to allow further spread of new progeny virions (83).

Antigenic drift, antigenic shift and highly pathogenic influenza viruses

Influenza virus causes seasonal outbreaks that result in up to 500,000 deaths every year (9). Unlike long-lived memory responses to other viruses such as yellow fever, immunity conferred by influenza virus infection or vaccination may not be protective to subsequent exposure of influenza. This is primarily due to antigenic drift (89). The influenza RNA-dependent RNA polymerase replicates with low fidelity, meaning that nucleotide "errors" are commonly introduced (at a rate of 1 in 1000 nucleotides) (83,89). These point mutations in the viral genome can result in antigenic and functional changes in viral proteins, affecting host immunity and/or viral infectivity. Antigenic drift is also the reason that influenza vaccination is recommended yearly (discussed further below) (89).

In addition to point mutations in the viral genome, influenza can also undergo major genomic changes through "swapping" of the segmented RNA molecules. This is called antigenic shift, and is the basis for the genesis of influenza pandemics (89). This reassortmant of genetic material occurs when at least two different influenza viruses infect the same cell, resulting in progeny virions with a novel combination of influenza RNA segments (and thus a novel combination of proteins). Generation of novel influenza strains primarily occurs from reassortment in swine (90). This is because epithelial cells in swine express sialic acid receptors of both the α2,6 and the α2,3 conformations (89,90). Influenza strains primarily circulating in humans preferentially bind to the α2,6 conformation (in the upper respiratory tract), whereas avain strains typically bind receptors of the α2,3 structure (systemically) (83). This is one critical barrier that prevents transmittance of highly pathogenic avian strains to humans. Novel influenza strains created from genetic shifting are a pertinent public health threat because often the general population lacks any pre-existing immunity to such viruses. There have been 5 influenza

pandemics, and the first pandemic of the 21st century occurred from the emergence of the triple reassortant 2009 pandemic H1N1 influenza virus (discussed further below) (90).

In birds, influenza virus is systemic (91). This is primarily due the presence of a multibasic cleavage site on the HA trimer in avian strains (91,92). In human strains, cleavage of HA is restricted to cellular proteases primarily found in the respiratory tract (such as trypsin), thus limiting infection to that compartment (92). However, in avian strains, this multibasic cleavage enhances viral tropism to epithelial cells of the digestive tract and possibly other organs as well (91,92). Therefore, reassortment of a contagious human virus with an HA from an avian strain could result in a severely lethal influenza virus in humans. In fact, in 2003 a novel avian strain, H5N1, emerged in China (10). Despite a 60% mortality rate, the highly pathogenic strain has shown limited human to human transmission, preventing a pandemic outbreak for the time being (10). However, as mentioned, the influenza genome is highly susceptible to mutations, and it has been demonstrated that only 5 mutations in HA of H5N1 are required for human to human transmission (10). Because influenza viruses do not readily transmit between birds and humans, it is thought that humans become infected with avian strains due to close contact with poultry (93). Recently, another novel avian strain, H7N9, emerged in China in March 2013 (94). H7N9 was not previously detected in humans until this point in time (94). Similarly, this virus does not appear to transmit well among humans, but those infected become severely ill (94). Persistent surveillance of these highly pathogenic influenza strains is important part of preventing future pandemics. Further, it is clear that obese individuals are more susceptible to influenza severity caused by seasonal strains and the 2009 pH1N1 strain, and thus obese individuals may be even more susceptible to severe infection outcomes from these avian strains (2).

The 2009 pandemic H1N1 influenza virus

The 2009 pandemic H1N1 influenza A virus (pH1N1) is unique in several aspects. Despite causing greater disease severity in animal models compared to seasonal H1N1 strains (95-98), the pH1N1 virus caused relatively mild illness in the majority of humans without predisposing risk factors (13,99). Further, in contrast to seasonal influenza epidemics, children and nonelderly adults were more susceptible to pH1N1 infection compared with elderly individuals (15,100). It has been estimated that approximately 90% of pH1N1 deaths occurred in the nonelderly population (101). Further epidemiological evidence suggests the lower susceptibly in elderly individuals is likely due to the presence of anti-hemagluttinin antibodies generated from previous exposure to pre-1950 influenza strains that cross-react with the novel pH1N1 virus (100,102-104). However, the majority of the population is naïve to these past circulating influenza strains. Further, recently circulating (pre-2009) seasonal strains and influenza vaccines did not elicit a robust cross-reactive neutralizing antibody response. Therefore, most individuals lacked pre-existing neutralizing antibody protection against pH1N1 infection (102,104-107).

Innate defenses to influenza virus infection in the lung

Influenza virus is primarily spread through mucous or air-born aerosols. The initial responders to influenza virus infection are also the primary target of the virus, respiratory epithelial cells (108). Influenza virus pathogen associated molecular patterns (PAMP) trigger induction of innate antiviral responses in epithelial cells. The primary pattern recognition receptors (PRR) for invading influenza virions include endosomal toll like receptors 3/7 (TLR3/7) and cytoplasmic retinoic acid inducible gene I (RIG-I), all of which recognize

influenza vRNA (108,109). PRR recognition of these PAMPs triggers activation of several inflammatory pathways that ultimately induce the production of type I interferons (IFN), chemokine production and inflammatory cytokine production (108,110,111). IFNα and IFNβ are secreted within a few hours after an infected cell recognizes the invading virus, and these type I interferon's are critical for communicating the presence of a viral infection to neighboring epithelial cells, making them poised to fight the ensuing infection (110,111). Chemokines produced from infected epithelial cells result in a robust infiltration of early responding innate immune cells (108,110,111). Simultaneously, innate immune cells, such as DCs and alveolar macrophages already present in the lung at the time of infection help to propagate this inflammatory response by producing cytokines and chemokines as well (108,111).

Approximately the first 5 days of the immune response to influenza virus infection is predominantly comprised of innate defenses (112). Macrophages, NK cells, DCs and neutrophils migrate into the lung in attempt to combat the infection (111). Macrophages and neutrophils are critical for phagocytizing virus particles, infected cells and inflammatory debris (108,111). NK cells target infected cells for lysis, distinguishing infected from uninfected cells by conserved cellular patterns. Lastly, DCs engulf viral particles, and present influenza virus antigens on major histocompatibility complexes I and II (MHCI and MHCII) to stimulate induction of the adaptive immune response (108,111).

Adaptive immunity to influenza virus

Activated dendritic cells presenting influenza virus antigen migrate to the draining lymph node of the lung to trigger activation of influenza-specific T cells and B cells (113,114). $CD4^+$ T cells recognize cognate antigen on MHCII molecules and $CD8^+$ T cells bind influenza epitopes

on MHCI molecules (114,115). T cells are constantly surveying the blood and lymph, and those specific for influenza virus will bind to MHC molecules and become activated and undergo clonal expansion in draining lymph nodes (114,116). Influenza-specific T cells accumulate in the draining lymph node, and can be detected in the lung as early as 5-6 days post-infection (dpi) (113,117). However, the number of infiltrating T cells peaks between 8 and 10 dpi (117). Effector $CD8^+$ T cells are critical for controlling the infection by targeting infected cells by lysis (113). Further TH1 cells, the primary $CD4^+$ T cell lineage generated during influenza, can also target infected cells for lysis (116). Additionally, $CD4^+$ T cells are critical for proper induction of antibody defenses to influenza virus (113).

Memory responses to influenza virus infection

Following robust expansion of influenza-specific T cells, a majority of the cells undergo apoptosis following viral clearance (118). However, a small proportion of these cells become long-lived memory T cells (118). Memory T cell responses are critical for protection against subsequent influenza virus infections. Although the exact mechanisms regulating the generation and maintenance of memory T cells are unclear, a number of modulatory factors have been defined, including inflammatory responses during the primary infection, cellular metabolism, and tissue migration (118,119). Memory T cells consist of primarily two different types, central memory T cells (Tcm) and effector memory T cells (Tem (118)). Tem are primarily found at the site of infection and are early responders to re-infection, serving as an early control of viral replication (118). Tcm are primarily found in circulation and mount a more robust and dynamic response to ultimately resolve a secondary infection (118).

Antibodies are the earliest line of defense protecting from influenza virus infection. B cells containing a B cell receptor specific to influenza antigens primarily recognize cognate antigen in draining lymph nodes through DC presentation (120). B cells can become activated, independent of T cell help, and these are primarily early sources of influenza-specific antibodies referred to as short-lived plasma cells (120,121). Additionally, the majority of activated B cells migrate to the germinal center of the draining lymph node where they interact with follicular helper T cells (Tfh) through MHCII and costimulatory molecules (120,121). This interaction is critical to the formation of effective antibody defenses because it triggers the generation of long-lived plasma cells and memory B cells (120,121). Long-lived plasma cells home to bone marrow, where they continue to secrete influenza antibodies for extended periods of time (likely throughout a lifetime) (120,121). Influenza-specific memory B cells can be found in circulation and in nearly every tissue and induce an accelerated and robust plasma cell response following re-infection (120). Influenza memory responses are the basis for effective influenza vaccination.

Influenza virus vaccination

Vaccination to influenza virus is widely accepted as the best measure to protect against influenza infection and to limit influenza infection severity (122,123). An abundance of research focuses on novel approaches to vaccinate individuals to the ever-changing influenza strains (123). The primary methods of vaccination include intramuscular immunization with the trivalent inactivated influenza vaccine (TIV) or intra-nasal administration of a live-attenuated influenza vaccine (LAIV) (122,123). Both vaccines include the three influenza strains, two type A strains (H1N1 and H3N2) and one B strain (122,123). These strains are chosen based on influenza surveillance data indicating the most actively circulating strains. During the 2013-2014

influenza season, a quadrivalent vaccine was available, including two influenza A strains and two B strains (123). At this point, it is unclear which type of vaccine (TIV vs. LAIV) offers better protection, but both vaccines have been shown to protect against influenza infection in humans (122,124). The purpose of influenza vaccination is to induce long-lived, protective antibody and memory T cell responses that serve to protect upon exposure to influenza virus (124). Vaccine antigen is taken up by dendritic cells in draining lymph nodes of the arm (TIV) and the respiratory tract (LAIV) where it can be presented to T cells and B cells as described above.

Influenza vaccines have been shown to reduce the number of individuals infected with influenza and to reduce illness severity in the infected (122,124). However, there is some evidence suggesting that obese individuals may not respond to vaccination to the same extent as healthy weight individuals (2). Obesity was associated with a poor antibody response to hepatitis B vaccination (125,126). Additionally, overweight children displayed significantly lower anti-tetanus immunoglobulin G (IgG) antibodies in response to vaccination compared with healthy weight children (127). Interestingly, it has been reported that using a larger vaccine needle length resulted in significantly higher antibody titers to hepatitis B surface antigen in obese adolescents (128). Studies from our lab have demonstrated that obese individuals have impaired cellular and humoral responses to TIV immunization. Although obese individuals are able to mount a comparable antibody response one month after vaccination compared with healthy weight adults, one year after vaccination obese individuals display a reduced ability to maintain influenza antibody levels (12). Further, both influenza-specific $CD4^+$ and $CD8^+$ memory T cell responses following vaccination are blunted in obese adults (11,12). Taken together, obesity impairs

influenza vaccination responses, potentially predisposing this at-risk population to greater infection severity.

Heterologous immunity

Neutralizing antibodies are critical for the control and even prevention of influenza infection (120). In their absence, influenza-specific memory T cells are critical regulators of viral spread and influenza severity (113,129). A number of studies in animals and humans have demonstrated that prior exposure to seasonal influenza viruses or vaccination can induce cross-reactive memory T cells that have the capacity to limit pH1N1 disease severity (107,130-135). In mice, seasonal influenza virus infection or vaccination elicits a memory T-cell response that can prevent morbidity and mortality to a lethal pH1N1 challenge (133,136-139). Additionally, seasonal influenza A-specific memory T cells from humans, naïve to the pH1N1 virus, are capable of recognizing pH1N1 and can directly lyse pH1N1-infected target cells (131). Therefore, the ability of cross-protective memory T cells to control pH1N1 infection is a critical mediator for the relatively benign symptoms experienced by a majority of those infected (131,140).

Although the majority of research on heterologous immunity to influenza infection focuses on T cell responses, cross-reactive antibody protection to pH1N1 cannot be ignored. Non-neutralizing antibodies recognizing conserved epitopes, such as NP antibodies, have been shown to contribute heterologous protection to influenza infection, reducing viral titers and infection severity in mice (141,142). Although it is currently unclear how non-neutralizing antibodies mediate protection to influenza virus, it is likely achieved through induction of antibody complexes in the respiratory tract. An additional mechanism by which antibodies may

confer protection during a heterologous pH1N1 infection is through accelerated production (compared with antibody production in naïve mice) of homologous pH1N1 antibodies. This is likely triggered by cross-reactive memory $CD4^+$ cells that facilitate accelerated B cell activation and antibody production (137,142).

Mechanisms by which obesity may impair immune cell function

It is well known that obesity is associated with a state of chronic, low-grade inflammation both in white adipose tissue (WAT) and systemically (143-146). Additionally, obesity is characterized by altered levels of circulating hormones and nutrients such as glucose and lipids. Circulating and tissue resident immune cells are thus exposed to an energy rich environment in the context of altered concentrations of metabolic hormones and inflammatory cytokines. Understanding how this pro-inflammatory, excess energy milieu impacts immune cell function is key in understanding greater susceptibility to pH1N1.

Hyperinsulinemia and insulin resistance are common features of obesity; however, there is little known regarding the immunomodulatory effects of excess insulin or impaired insulin signaling in the context of obesity. Monocytes have been shown to express insulin receptors and are insulin sensitive immune cells (147-150). Interestingly, resting T cells are insulin insensitive in that the insulin receptor is absent from the plasma membrane. However, upon activation, effector T cells upregulate *de novo* emergence of insulin receptors (151,152). Insulin signaling induces glucose uptake, amino acid transport, lipid metabolism and can modulate T cell activation and function (151,153). Furthermore, insulin promotes an anti-inflammatory T_H2 cell phenotype (152), and MacIver et al. speculate that insulin resistance in obesity may actually enhance T_H1 cell development (154). Macrophage function and ER stress responses are also

modulated by insulin receptor signaling (1,2). Thus, it is clear that insulin can have potent effects on immune cell metabolism and function, but the effects of hyperinsulinemia or insulin resistance on immunity remain relatively unknown.

Leptin and immunity in the obese

The primary adipose derived immunomodulatory adipokines include leptin, adiponectin, and the pro-inflammatory cytokines: tumor necrosis factor α (TNF-α), interleukin-6 (IL-6) and IL-1β (144,145,155). Adiponectin, levels of which are decreased during obesity, has been shown to alter NK cell cytotoxicity and cytokine production by human myeloid cells (156,157). Conversely, there is excess production of TNF-α, IL-6 and IL-1β in WAT of the obese (145). These cytokines can be secreted into circulation and potentially have distal effects; however, exactly how chronic production of these cytokines impacts cellular immunity remains to be elucidated. It is possible that chronic exposure to pro-inflammatory cytokines may desensitize immune cells to inflammatory responses during an actual infection (158).

The pleiotropic effects of leptin on immune cell activity are highly diverse (52), and the function of nearly every innate immune cell has been shown to be modulated by leptin signaling (159-163). In monocytes, leptin upregulates pro-inflammatory cytokine production of IL-6, IL-12 and TNF-α as well as phagocytic activity (53,164,165). In polymorphonuclear neutrophils of healthy individuals, leptin signaling induced chemotaxis, reactive oxygen species (ROS) generation and influences oxidative capacity (163,166,167). NK cells are highly influenced by leptin signaling, including aspects of differentiation, proliferation, activation and activity (161,168). Given the importance of leptin to innate immune cell function, it follows that nearly all innate immune cells are impaired in mice lacking intact leptin signaling (2).

Leptin also plays a critical role in regulating adaptive immunity (159,162). Leptin is an important source of pro-survival signals to double-positive and single-positive thymocytes during the maturation of T cells (169). Leptin has been shown to play a key role in lymphopoieses and myelopoieses given that *ob/ob* mice have only 60% as many nucleated cells in bone marrow as compared with wild-type controls (170). In the presence of a polyclonal stimulator, leptin can increase T cell proliferation and can modulate expression of activation markers on both $CD4^+$ and $CD8^+$ T cells (171).

Although several papers have discussed how leptin may be required for, or may enhance immune cell function, few have taken into consideration how hyperleptinemia in obese individuals may modulate immune cell function (172). Additionally, elevated levels of leptin have been shown to induce a state of central leptin resistance. Indeed, studies have demonstrated that T cells (162) and NK cells (173) can become resistant to leptin in rodent models of obesity. Leptin signals through a variety of pathways, the most studied being the Jak/Stat signaling pathway. Leptin receptor activation results in the translocation of the transcription factor, STAT-3, into the nucleus and subsequent transcription of leptin induced genes, including suppressor of cytokine signaling-3 (SOCS-3). SOCS-3 functions as a negative feedback mediator of Jak/Stat signaling, and thus may play an important role in impairing leptin signaling and contributing to central and peripheral leptin resistance (174). Leptin resistance, induced by hyperleptinemia, would obviously not occur in *ob/ob* mice, which is another reason these mice are not the best model for studying obesity-related immune dysfunction. Although it is widely accepted that leptin resistance occurs centrally in the hypothalamus (174-176), peripheral leptin resistance requires further investigation. Additionally, it is likely that differing immune cells respond differently to hyperleptinemia.

Additional considerations of the consequences of obesity on immunity

In addition to perturbations in circulating levels of nutrients and hormones, there are a variety of other pathophysiological complications of obesity that may contribute to excessive antiviral responses and lung damage during influenza infection. Obesity induces a state of oxidative stress (177), which has been shown to increase influenza severity in mice (178). Further, a hallmark of obesity is a state of chronic, low-grade inflammation (2), which may compromise the immune response to influenza infection or vaccination. Finally, obesity is associated with distinct changes in the intestinal microbiome (179), which may potentially impact antiviral responses given that manipulation of the intestinal microbiota in mice can influence influenza infection outcome (180).

Metabolic profiling and infectious disease

Given the large number of mechanisms that may contribute to alterations in immune processes during influenza infection in the obese, narrowing focus to one particular mechanism, cell type or molecular pathway may not be the best approach to addressing this problem. Perhaps, given the complexity of obesity, a systems biology approach may be useful in identifying the complicated interactions of underlying mechanisms driving greater infection severity. Obesity is inherently a metabolic disease, and therefore, of the many integrative systems approaches, we believe metabolic profiling could be a useful tool in identifying perturbations in lung-specific and systemic metabolites altered by obesity during influenza infection.

Metabolomics is a technique that allows for biochemical profiling of all small molecules that constitute the metabolome (181). Metabolic profiling is useful because it provides a more

global view of complex processes occurring during disease and can actually serve as a snapshot of cellular processes that have just occurred on a cellular, tissue or systemic level (181). Standard processing of samples for metabolomics typically involves identifying and quantitating metabolite levels using ^{1}H Nuclear Magnetic Resonance (^{1}H NMR) or Mass Spectometry (MS). ^{1}H NMR doesn't not require separation of compounds whereas MS requires prior separation of analytes (commonly through gas chromatography or liquid chromatography separation) (181). Uncovering metabolic biomarkers and patterns of altered metabolites would provide a more global view of the impact of obesity on dynamic infection responses and simultaneously may address the complicated interactions of the molecular underpinnings driving obesity-induced influenza mortality. Metabolomics has been used to characterize the metabolic consequences of several types of infections in mice including parasitic (182,183), viral (184,185) and bacterial infections (186). Further, metabolomic analyses of models of lung inflammation have also identified unique metabolites associated with lung damage or greater inflammation (187-189). In all of the referenced models of infectious and inflammatory diseases, metabolomics was able to identify novel biomarkers and metabolic signatures discriminating infected and uninfected groups. In some cases, metabolomics has been used as a novel technique to improve diagnostic measures (184,185), whereas in other instances metabolomics has been used to enhance understanding of pathways driving disease severity (186-188). Identification of biomarkers or predictive metabolic signatures could be used in clinical settings to enhance influenza diagnosis and/or treatment of severely infected obese individuals.

CHAPTER III: DIET-INDUCED OBESE MICE EXHIBIT ALTERED HETEROLOGOUS IMMUNITY DURING A SECONDARY 2009 PANDEMIC H1N1 INFECTION[1]

Introduction

The novel 2009 pandemic H1N1 influenza A virus (pH1N1) is unique in several aspects. Despite causing greater disease severity in animal models compared to seasonal H1N1 strains (95-98), the pH1N1 virus caused relatively mild, uncomplicated symptoms in humans (13,99). Further, in contrast to seasonal influenza epidemics, children and nonelderly adults were disproportionately susceptible to pH1N1 infection compared with elderly individuals (15,100), with estimates that approximately 90% of pH1N1 deaths occurred in the nonelderly population (101). Clinical and epidemiological data suggest the lower susceptibly in individuals over 65 y of age is likely due to the presence of cross-reactive anti-hemagglutinin antibodies generated from previous exposure to pre-1950 influenza strains (100,102-104). Because a majority of the population is naïve to these past circulating influenza strains, and recently circulating (pre-2009) seasonal strains and influenza vaccines did not elicit a robust cross-reactive antibody response, most individuals lacked neutralizing antibody protection against pH1N1 infection (102,104-107).

Although antibodies are important for the control and even prevention of influenza infection, in their absence, influenza-specific T cells are essential in limiting influenza severity

[1]This chapter was published in the *Journal of Immunology*:
J. Justin Milner, Patricia A. Sheridan, Erik A. Karlsson, Stacey Schultz-Cherry, Qing Shi, Melinda A. Beck. *J Immunol*. 2013 Sep; 191(5): 2474-85.

(113,129). Several recent studies in animals and humans have demonstrated that previous exposure to seasonal influenza strains or vaccination can induce cross-reactive memory T cells that have the capacity to limit pH1N1 disease severity (107,130-135). In mice, seasonal influenza viruses and vaccines elicit a memory T-cell response that can prevent morbidity and mortality to a lethal pH1N1 challenge (133,136-139). Additionally, seasonal influenza A-specific memory T cells from humans (naïve to pH1N1) are capable of recognizing pH1N1 epitopes and can directly lyse pH1N1-infected target cells (131). Therefore, the ability of cross-protective memory T cells to control pH1N1 infection could explain the relatively benign symptoms experienced by a majority of those infected (131,140). However, cross-reactive antibody protection to pH1N1 cannot be ignored. Non-neutralizing antibodies recognizing conserved epitopes, such as anti-nucleoprotein (NP) antibodies, have been shown to contribute heterologous protection to influenza infection, reducing viral titers and infection severity in mice (141,142). Additionally, a primary seasonal infection can lead to an accelerated production of pH1N1 antibodies during a heterologous pH1N1 infection, which may facilitate pH1N1 viral clearance (137,142).

Another novel characteristic of the pH1N1 virus is that obesity, defined as a BMI $\geq$ 30kg/m^2, was considered to be an independent risk factor for increased morbidity and mortality following infection (4-7,190). Obesity is a global public health concern, affecting more than one-in-ten of the world's adult population (3). It is well-established that obesity impacts several aspects of the immune response and increases susceptibility for a variety of pathogens, including influenza virus (2). Although recent investigations in mice and humans have begun to elucidate potential mechanisms by which obesity impairs anti-viral immunity to influenza infection, the specific factors contributing to the increased severity observed in the obese population remain unclear (2). We have previously demonstrated that obese mice and humans exhibit impaired

memory $CD8^+$ T-cell responsiveness to influenza stimulation (12,78). Further, obese mice display impaired responsiveness to influenza vaccination (68) , and obese humans are unable to maintain long-term influenza antibody levels following vaccination (12). Therefore, given the protective nature of cross-reactive antibody and T-cell responses, we hypothesized that obesity impaired heterologous immunity induced by previous influenza exposure, resulting in greater pH1N1 infection severity.

In this study, we utilized a model in which lean and obese mice were initially infected with a sublethal dose of influenza A/PR/8/34 (H1N1, PR8). After 5 wk (to allow contraction of effector T cell responses), mice were challenged with a lethal dose of heterologous pandemic A/Cal/04/09 (H1N1, pH1N1). Similar to results shown previously in lean, chow fed mice (133), we found that priming with PR8 effectively prevented mortality from pH1N1 infection in both lean and obese mice in the absence of cross-reactive neutralizing antibodies. However, obese mice exhibited a lower level of cross-reactive pH1N1 nucleoprotein (NP) antibodies 5 wk after the PR8 infection, and a lower proportion of obese mice generated pH1N1 HAI antibodies following the secondary challenge. Consequently, obese mice had greater lung viral titers, more lung pathology as well as an increased number of cytotoxic memory $CD8^+$ T cells in lung airways during the pH1N1 infection. Given the excessive inflammation, infiltration, lung damage and cytotoxic $CD8^+$ T-cell responses in the lungs of obese mice during the lethal pH1N1 challenge, we investigated the impact of obesity on regulatory T cells (Tregs) as a potential mechanism for the inability to control the antiviral responses in the lung. Unexpectedly, obese mice had nearly twice as many Tregs in the lung airways during the heterologous secondary pH1N1 infection compared with lean mice. However, *ex vivo* analysis of Treg function revealed that Tregs isolated from obese mice were significantly less suppressive than those isolated from

lean mice. Therefore, an excessive inflammatory response in the lungs, potentially due to a combination of elevated viral titers and impaired Treg function, may be a mechanism by which obesity enhances pH1N1 infection severity.

Materials and methods

Mice and diets

Weanling, male, C57BL/6J mice were obtained from The Jackson Laboratory (Bar Harbor, ME) and fed a low fat diet with 10% kcal fat (Research Diets D12450B) or high fat diet with 45% kcal fat (Research Diets D12451, New Brunswick, NJ). In addition to inducing weight gain, high fat diets are considered to be pro-inflammatory (191). Mice were maintained on the diets for 15-18 wk as described below. Mice were housed in isolation cubicles at the University of North Carolina Animal Facility (fully accredited by the American Association for Accreditation of Laboratory Animal Care). All experimental procedures involving mice were approved by the UNC Institutional Animal Care and Use Committee.

Influenza virus and infection in mice

Influenza A/Puerto Rico/8/34 (H1N1, PR8), obtained from American Type Culture Collection (Manassas, VA), was utilized for primary infections. Pandemic influenza A/California/04/09 (H1N1, pH1N1) was obtained from BEI resources (Manassas, VA) and was used for secondary infections. Both PR8 and pH1N1 were propagated in the allantoic cavities of 10-12-day-old embryonated chicken eggs. At 72 h post-infection, allantoic fluid from eggs was harvested and clarified by centrifugation at 5000 x rpm for 10 min at 4°C, aliquoted and stored at

-80°C. The stock viral titers of PR8 and pH1N1 were determined by a modified 50% tissue culture infective dose ($TCID_{50}$) in Madin-Darby canine kidney cells using hemagglutination as an endpoint (79) and evaluated by the method of Reed and Muench (192). For influenza inoculations, mice were lightly anesthetized by isoflurane inhalation and inoculated via non-invasive oral aspiration (193,194) with 0.05mL of viral inoculum diluted in PBS. For re-challenge studies, mice were maintained on the designated low fat or high fat diet for 15 wk and then infected with 11.4 $TCID_{50}$ PR8 for a primary infection. Mice were monitored and weighed daily for 14 days post-infection (dpi) following the primary PR8 infection. Five weeks after the primary PR8 infection, a similar period of time as performed by others (78,139,142,195), mice were rechallenged with $5x10^3$ $TCID_{50}$ pH1N1, a previously determined lethal dose (approximately 10 LD_{50}). Following the secondary pH1N1 infection, mice were weighed daily. For isolation of Treg cells from mouse splenocytes or harvesting of sera during the primary PR8 infection, mice were maintained on a high fat or low fat diet for 18 wk.

Quantitation of viral titers

Viral titers in lung tissue were determined by a modified $TCID_{50}$ using hemagglutination as an endpoint as previously described (196). Briefly, the lung tissue from lavaged mice was harvested and frozen in liquid nitrogen for subsequent processing. The supernatant from each homogenized lung was collected, serially diluted and added to 80% confluent Madin-Darby canine kidney cells in replicates of six in 96-well pates. $TCID_{50}$ was determined using the Reed and Muench method (192), and values were normalized to lung tissue weight (78).

Hemagglutination inhibition and microneutralization assays

Sera were collected from individual mice, at days 0 (five weeks after the primary PR8 infection, naïve to pH1N1), 5, 8 and 14 following the secondary pH1N1 challenge and hemagglutination inhibition (HAI) titers were determined. Briefly, sera were treated with receptor destroying enzyme (RDE; Denka Seiken, Tokyo, Japan) overnight, followed by inactivation at 56^{o}C for 1 h, and a final dilution to 1:10 with PBS. RDE-treated sera were then incubated with either pH1N1, PR8 or influenza A/Victoria/361/2011 (negative control) for 15 min at room temperature (primary PR8 infection sera was incubated with PR8 alone). After a 1 h incubation at 4^{o}C with either 0.5% turkey RBC (PR8, pH1N1) or 0.5% chicken RBC (PR8, A/Victoria/361/2011), HAI titer was determined by the reciprocal of the highest dilution of serum to completely inhibit hemagglutination. Positive and negative controls as well as back titrations of virus were included on each individual plate.

Microneutralization assays were performed on sera from PR8-infected mice at 35 dpi as previously described (197). Briefly, 100 $TCID_{50}$ of either PR8 or CA/09 were added to two-fold dilutions of RDE-treated sera, and serum-virus mixtures were incubated at 37^{o}C, 5% CO_2 for 1 h. Following incubation, 3 x 10^5 MDCK cells were added to each well and plates were incubated overnight at 37^{o}C, 5% CO_2. Plates where then fixed with 80% acetone, blocked for 2 hours at room temperature and an ELISA was performed using mouse anti-influenza A NP monoclonal antibody mixture (BEI Resources) followed by Peroxidase-conjugated goat anti-mouse IgG (Jackson Immunoresearch, West Grove, PA). ELISA plates were developed for 10 min using Substrate Reagent (R&D Systems, Minneapolis, MN), stopped using a 2N H_2SO_4 solution and absorbance of each well was read at 450nm. Wells were considered positive for microneutralization at an OD below or equal to 50% of the MDCK cells being infected.

Influenza nucleoprotein ELISA

Anti-nucleoprotein antibodies in the sera of lean and obese mice 35 days after the primary PR8 infection were measured by ELISA. Briefly, 8ug/mL of purified pH1N1 nucleoprotein (A/California//06/2009, Immune Technology Corp., New York, NY) was coated on ELISA plates (BD Falcon, San Jose, CA) overnight at 4^{o}C in coating buffer. Influenza A/Cal/04/2009 NP was not commercially available, so purified NP from the A/Cal/06/2009 pandemic strain was used. Subsequently, ELISA plates were blocked with 1% BSA for 1h at 37^{o}C, washed and then incubated with mouse sera (1:400 dilution) overnight. Following the overnight incubation, plates were washed and incubated with HRP-conjugated goat anti-mouse IgG (Invitrogen, Carlsbad, CA) antibody (1:2000 dilution) for 1h at 37^{o}C. After washing, the assay was developed with the TMB Substrate Kit (Thermo Scientific, Rockford, IL) per manufacturer's instructions. Optical density was measured at 405nm, and the optical density of uninfected control sera was subtracted from the 35 dpi experimental samples.

Lung histopathology

At 5 dpi, the left lobe of the lung was harvested from lean and obese mice, inflated with 4% paraformaldehyde and maintained in 4% paraformaldehyde for 48 h, after which samples were transferred to 70% ethanol. Tissues were paraffin embedded, and three 5μm (separated by 100μm) sections (per lung sample) were processed for H&E staining by the UNC Animal Histopathology Core Facility. The extent of lung pathology was scored blindly according to relative degree of mononuclear infiltrate on a scale from 0 to 4: 0, no inflammation; 1, mild influx of inflammatory cells; 2, increased inflammation with ~25-50% of the total lung involved;

3, severe inflammation involving 50-75% of the lung; and 4, almost all lung tissue contains inflammatory infiltrate (78).

Bronchoalveolar lavage total protein and albumin measurements

To recover bronchoalveolar lavage (BAL) fluid, the trachea of killed mice were exposed and cannulated with a 22-guage angiocath, and the lungs were then lavaged with a series of 4 washes with unsupplemented HBSS, totaling 3.75mL (one 0.75mL and three 1mL washes). BAL fluid supernatant was collected from the initial 0.75mL lavage and was subsequently used for total protein, and albumin detection. The cells from the series of BAL washes for each mouse were combined for subsequent flow cytometry analysis. BAL fluid was harvested at 5, 8 and 14 days following the secondary pH1N1 infection. BAL supernatants from 5 and 8 dpi were diluted 1:10, and total protein was measured (BCA kit, Sigma Aldrich, St Louis, MO). BAL supernatants were diluted 15,000 fold prior to measuring albumin levels per manufacturer instructions of the Mouse Albumin ELISA Kit (Genway Biotech, Inc., San Diego, CA).

Quantitation of lung cytokine gene expression

Lung tissue samples were collected at day 0 (five weeks after the primary PR8 infection, naïve to pH1N1) and 5, 8, and 14 days following the secondary pH1N1 infection. Total RNA was isolated using the TRIzol method (Invitrogen), and reverse transcription was performed with use of the Superscript II First Strand Synthesis kit (Invitrogen) using oligo (dT) primers. Expression levels of cytokines and chemokines were quantified using qRT-PCR as previously described (79).

Flow cytometry

Splenocytes and cells from draining mediastinal lymph nodes (mLN) were isolated as previously described (78). For analysis of surface proteins of T-cell populations, single-cell suspensions were simultaneously incubated with Fc blocker (anti-CD16/CD32) and stained in PBS (with 1% FBS) with the following monoclonal antibodies: CD3 (APC/Cy7), CD62L (Brilliant Violet 421) and CD8 (PerCP) from BioLegend (San Diego, CA); CD4 (FITC, PE-Cy7), CD25 (PE-Cy7), CCR7 (APC), CD44 (PE-Cy7) and CD62L (E450) from eBioscience (San Diego, CA). MHC class I tetrameric complexes (PE) specific for the H-2D^b-restricted epitope of the nucleoprotein (NP, D^{b}NP$_{366-74}$; ASNENMETM) of PR8 were used to identify NP-specific T cells and the irrelevant LCMV tetramer D^{b}GP$_{33-41}$ (PE) was used as a negative control (NIH Tetramer Core Facility, Atlanta, GA). For intracellular cytokine and transcription factor staining, cells were fixed and permeabilized with the Foxp3/Transcription Factor Staining Buffer Set (eBiosciences) per manufacturer's instructions. Subsequently, cells were stained with Foxp3 (APC, eBioscience) for identification of Tregs. For detection of the intracellular cytokines IFN-γ (APC, eBioscience) and granzyme B (GzB, FITC, eBioscience), 1-5x10^5 BAL cells were stimulated under the following conditions for 6 h in the presence of Golgi Plug (BD Biosciences, San Jose, CA) per manufacturer instructions: incubated with heat-inactivated pH1N1 (inactivated by a 1 h incubation at 56°C) at a multiplicity of infection (MOI) of 1x10^{-3}; incubated with heat-inactivated pH1N1 (MOI=2x10^{-3}) with antigen-presenting cells (splenocytes from lean mice depleted of nonadherent cells) pulsed with heat-inactivated pH1N1 (MOI=0.1) at a ratio of 1 APC:15 BAL cells; or 0.08μg/mL of Con A. Samples were analyzed on a CyAn ADP Analyzer flow cytometer (Beckman Coulter, Inc., Fullerton, CA) and cytometry data were analyzed with FlowJo software (TreeStar, Ashland, OR). T-cell populations were analyzed by a doublet

exclusion gate for all cells followed by gating of $CD3^+$ T cells for further analysis of $CD4^+$ and $CD8^+$ T-cell populations.

Suppression Assay

Treg suppression assays were performed similar to De Rosa et al. (198). Tregs were isolated from pooled splenocytes of three naive lean or three naïve obese mice. $CD4^+CD25^+$ Tregs and $CD4^+CD25^-$ T effector cells (Teff) were isolated using the Dynabeads FlowComp Mouse $CD4^+CD25^+$ Treg Cells kit (Invitrogen) and stimulated with Dynabeads mouse anti-CD3/28 (0.5 bead/Teff; $5x10^4$ Teff per well). The Treg cells (≥95% $Foxp3^+$ by FACS analysis) and Teff cells (≤5% $Foxp3^+$) were cocultured at a ratio of 1:2 in round-bottom 96-well plates with complete RPMI medium. Only Teff cells from lean mice were used in the assay to eliminate concern of a discrepancy in obese mouse Teff cell proliferation. Cells were stimulated for 72 h, and cells were pulsed with [3^H]thymidine (PerkinElmer, Boston, MA) for the last 16 h of culture. Cells were harvested onto glass fiber filter paper (Brandel Inc., Gaithersburg, MD), and radioactivity was measured using a Wallac 1409 liquid scintillation counter (Wallac, Turku, Finland).

Statistical analysis

JMP Statistical Software (SAS Institute, Cary, NC) was used for all statistical analyses. Statistical significance for parametric data was evaluated using the two-tailed unpaired Student *t* test to compare dietary groups. For nonparametric data, the Wilcoxon signed rank test was used. Lastly, for the percentage of mice with HAI titers at each dpi, the 2-tailed Fisher's exact test was used. Differences between means were considered significantly different at $p<0.05$.

Results

Heterologous immune defenses prevent mortality from a lethal pH1N1 challenge in lean and obese mice.

To investigate the impact of obesity on heterologous immunity to a lethal pH1N1 infection, we utilized a diet-induced obese mouse model. To induce obesity, weanling, male C57BL/6J mice were fed a high fat (45% kcal from fat) diet or a low fat (10% kcal from fat) control diet for 15 wk (Fig. 3.1A). The OpenSource Diets® are composed of purified constituents and are matched in every aspect except for fat and carbohydrate content. Mice fed a high fat diet rapidly gained more weight than control mice and after 15 wk on the diet weighed approximately 33% more (Fig. 3.1B). Mice were maintained on the respective high fat or low fat diet throughout the course of the experiment, including both primary and secondary infections.

To test if obese mice had compromised heterologous defenses, lean and obese mice were initially infected with a sublethal dose of PR8 virus after the 15 wk of dietary exposure (Fig. 3.1A). As expected, obese mice lost significantly more weight (5.10±0.40g) compared with lean mice (3.54±0.31g) following the primary PR8 infection, but when normalized to pre-infection body weight, there were no differences in percent weight loss between lean and obese mice (Fig. 3.1C). PR8 infected mice were maintained on their respective diets for 5 wk to allow the mice sufficient time to recover. After 5 wk, having regained weight equivalent to initial weight status prior to the PR8 infection (data not shown), mice were infected with a lethal dose of pH1N1 virus. One-hundred percent of naïve (unprimed) lean and obese mice rapidly succumbed to the lethal pH1N1 infection at 6 dpi (Fig. 3.1D). However, of the mice previously infected with PR8, 100% of lean mice and 95% of obese mice survived the pH1N1 challenge. Contrary to the initial primary infection, both lean and obese mice began to lose weight early at 2 dpi following the

secondary pH1N1 infection, with obese mice nearly losing twice as much weight as lean mice over the course of the infection. However, once normalized to body weight, weight loss was not significantly different between the two groups (Fig. 3.1E).

Diet-induced obesity impairs primary and secondary influenza antibody responses.

We assayed sera for HAI antibodies 5 wk following the primary PR8 infection in lean and obese mice to confirm that the pH1N1 virus was heterologously distinct in our hands. We did not detect HAI antibodies to pH1N1 in sera from lean or obese mice previously infected with PR8 (Fig. 3.2A). Further, microneutralization assays confirmed that the PR8 infection did not induce cross-neutralizing protection to pH1N1 virus (Fig. 3.2B). Similarly, Guo et al. did not detect cross-neutralizing antibodies to pH1N1 in sera from PR8-infected mice (133). Therefore, reflective of what happened in the human population during the pH1N1 outbreak, PR8 infected mice lacked pH1N1cross-reactive neutralizing antibodies.

As expected, 5 wk after PR8 infection, lean mice displayed elevated HAI and microneutralization titers to PR8 but not pH1N1 (Fig. 3.2A/B). Surprisingly, none of the obese mice had detectable HAI antibodies to PR8, and obese mice had nearly a 4-fold lower PR8 microneutralization titer. Although PR8 HAI antibodies are not critical modulators of secondary infection outcome in this model, the striking deficiency in PR8 HAI antibodies prompted us to measure PR8 antibody levels during the primary PR8 infection to determine if the reduced antibody levels at 35 dpi were a result of decreased antibody generation. At 7 dpi following the primary PR8 infection, obese mice had a lower mean PR8 HAI titer and a lower percentage of obese mice (p=0.06) exhibited detectable PR8 HAI antibodies (Fig. 3.2C/D). However, by 9 dpi and through 14 dpi, obese mice had similar levels of HAI antibodies compared with lean mice.

Therefore, obese mice exhibited delayed antibody generation during the primary infection but were able to compensate and eventually exhibited similar levels to that of lean mice. However, by 35 dpi, obese mice did not have any detectable PR8 HAI antibodies (Fig. 3.2C/D), indicating that obesity also impairs antibody maintenance. Kim et al. demonstrated that obese mice have impaired responsiveness to influenza vaccination, but obesity-induced impairments in antibody responses following infection in mice have not previously been shown (68). Interestingly, we have similarly demonstrated that obese humans have an impaired ability to maintain long-term levels of influenza antibodies (12).

Because of the striking deficiency of PR8 HAI antibodies in the obese mice at 35 dpi, we also assessed pH1N1 HAI antibody levels following the secondary challenge. Previous studies in mice have demonstrated that a primary heterologous influenza infection can lead to an accelerated production of pH1N1 neutralizing antibodies during a secondary pH1N1 infection (137,142), which could potentially impact infection outcome. We did not detect HAI antibodies at 5 dpi in lean or obese mice; however, 72.7% of lean mice had HAI antibodies at 8 dpi. By 14 dpi, 100% of lean mice had HAI antibodies (Fig. 3.3A/B). In contrast to lean mice, 41.7% of obese mice generated detectable serum HAI antibodies at 8 dpi, and only 50% of obese mice had pH1N1 HAI antibodies at 14 dpi (Fig. 3.3A/B). Therefore, obese mice displayed altered antibody responses during both primary and secondary infections. Although PR8 HAI antibodies offer negligible protection during the secondary infection, we measured PR8 HAI antibodies to determine if the impairments in antibody production during the secondary infection were specific to pH1N1 or a more global defect. The differences between lean and obese mice were striking, as 75% (day 5), 72.7% (day 8) and 83.3% (day 14) of lean mice had detectable levels of HAI antibodies to PR8 during the secondary pH1N1 infection compared with 8.3% (day 5), 16.7%

(day 8) and 33.3% (day 14) of obese mice (Fig. 3.3C/D). As a negative control for all HAI titers from sera obtained during the secondary infection, influenza A/Victoria/361/2011 (H3N2) was assayed in addition to pH1N1 and PR8. Taken together, obese mice exhibited delayed or impaired antibody generation during primary and secondary influenza infections, respectively, and impaired antibody maintenance (35 days following the primary PR8 infection).

Although, PR8 antibodies do not neutralize pH1N1 virus infectivity (see Figure 3.2B), nucleoprotein (NP) specific antibodies generated during a heterologous primary influenza infection or through vaccination have been shown to control virus replication during influenza infections (141,199,200). Therefore, we next assayed the level of anti-pH1N1 NP antibodies in lean and obese mice at 35 dpi. Interestingly, we detected that obese mice had a significantly lower level of serum anti-pH1N1 NP antibodies (Figure 3.3E). Because NP antibodies can regulate viral burden (141), we next measured lung viral titers in lean and obese mice to determine if lower anti-NP antibody levels potentially impacted influenza viral titers during the secondary pH1N1 infection. At 5 dpi, obese mice had greater than a 10-fold higher mean virus titer (p=0.05) in the lungs compared with lean mice (Fig. 3.3F). Although viral replication is controlled through several cell types and effector responses, it is plausible that reduced NP antibody levels resulted in greater viral burden in the lungs of obese mice.

Obese mice develop greater lung airway inflammation following a secondary heterologous pH1N1 infection.

Given that obese mice exhibited elevated viral titers at 5 dpi, we next assessed how greater viral burden impacted lung inflammation and pathology. Enumeration of BAL cells following the secondary infection revealed that obese mice had nearly twice as many cells in the lung airways at 5 dpi (Fig. 3.4A). Conversely, in the draining mLN, lean mice had approximately

twice as many immune cells as obese mice at 5 dpi (Fig. 3.4B). Despite the lack of differences in inflammatory cytokine expression (Table 3.1), obese mice had elevated lung pathology scores (Fig. 3.4C) and a greater level BAL fluid protein at 5 dpi (Figure 3.4D). To determine if the elevated level of immune cell infiltration and inflammation in the lungs resulted in damage to the integrity of the respiratory epithelium in obese mice, we assayed albumin levels in the lung airways. Consistent with heightened infiltrate and pathology at 5 dpi, we detected greater levels of BAL albumin at 5 dpi in obese mice (Figure 3.4E).

Obese mice have a heightened memory $CD8^+$ T-cell response in the lung airways following a lethal secondary pH1N1 infection.

The protective role of memory T cells during secondary heterologous influenza infections is well established (201,202). Further, several recent investigations have demonstrated that exposure to seasonal influenza strains or vaccination can elicit memory T cells that are able to recognize viral epitopes of pH1N1, conferring cross-protection (107,137). Both $CD4^+$ and $CD8^+$ memory T cells have been shown to be important in limiting disease severity in several models of pH1N1 rechallenge studies (133,137,139).

To determine if obesity influenced the distribution and activation of cross-reactive T cells, BAL cells from mice previously infected with PR8 5 wk earlier and then challenged with pH1N1 were stimulated with heat-inactivated pH1N1 virus, pH1N1-pulsed APCs or the polyclonal mitogen, Con A, at days 5, 8 and 14 following the secondary pH1N1 infection. Figure 3.5A demonstrates that all three methods of stimulation induced a robust IFN-γ response in cross-reactive $CD4^+$ T cells at 5 dpi. As expected, the addition of influenza-pulsed APCs in culture with BAL cells resulted in an elevated IFN-γ response compared with BAL cells incubated with heat-inactivated virus alone. Obesity did not impair IFN-γ or GzB production by

memory $CD4^+$ T cells in response to the stimuli (Fig. 3.5B/C). There were no differences in $CD4^+$ T-cell IFN-γ median fluorescence intensity (MFI) or GzB MFI (data not shown).

Next, we investigated potential differences in $CD4^+$ effector memory T cells between lean and obese mice as we have previously demonstrated that obese mice have an impaired $CD8^+$ effector memory T-cell response (78). Effector memory T cells were distinguished by lack of expression of the cell adhesion molecule, CD62L, which is inherently absent or low on effector memory T cells (203). Because we detected differences in viral titers and lung pathology at 5 dpi, we focused on effector memory T-cell populations specifically on this day. However, we did not detect any differences in IFN-γ or GzB production of $CD4^+CD62L^-$ effector memory T cells between lean and obese mice (Fig. 3.5D/E). This suggests, at least partially, that cross-reactive $CD4^+$ T-cell cytotoxic responses are intact in obese mice.

We also determined how obesity affected the cross-reactive $CD8^+$ T-cell responses under the same conditions described for $CD4^+$ T cells. Approximately, 4-5% of $CD8^+$ T cells from lean and obese mice produced IFN-γ following stimulation with influenza-pulsed APCs at 5 dpi (Fig. 3.6A). After day 5, the magnitude of the $CD8^+$ T-cell response declined in both lean and obese mice (Fig. 3.6B/C). Interestingly, obese mice had a strikingly elevated number of $CD8^+IFN\text{-}\gamma^+$ and $CD8^+GzB^+$ T cells at 5 dpi (Fig. 3.6B/C). Further analysis of the $CD8^+$ memory T-cell population revealed that obese mice had an elevated number of $CD8^+CD62L^-IFN\text{-}\gamma^+$ T cells and a significantly greater number of $CD8^+CD62L^-GzB^+$ effector memory T cells at 5 dpi as well (Fig. 3.6D/E). There were no differences in CD8+ IFN-γ MFI or GzB MFI (data not shown).

We used whole virus in BAL cell stimulations, and thus we were assessing the total polyclonal response of the $CD4^+$ and $CD8^+$ memory T-cell pool. Since we detected significant differences in the number of GzB producing effector memory $CD8^+$ T cells in obese mice, we

next examined GzB production by effector memory T cells specific for a specified viral epitope. As NP from PR8 shares 91% similarity with the pH1N1 NP (142), we used the influenza tetramer D^bNP_{366-74}, allowing for detection of T cells specific for the PR8 NP_{366-74} epitope during the secondary pH1N1 infection. Figure 6F demonstrates that obese mice had a greater number of NP_{336-74} specific T cells producing GzB following stimulation. Further, obese mice had a significantly greater number of NP_{366-74} specific $CD8^+CD62L^-$ T cells, and a significantly greater proportion of these cells produced GzB (Fig. 3.6G). The elevated cross-reactive $CD8^+$ T-cell response could be attributed to the greater viral burden detected in the lungs of obese mice at 5 dpi. It is likely that greater viral load induced excessive recruitment of $CD8^+$ T cells to the lungs, and perhaps the elevated $CD8^+$ T-cell response was required to control the excess viral burden in the absence of proper antibody defenses.

Obese mice have a greater number of $CD4^+CD25^+Foxp3^+$ Tregs in the lung airways at 5 dpi.

Numerous factors could contribute to the increased lung inflammation, lung infiltration, lung damage and memory $CD8^+$ T-cell responses in obese mice. Enhanced inflammatory responses in the lungs between 1-5 dpi or altered expression of lung trafficking molecules on immune cells could result in the observed differences in infiltration in the lung at 5 dpi. However, we did not detect any differences in the percentage of mLN $CD8^+$ T cells expressing the trafficking molecules CD44, CD62L and CCR7 at 5 dpi, nor did we find any differences in mLN or lung chemokine expression at 0 or 5 dpi (mLN data not shown).

We observed greater infiltration, lung damage and heightened $CD8^+$ T-cell responses in the lungs of obese mice, and Tregs have been shown to regulate all of these parameters in other respiratory infection models (204,205). Further, obesity has been reported to result in a

deficiency of anti-inflammatory Tregs in metabolic tissues such as white adipose (206) and the liver (207). We therefore proceeded to investigate this unique cell type in the secondary infection model as a potential mechanism for increased inflammation in the obese mice. Figure 3.7A represents the gating scheme used to distinguish Tregs and demonstrates the Treg distribution in the lung airways and mLN in lean and obese mice at 5 dpi. Although, $CD25^{-}Foxp3^{+}$ Tregs were present in the lung airways and mLN following the secondary infection, the majority of $Foxp3^{+}$ T cells were $CD25^{+}$ (Fig. 3.7A). BAL Treg number peaked at 5 dpi in obese mice and continually decreased in number, whereas lean mice had consistent numbers of BAL Tregs from 5 to 8 dpi with a similarly low level of Tregs by 14 dpi (Fig. 3.7B). Interestingly, obese mice had more than twice as many BAL Tregs at 5 dpi and nearly half as many mLN Tregs (Fig. 3.7C) compared with lean mice. Consistent with two recent publications investigating Tregs during a primary influenza infection (208,209), the mLN in lean and obese mice contained a greater number of Tregs than the BAL compartment following infection (Fig. 3.7C). There is little known regarding memory Tregs during influenza infection nor the distribution and function of Tregs during a secondary influenza infection. One would expect a greater presence of suppressive Treg cells to result in a dampening of the inflammatory and cytotoxic responses in the lungs of obese mice (210). However, we observed the opposite, and therefore investigated the possibility that obese mice have impaired Treg suppressive function.

Tregs isolated from obese mice are less suppressive than those from lean mice.

To compare Treg activity from lean and obese mice, we used a well-established suppression assay (198). Tregs isolated from splenocytes were cocultured in the presence of $CD4^{+}CD25^{-}$ Teff cells isolated from lean mice. Tregs from lean and obese mice were only

cocultured with Teff cells isolated from lean mice to eliminate any possibility of a discrepancy in Teff proliferation between lean and obese mice. Figure 3.8A demonstrates that isolated Treg populations were greater than 95% $Foxp3^+$ from both dietary groups, and less than 5% of Teff cells isolated from lean mice were $Foxp3^+$, confirming pure populations of isolated cells. Interestingly, after a 72 h anti-CD3/CD28 polyclonal stimulation, Tregs isolated from obese mice were found to be significantly less suppressive (Fig. 3.8B). After normalizing to lean Treg activity, Tregs isolated from obese mice were 41% less suppressive (Fig. 3.8C). Therefore, diet-induced obesity dramatically impaired Treg suppressive activity. There are a wide variety of mechanisms that could contribute to the impaired Treg function in obese mice. The level of Foxp3 expression in Treg cells is important for suppressive activity as experimental reduction in Foxp3 results in impaired Treg suppressive function (211,212). Thus, we assayed Foxp3 protein expression levels in Tregs from splenocytes of lean and obese mice, but we did not detect differences in Foxp3 levels (Fig. 3.8D) suggesting that impairment in Treg function is due to a mechanism unrelated to Foxp3 expression.

Discussion

Globally, greater than 1.4 billion adults are overweight, and approximately 500 million of these individuals are obese (3). In 2009, obesity was reported to be an independent risk factor for hospitalization and death following pH1N1 influenza infection (5-7). Given the prevalence of obesity and the consistent threat of influenza epidemics and pandemics, understanding how excess adiposity affects the immune response to influenza infection is important in potentially developing therapies to limit morbidity and mortality in this at-risk population.

During the 2009 pandemic, a majority of individuals (nonelderly) lacked pre-existing neutralizing antibody protection to pH1N1 (102,104-107). Therefore, a number of investigations have focused on the protectiveness of heterologous immunity to pH1N1 infection, conferred from previous exposure to circulating influenza strains or vaccines (131,139,140). Human studies and mouse models have demonstrated that cross-reactive T cells and cross-reactive non-neutralizing antibody defenses can limit viral load and protect from a lethal heterologous influenza infection (102,131,133,142). Additionally, prior heterologous infection can accelerate pH1N1 antibody generation during a secondary pH1N1 infection, thus providing an additional mechanism by which heterologous immunity can limit pH1N1 infection severity (137,142). However, obese humans and mice have been shown to have impaired memory T-cell and humoral responses following vaccination or infection (12,68,78,213). Thus, we developed a mouse model to investigate if obesity results in enhanced pH1N1 infection severity due to impairments in heterologous immune defenses.

In this study, obesity did not impair the overall ability of heterologous immunity to prevent mortality from pH1N1 infection as 95% of PR8 primed obese mice survived the lethal secondary heterologous infection, whereas none of the naïve, obese mice survived the pH1N1 infection. However, heterologous cellular and humoral responses were significantly altered by obesity, and obese mice displayed greater lung damage during the secondary pH1N1 infection. Obese mice exhibited a significant delay or impairment in antibody generation during both primary and secondary influenza infections. Further obese mice displayed significantly lower levels of cross-reactive anti-pH1N1 NP antibodies following the primary PR8 infection. Subsequent investigation of viral titers confirmed that obese mice had a greater lung viral titer at 5 dpi, perhaps due to reduced levels of cross-reactive anti-NP antibodies. Consistent with greater

viral load, obese mice had an elevated number of infiltrating cells into the lung airways, heightened lung pathology, and greater BAL total protein and albumin levels. Analysis of cross-reactive T-cell responses demonstrated that obesity led to a heightened $CD8^+$ T-cell response in the lung airways, but obesity did not impact cross-reactive $CD4^+$ T-cell distribution during the secondary infection. These data point towards a model in which reduced levels of anti-NP antibodies resulted in greater lung viral burden, which subsequently induced greater immune cell infiltration, lung damage and heightened $CD8^+$ T-cell responses in obese mice. Lastly, we investigated the impact of obesity on Treg distribution during the secondary infection model. We found that obese mice had a greater number of BAL Tregs at 5 dpi, but *ex vivo* analysis revealed Tregs isolated from obese mice were significantly less functional than Tregs from lean mice. Therefore, perhaps obese individuals experienced greater pH1N1 infection severity due to a combination of impaired pH1N1 heterologous antibody defenses and excessive antiviral immune responses in the lungs, which could not be controlled properly due to dysfunctional Tregs.

Despite a lack of neutralizing antibody protection, antibody defenses may still impart protection to a lethal pH1N1 infection in our model. A protective role for cross-reactive non-neutralizing antibodies during influenza infection has been well established (141,142,199,200). LaMere et al. demonstrated that intact antibody defenses (i.e. somatic hypermutation and class-switch recombination) were required for proper heterologous immunity in the classical X31 prime, PR8 challenge, heterologous infection model (141). Further, influenza NP vaccination or passive transfer of NP immune serum can limit viral replication in the lungs of PR8 infected mice (141). Therefore, non-neutralizing antibodies can impart antiviral activity, although the exact mechanisms by which anti-NP antibodies function remain unclear (141). Interestingly, NP was detected in the 2008/09 trivalent inactivated vaccine, and some individuals demonstrated

increased levels of anti-NP antibodies following vaccination (200). Therefore, non-neutralizing NP antibody protection is clinically relevant as well. The non-neutralizing influenza antibody repertoire can also include antibodies targeting other internal viral proteins such as the matrix protein (M1) and nonstructural protein 1 (NS1) (141,142). However, the protective role of antibodies specific to these proteins is less established and likely less protective compared with anti-NP antibodies (141,142).

Another mechanism by which heterologous immunity may protect against pH1N1 is through the acceleration of homologous pH1N1 antibodies produced during a secondary pH1N1 challenge. A primary heterologous infection followed by a pH1N1 challenge has been shown to result in significantly enhanced production of pH1N1 neutralizing antibodies (137), split pH1N1 antibodies and anti-NP antibodies compared with naïve mice infected with pH1N1 (142). It is likely that cross-reactive $CD4^+$ T cells facilitate this accelerated homologous pH1N1 antibody production (137). We did not detect pH1N1 HAI antibodies at the early time-point of 5 dpi, however, we found that a significantly lower proportion of obese mice exhibited detectable pH1N1 HAI antibodies 14 days after the secondary challenge. Therefore, it is unlikely that this aspect of heterologous immunity contributed to the observed outcomes in lean and obese mice. Of particular note, we found that obese mice displayed a delayed production and impaired maintenance of PR8 antibodies following the primary, sublethal PR8 infection. Further, obese mice had significantly lower mean PR8 HAI titers during the secondary infection, and a lower proportion of obese mice had detectable PR8 HAI antibodies at all of the time points assayed. Although PR8 HAI antibodies did not mediate protection in this model *per se*, the dramatic impact of obesity on influenza antibody responses has clear public health implications. Kim et al. demonstrated that obesity impairs the antibody response to pH1N1 vaccination in mice (68),

but it has not been reported that obesity alters antibody responses during the context of an infection.

Excessive antiviral and inflammatory immune responses in the lung, contributing to severe immunopathology, are known to be one of the primary causes of influenza-related morbidity and mortality (214,215). Further, fatal pH1N1 infection is associated with enhanced inflammation with high numbers of $CD8^+GzB^+$ cytotoxic T cells and excess local production of IFN-γ in the lung (215). We similarly detected greater inflammation, lung pathology and a greater number of $CD8^+GzB^+$ cytotoxic T cells in the lungs of obese mice infected with pH1N1. Although, only mild symptoms were experienced by a majority of individuals infected, severe immunopathology may partly explain why certain at-risk groups, such as obese humans, experienced a worse outcome to pH1N1 infection.

Obesity is characterized by a state of chronic inflammation, likely due, in part, to the simultaneous deficiency of Tregs in metabolic tissues (206). Because obesity negatively impacts Treg distribution, we hypothesized that obese mice would have fewer Tregs in their lungs, offering a potential explanation for the greater lung infiltration, inflammation, pathology, damage and the heightened memory $CD8^+$ T-cell responses detected in the lung airways at 5 dpi. Tregs have been shown to regulate all of these parameters in other respiratory infection models (204,205,216). Contrary to our expectations, we found that obese mice had nearly twice as many Tregs in the lung airways at 5 dpi compared with lean mice. Subsequent investigation of Treg function revealed that Tregs isolated from obese mice were 41% less suppressive than those isolated from lean mice. Therefore, impaired Treg function may have contributed to the excessive antiviral responses observed in the lungs of obese mice at 5 dpi. Although, we did not

show impaired Treg suppressive function *in vivo* during the infection, the suppression assay suggests that *in vivo* function may be impaired as well.

Betts et al. demonstrated that a primary influenza infection results in a robust, antigen-specific Treg response, and influenza infection-induced Tregs were able to suppress antigen-specific $CD4^+$ and $CD8^+$ T-cell proliferation and cytokine production (209). Further, a recent study by Brincks et al. reported that during secondary influenza infections, antigen-specific memory Tregs exhibit accelerated accumulation in the lungs and mLN compared with primary infection responses and control memory $CD8^+$ T-cell proliferation in a MHC class II dependent antigen-specific manner (217). Interestingly, depletion of memory Tregs resulted in heightened $CD8^+$ T-cell responses, pulmonary inflammation and lung cytokine expression during a secondary influenza infection (217). It is possible that obesity-induced alterations in memory Treg responses could have contributed to the aberrant inflammatory responses observed in obese mice during the secondary pH1N1 infection.

We utilized a mouse model of diet-induced obesity and heterologous influenza infection in attempt to mirror clinical and epidemiological evidence. We found lower levels of non-neutralizing influenza NP antibodies, heightened cross-reactive $CD8^+$ T-cell responses, greater viral titers and lung pathology, and impaired Treg function in obese mice. We propose that impaired antibody protection resulted in greater viral burden, which subsequently drove heightened inflammatory responses that were not properly controlled by dysfunctional Tregs. This study and numerous others have demonstrated obesity negatively impacts the immune response to influenza infection (67,68,78,79,81,82,213). Yet, the exact cellular and molecular mechanisms by which excess adiposity contributes to altered antiviral defenses remain unclear (2). It is possible that one global defect in all immune cells can explain impaired functionality in

the obese, but it is more likely that a complex combination of altered signaling pathways and responses ultimately impairs immunity and results in greater influenza susceptibility (2).

Tables and Figures

Table 3.1 Similar levels of lung cytokine and chemokine expression during a secondary heterologous pH1N1 challenge in lean and obese mice

Gene	Dietary Group	Day 0	Day 5	Day 8	Day 14
TNF-α	*Lean*	1.00±0.11	1.92±0.44	0.89±0.12	1.12±0.10
	Obese	0.83±0.09	2.20±0.51*	0.78±0.09	0.84±0.12
IL-1β	*Lean*	1.00±0.11	1.75±0.29*	0.69±0.10	0.59±0.07*
	Obese	3.07±1.13	2.64±0.57	0.59±0.10*	0.53±0.08*
IFN-γ	*Lean*	1.00±0.32	6.33±0.69*	2.41±0.29*	1.96±0.10
	Obese	0.71±0.15	6.58±1.69*	2.01±0.19*	1.81±0.11*
IL-10	*Lean*	1.00±0.18	6.62±0.83*	2.84±0.29*	0.94±0.05
	Obese	1.11±0.34	8.31±5.09	4.09±0.69*	1.40±0.42
RANTES	*Lean*	1.00±0.51	0.69±0.08	1.08±0.20	0.64±0.20
	Obese	0.48±0.0.08	0.73±0.15	0.76±0.09	0.79±0.15
MCP-1	*Lean*	1.00±0.11	14.25±1.34*	1.32±0.18	0.77±0.05
	Obese	0.73±0.01	23.99±7.49*	2.20±0.83*	0.86±0.11

Table 3.1: Values represent mean fold increase over uninfected control ± SEM (n=4-6), *$p<0.05$ compared with 0 dpi within same dietary group. There were no statistical differences between lean and obese mice at any time point.

Figure 3.1 Sublethal influenza A/PR/8/34 infection induces heterologous protection against a lethal pH1N1 challenge in lean and diet-induced obese mice

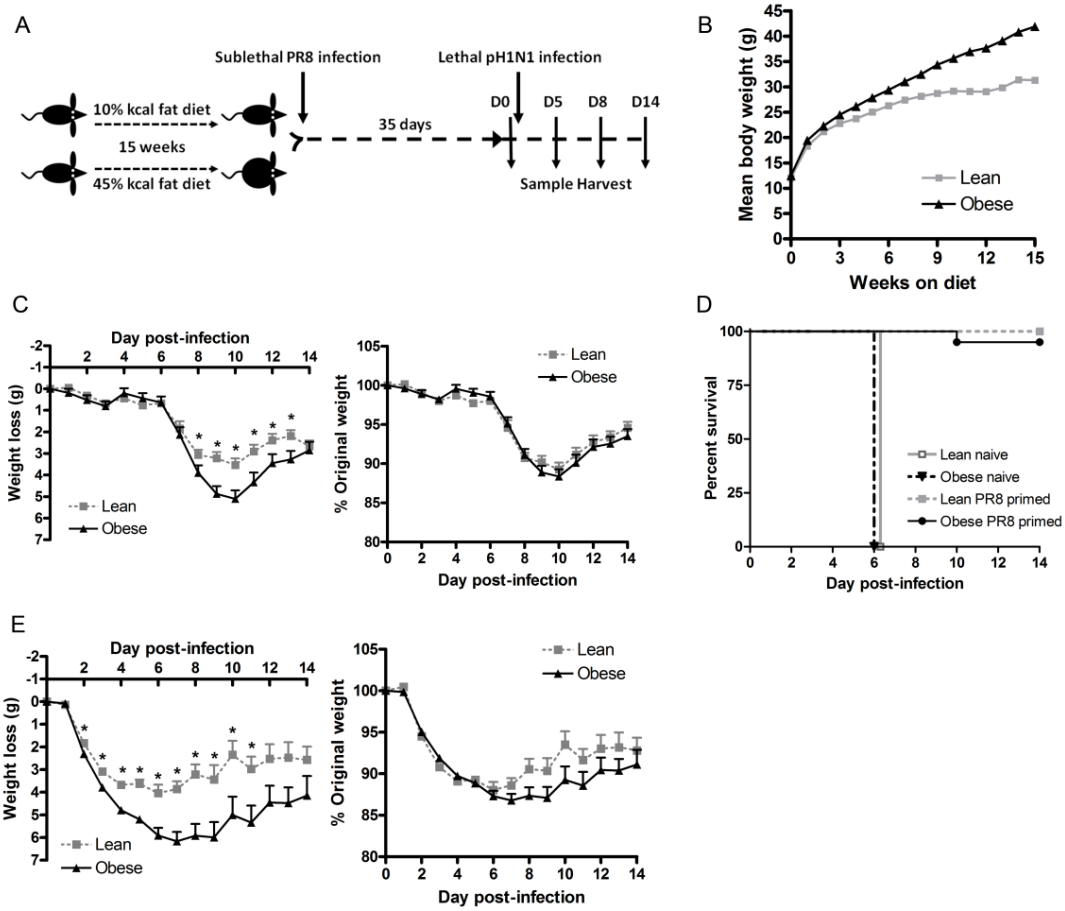

Figure 3.1: A, Weanling, male C57BL/6J mice were placed on a high fat or low fat, control diet for 15 wk. Lean and obese mice were infected with a sublethal dose of influenza A/PR/8/34. Thirty-five days after the primary infection, mice were challenged with a lethal dose of pH1N1 and samples were harvested at day 0 (naïve to pH1N1), and 5, 8 and 14 dpi. B, Mice fed a high fat diet gain significantly more weight than mice fed a low fat, control diet ($n \geq 40$ per group). After one week and throughout dietary exposure, high fat diet fed mice weigh significantly more than low fat diet fed mice. C, Fifteen weeks after mice were placed on the designated diets, mice were inoculated with a sublethal dose of PR8, and weight loss was monitored daily. D, Five weeks after the primary PR8 infection, PR8 primed (two cohorts of n=46) and naive mice (n=3-4) were challenged with a lethal dose of pH1N1. The naïve mice rapidly succumbed to the pH1N1 challenge, whereas primed mice did not. E, Secondary pH1N1 infection weight loss. Diet-induced weight gain graphs and infection weight loss graphs represent means ± SEM of at least two independent experiments. *$p<0.05$ compared with obese mice.

Figure 3.2 Obese mice exhibit delayed antibody production and impaired antibody maintenance following a sublethal PR8 infection

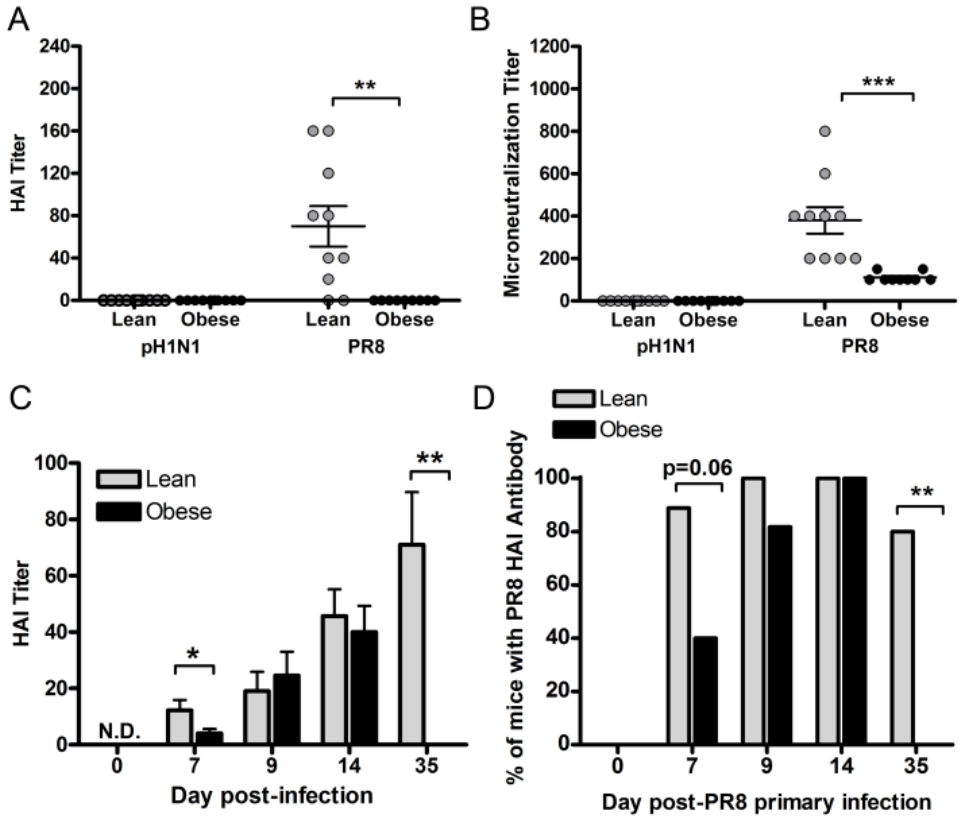

Figure 3.2: A and B, HAI (A) and microneutralization (B) titers of sera from lean and obese mice 5 wk after a primary PR8 infection, demonstrating that PR8 does not elicit a cross-neutralizing pH1N1 antibody response (n=9-10). C and D, PR8 HAI titer (C) and percentage of mice with detectable PR8 HAI antibodies (D) following a sublethal PR8 infection (n=8-11). The limit of detection for HAI and microneutralization titers is 10. Each data point represents an individual animal. Bars represent mean HAI $\pm$ SEM or percentage of mice with detectable PR8 HAI. *$p<0.05$, **$p<0.005$, ***$p<0.0005$.

Figure 3.3 Obese mice have lower levels of cross-reactive anti-pH1N1 nucleoprotein antibodies and exhibit greater lung viral titers during a secondary pH1N1 infection

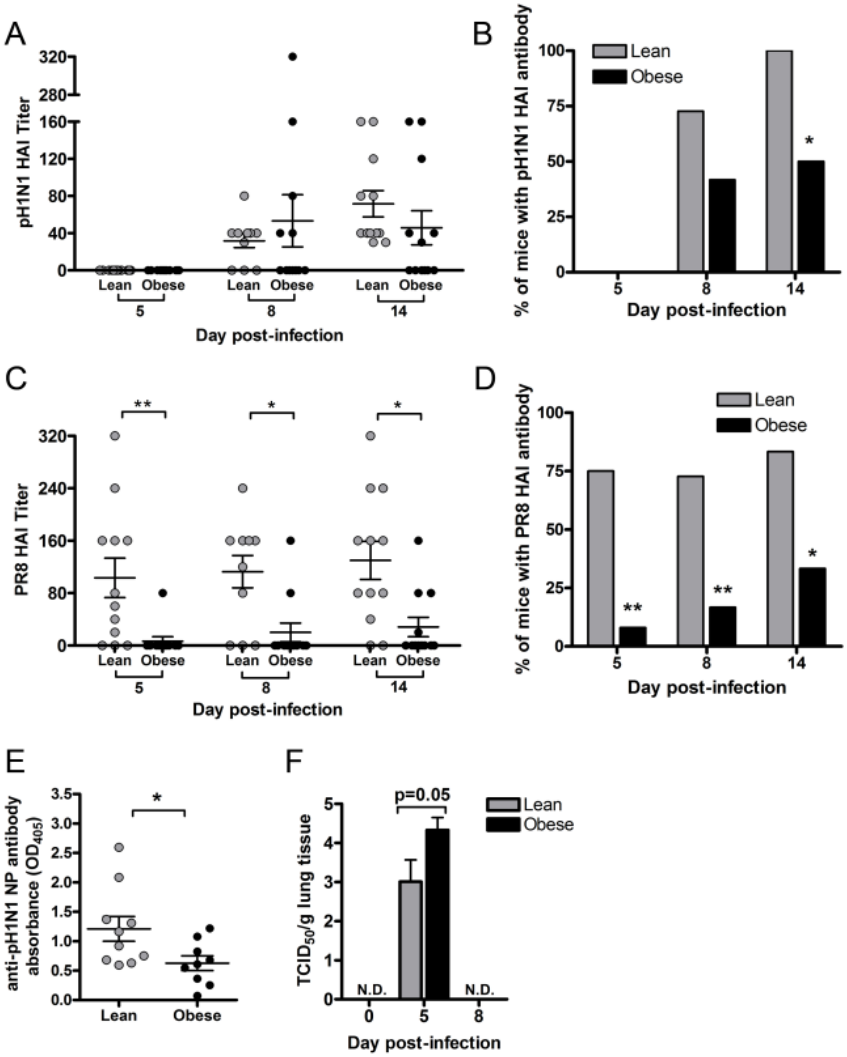

Figure 3.3: A and B, Serum pH1N1 HAI titer (A) and percentage of mice with detectable pH1N1 HAI antibodies (B) during a secondary heterologous pH1N1 challenge, n=10-12. C and D, Serum PR8 HAI titer (C) and percentage of mice with detectable PR8 HAI antibodies (D) during a secondary heterologous pH1N1 challenge, n=10-12. The limit of detection for HAI titers is 10. E, Obese mice have lower levels of serum cross-reactive anti-pH1N1 NP antibodies 5 wk after a primary PR8 infection, n=9-10. F, Obese mice have a greater viral burden at 5 dpi during the pH1N1 rechallenge (n=12). No virus was detected (N.D.) at 0 or 8 dpi, n=5-6 at 0 and 8 dpi. Each data point represents an individual animal. Bars represent percentage of mice with detectable HAI antibody or mean viral titer $\pm$ SEM. *p<0.05, **p<0.005 compared with lean mice.

Figure 3.4 Obese mice exhibit a greater inflammatory and pathological response in the lungs following a secondary heterologous pH1N1 challenge

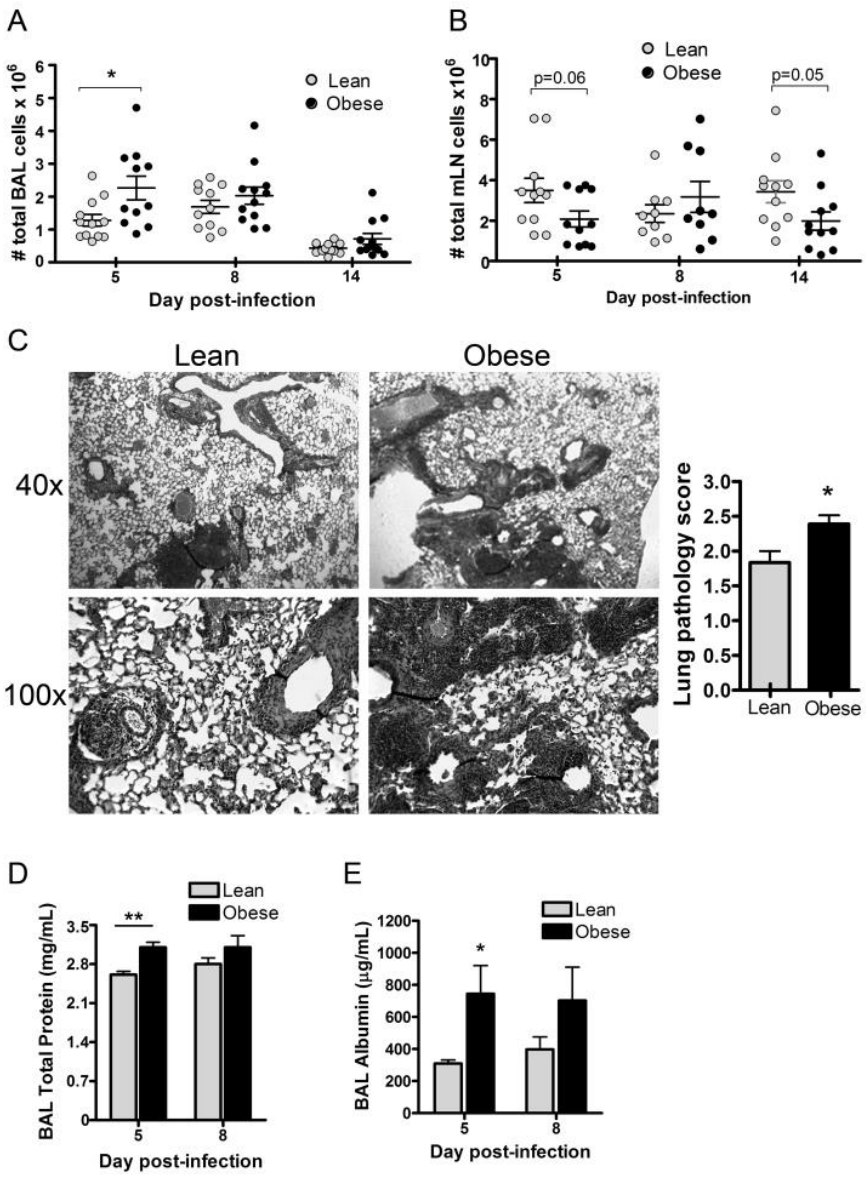

Figure 3.4: A and B, Enumeration of BAL cells (A) and mLN cells (B) at 5, 8 and 14 dpi following the secondary pH1N1 challenge, n=9-12. Each data point represents an individual animal. C, Representative H&E stained lung histology slides at 40x and 100x magnification and pathology score at 5 dpi, n=3-4. D, Total protein in BAL fluid at 5 and 8 dpi, n=5-6. E, Albumin levels in BAL fluid at 5 and 8 dpi, n=5-6. Bars represent mean $\pm$ SEM, *p<0.05, **p<0.005 compared with lean mice.

Figure 3.5 Exposure to PR8 elicits a rapid and robust memory CD4$^+$ T-cell response following pH1N1 infection in both lean and obese mice

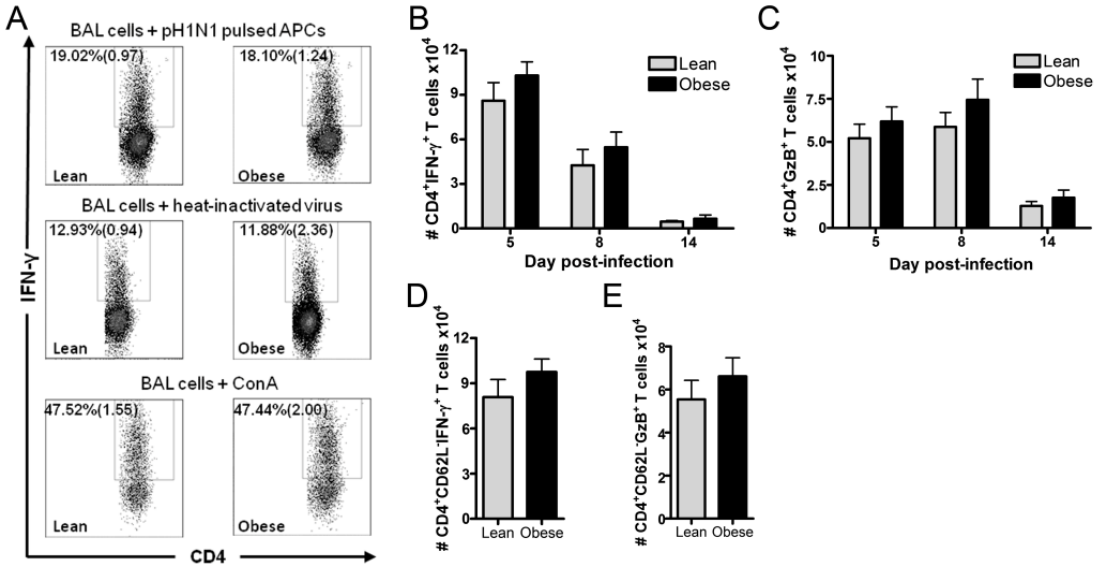

Figure 3.5: BAL cells from mice challenged with a secondary heterologous pH1N1 infection were stimulated for 6h with heat-inactivated pH1N1 (n=5-6), pH1N1 pulsed APCs (n=4-6) or Con A (n=5-6). A, Representative flow cytometry gating scheme at 5 dpi, including mean % (SEM). B and C, Number of IFN-γ (B) and GzB (C) producing CD4$^+$ T cells after stimulation with pH1N1 pulsed APCs, n=4-6. D and E, Number of IFN-γ (D) and GzB (E) producing effector memory CD4$^+$ T cells after stimulation with pH1N1 pulsed APCs at 5 dpi, n=4-6. Each bar represents the mean ± SEM.

Figure 3.6 Obese mice have enhanced cross-reactive $CD8^+$ T-cell responses at 5 dpi after a secondary heterologous pH1N1 challenge

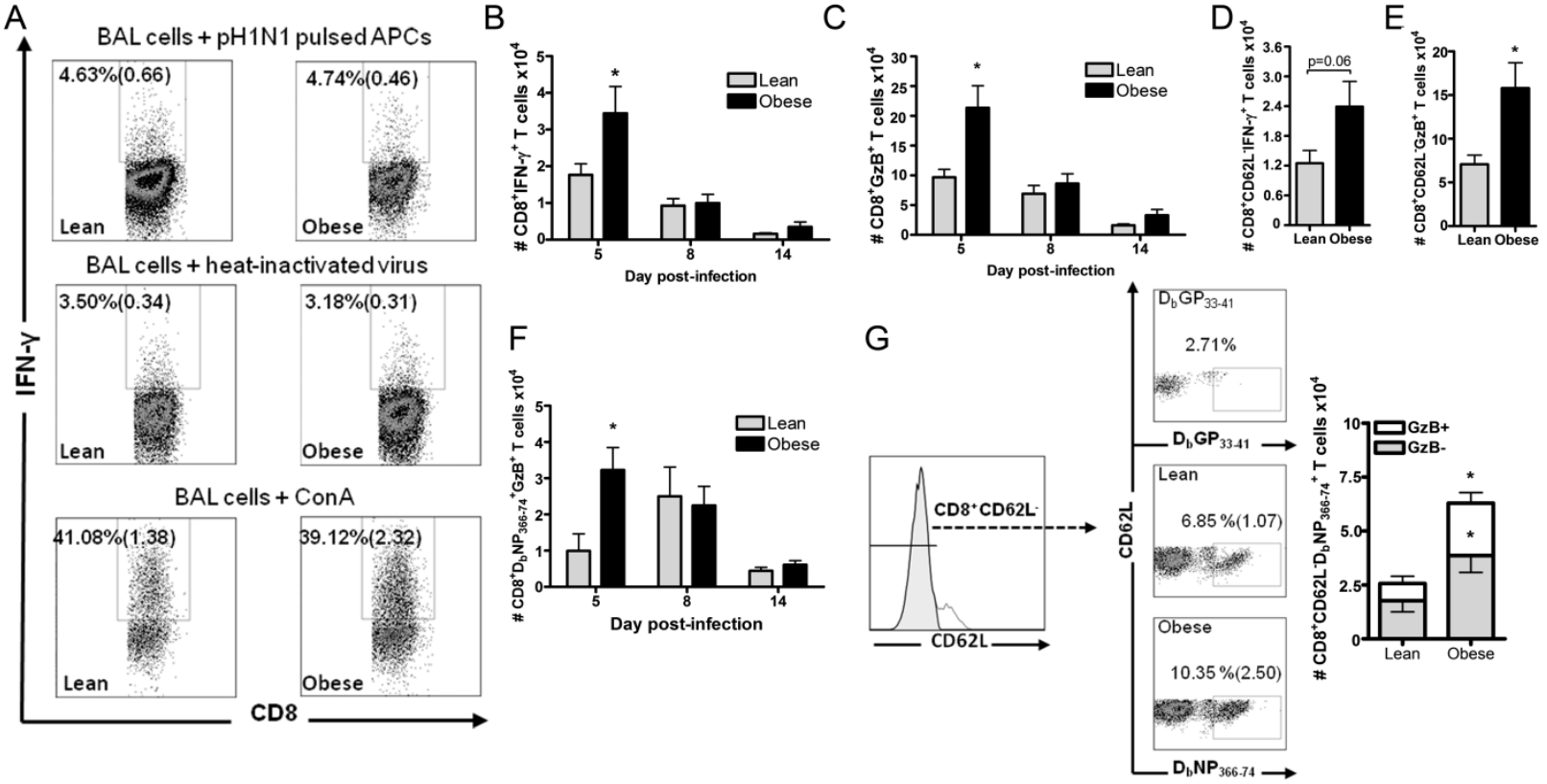

FIGURE 3.6: A, BAL cells from mice challenged with a secondary heterologous pH1N1 infection were stimulated as described in the legend to Figure 4. A, Representative flow cytometry gating scheme at 5 dpi, including mean percentage (SEM), n=4-6. B and C, Number of IFN-γ (B) and GzB (C) producing $CD8^+$ T cells after stimulation with pH1N1 pulsed APCs, n=4-6. D and E, Number of IFN-γ (D) and GzB (E) producing effector memory $CD8^+$ T cells after stimulation with pH1N1 pulsed APCs at 5 dpi, n=4-6. F, Enumeration of GzB producing, NP_{366-74} specific $CD8^+$ T cells in the BAL compartment, n=4-6. G, Comparison of GzB production by NP-specific effector memory $CD8^+$ T cells stimulated with APCs at 5 dpi, n=4-6. Each bar represents the mean ± SEM, *$p<0.05$ compared with lean mice at 5 dpi.

Figure 3.7 Obese mice have a greater number of Tregs in the lung airways during a heterologous secondary pH1N1 challenge

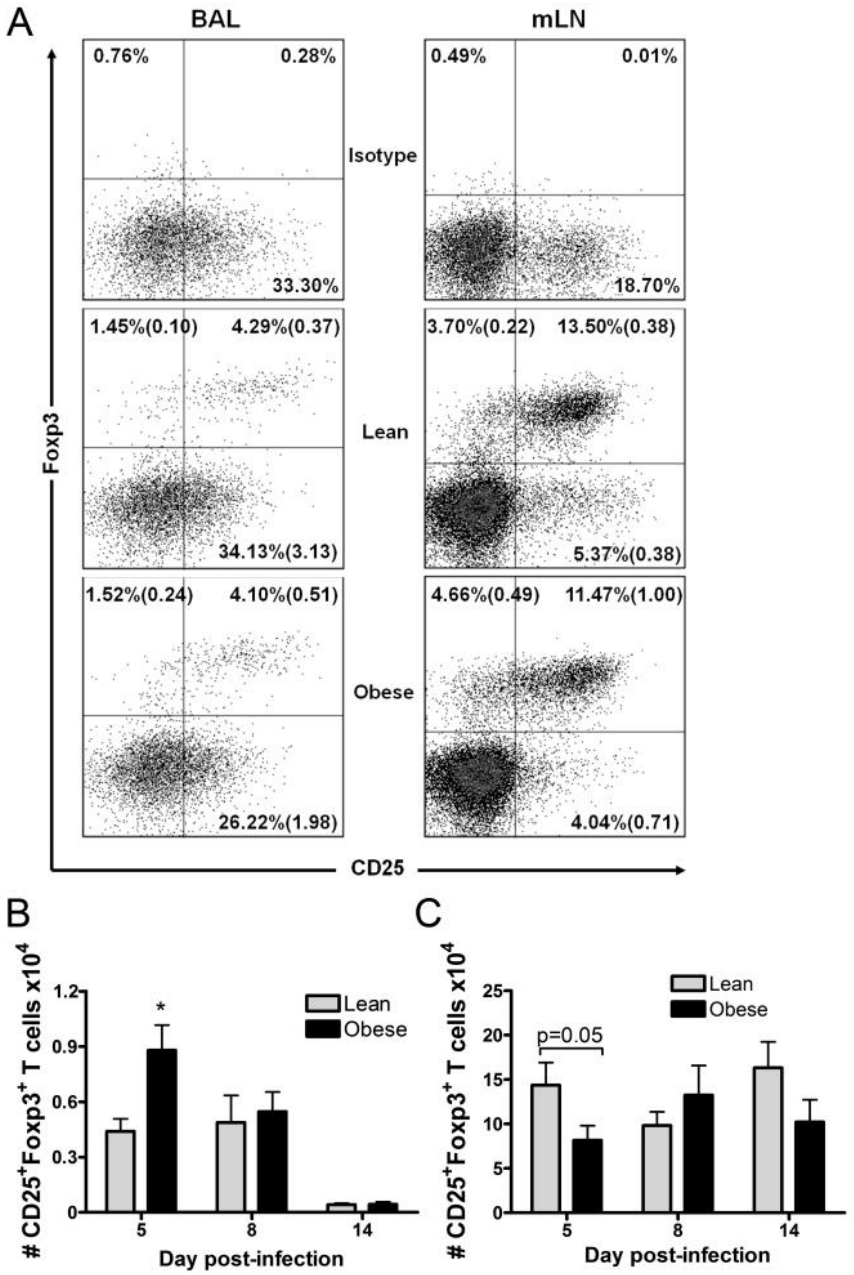

Figure 3.7: A, Representative BAL (n=5-6) and mLN (n=10-12) $CD4^{+}CD25^{+}Foxp3^{+}$ Treg gating scheme at 5 dpi, including mean percentage (SEM). B and C, Enumeration of Tregs in BAL fluid (B) and mLN (C). Each bar represents the mean ± SEM, and *$p<0.05$ compared with lean mice at 5 dpi.

Figure 3.8 Tregs isolated from obese mice are significantly less suppressive than Tregs isolated from lean mice

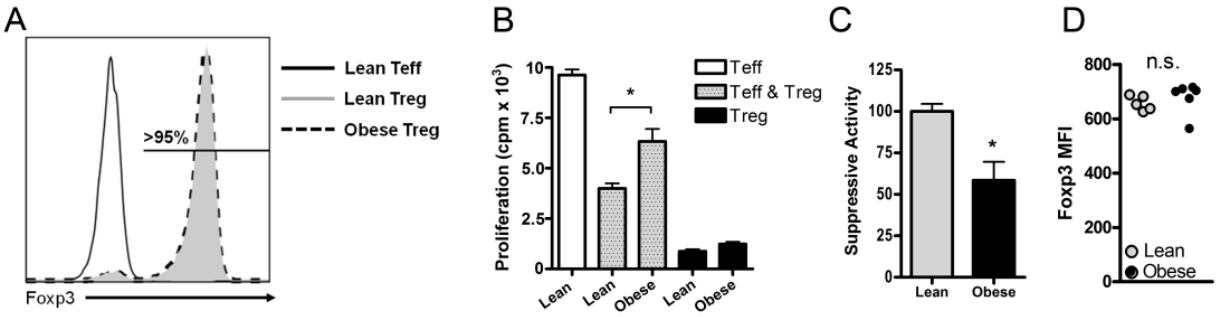

Figure 3.8: Pooled $CD4^+CD25^-$ Teff cells and $CD4^+CD25^+$ Tregs were isolated from splenocytes of naïve lean (n=3) and obese mice (n=3). A, Greater than 95% of isolated Tregs expressed Foxp3 from lean and obese mice, and less than 5% of Teff cells expressed Foxp3 as determined by FACS analysis, confirming pure populations of cells. B, Suppression assay comparing functionality of lean Tregs and obese Tregs cocultured with lean Teff cells at a ratio of 1:2 in the presence of anti-CD3/CD28 for 72 h. C, Normalized suppressive activity of isolated Tregs. D, Foxp3 median fluorescence intensity (MFI) of Tregs from splenocytes of lean and obese mice. Each data point represents an individual animal, n=5-6. Each bar represents the mean $\pm$ SEM, and *$p<0.05$ compared with lean mice.

CHAPTER IV: DIET- AND GENETIC-INDUCED OBESITY RESULTS IN GREATER LUNG DAMAGE AND MORTALITY DURING A PRIMARY 2009 PANDEMIC H1N1 INFLUENZA VIRUS INFECTION IN MICE

Introduction

The triple reassortant H1N1 influenza virus, responsible for causing the 2009 influenza pandemic outbreak, continues to circulate and cause epidemics globally (218). The 2009 pandemic H1N1 strain (pH1N1) was novel in several aspects. Despite infecting up to 89 million people in the US alone (16), pH1N1 infection symptoms were relatively mild (13,99). However, certain at risk groups exhibited greater morbidity and mortality following infection, including individuals with underlying health conditions such as asthma, type 2 diabetes, COPD, smokers and pregnant women (4,13,15). Further, several epidemiological investigations identified obesity as an independent risk factor for hospitalization and death to pH1N1 infection (72-75). Globally, more than 500 million individuals are obese (BMI≥kg/m^2) (3). Therefore, understanding the mechanisms by which obesity drives greater pH1N1 infection severity is critical for solving this widespread global public health issue and will ultimately facilitate identification of novel vaccination or therapeutic approaches.

Vaccination is considered the best available measure for preventing infection and limiting influenza severity (219). We have previously demonstrated that obese humans exhibit impaired influenza vaccination responses. Following trivalent influenza vaccine (TIV) immunization, circulating memory T cell activation induced by vaccine strains was impaired in obese individuals (BMI≥30) compared with healthy weight adults (11,12). Although short term TIV

antibody responses are intact, obese individuals displayed a greater decline in influenza antibodies one year after vaccination (12). At this point in time, it is not clear whether obese individuals are more susceptible to influenza infection, only that illness is more severe in those infected.

Similar to obese humans, obese mice exhibit greater mortality from influenza infection compared with lean control mice (2). It is well established that obesity alters inflammatory responses and the function of a variety of innate and adaptive immune cell populations (2). Further, during the context of influenza infection, obese mice exhibit heightened inflammatory responses in the lung, impaired lung epithelial wound healing, blunted antibody responses and aberrant memory T cell responses (14,67,68,78,82). However, the underlying cellular and molecular mechanisms for greater influenza mortality in obese mice remain unclear. Excess adiposity triggers a number of metabolic and physiologic perturbations such as insulin resistance, hyperleptinemia, greater oxidative stress, low-grade chronic inflammation and alterations in a variety of circulating nutrients and hormones, all of which could potentially affect influenza immunity (2).

Herein, we demonstrate that high fat diet (HFD) induced obese mice are more susceptible to intranasal pH1N1 infection compared with lean, low fat diet (LFD) fed and lean, chow diet (CD) fed mice. For the first time, we also demonstrate that mice fed a purified LFD exhibit greater pH1N1 mortality compared with CD fed mice. We then explored the impact of obesity (independent of diet) on pH1N1 infection severity. A genetic model of obesity was used, wherein leptin signaling was disrupted in hypothalamic neurons, providing a robust model of obesity independent of HFD effects. Similar to diet-induced obesity, genetic-induced obesity resulted in greater pH1N1 mortality.

Analysis of infection responses revealed that diet and genetically-induced obese mice had relatively similar levels of lung immune cell infiltration, lung pathology, inflammatory cytokines, and virus titers despite a striking difference in mortality compared with lean control mice. However, both models of obesity exhibited greater lung airway damage during pH1N1 infection compared with lean controls. Analysis of immune cells resident in the bronchoalveolar compartment revealed that obese mice had fewer macrophages but similar numbers of neutrophils and NK cells. Further, obese mice had fewer activated regulatory T cells in the lung airways during infection. Of interest, we have previously demonstrated that Tregs isolated from obese mice exhibit impaired suppressive function (14).

We next addressed the immunomodulatory role of leptin during the context of pH1N1 infection in obese mice. Obesity is characterized by a state of hyperleptinemia, and it has previously been demonstrated that leptin antibody treatment during pH1N1 infection limits infection mortality in obese mice (82). Further, leptin is a critical regulator of effector and regulatory T cell responses (220). In our study, both diet and genetic models of obesity exhibited hyperleptinemia prior to and during the pH1N1 infection. We also detected a greater concentration of leptin in the lung airways of obese mice during pH1N1 infection. We then investigated if disruption of leptin signaling in T cells ($LepR^{T-/-}$) ameliorates infection severity in obese mice. $LepR^{T-/-}$ and $LepR^{Tfl/fl}$ mice (fully floxed, littermate control mice) were maintained on a high fat diet or standard chow diet for approximately 15 wks, with no differences in weight gain between $LepR^{T-/-}$ and $LepR^{Tfl/fl}$ mice. Subsequently, mice were infected with pH1N1, and as expected obese $LepR^{Tfl/fl}$ mice exhibited greater mortality than lean $LepR^{Tfl/fl}$ mice. However, there were no differences in mortality between obese $LepR^{Tfl/fl}$ and obese $LepR^{T-/-}$ mice. Therefore, pH1N1 mortality is not likely mediated by leptin signaling in T cells.

Materials and methods

Mice and diets

Diet-induced obesity was achieved by maintaining weanling, male C57BL6/J mice (obtained from The Jackson Laboratory, Bar Harbor, ME) on a HFD (60% kcal fat, Research Diets D12492, New Brunswick, NJ), and lean mice were maintained on a LFD (10% kcal fat, 35% kcal sucrose,

Research Diets D12450B) or a standard CD (14.02% kcal fat) for approximately 15 weeks. Genetically-induced obesity was achieved by crossing fully floxed leptin receptor mice on a C57BL6/J background (generously provided by Alyssa Hasty) with C57BL/6J-Tg(Nkx2-1-cre)2Sand/J mice purchased from the Jackson Laboratory. Fully floxed mice expressing the Cre transgene under control of the Nk2.1 promoter, lack leptin receptor signaling in hypothalamic neurons ($LepR^{H-/-}$) and become obese due to hyperphagia (221). Additionally, $LepR^{H-/-}$ mice do not breed properly; therefore $LepR^{H+/-}$ and $LepR^{Hfl/fl}$ (fully floxed leptin receptor) mice were used for breeding (221).

Disruption of leptin signaling in T cells was achieved by crossing fully floxed leptin receptor mice with B6.Cg-Tg(Lck-cre)548Jxm/J (expressing Cre under control of the Lymphocyte-specific protein tyrosine kinase, Lck, promoter) mice purchased from the Jackson Laboratory. For obesity studies, mice lacking leptin receptor signaling in T cells ($LepR^{T-/-}$) and littermate control fully floxed mice ($LepR^{Tfl/fl}$) were maintained on a high fat diet (60% kcal fat, Research Diets D12492) or a standard chow diet for 15-17 wks.

Hypothalamic and T cell leptin receptor conditional knockout mice were genotyped as previously described (221). Mice were housed in isolation cubicles at UNC, which is fully

accredited by the American Association for Accreditation of Laboratory Animal Care. All procedures involving the use of mice were fully approved by the UNC Institutional Animal Care and Use Committee.

Influenza virus infection and viral titers

Influenza A/Cal/04/09 (BEI Resources, Bethesda, MD) was propagated in embryonated hen's eggs and titered via a modified $TCID_{50}$ using hemagglutination as an endpoint as previously described (2,78). Mice were lightly anesthetized via isoflurane inhalation and were infected intranasally with $5.8x10^2$ $TCID_{50}$ or $1.3x10^3$ $TCID_{50}$ as described in figure legends. For influenza viral titers of infected mice, BALF was titered via a modified $TCID_{50}$ in replicates of four.

Serum and BALF measurements

BALF was obtained as previously as previously described (14). Serum and BALF leptin were measured with use of an ELISA kit per manufacturer's instructions (Invitrogen, Carlsbad, CA). ELISA kits were used to measure serum TAG (Pointe Scientific, Canton, MI) and adiponectin (Abcam, Cambridge, UK). Further, BALF albumin was measured with the Mouse Albumin ELISA Kit (Genway Biotech, Inc., San Diego, CA). Total protein in BALF was measured via standard BCA assay (BCA kit, Sigma Aldrich, St Louis, MO). BALF cytokines (IL-4, IFNγ, MCP-1, RANTES, KC, IL-17A, IL-10 and TNFα) were measured via a BioRad Bio-Plex assay per manufacturer's instructions (Hercules, CA).

Lung Histopathology

The left lobe of the lung was inflated and fixed with 10% neutral buffered formalin. Fixed lung was embedded in paraffin and processed for H&E staining by the UNC Animal Histopathology Core Facility. Lung pathology was blindly scored from 1-4 based on varying degree of immune cell infiltration and inflammation as described previously (78).

Flow Cytometry

Lungs, spleen, mLN and BAL cells were stained for flow cytometry as previously described. For staining of BAL cells from uninfected mice, samples were pooled from 2 individual mice to obtain a sufficient number of cells. The following antibodies were used: CD4 (FITC, PE-Cy7), CD103 (PE), Foxp3 (APC), Ly6G (FITC), NK1.1 (PE-Cy7) and F4/80 (APC) from EBioscience (San Diego, CA) and CD8 (PerCP) and CD3 (APC-Cy7) from BioLegend (San Diego, CA) and CD25 (FITC) from BD Biosciences (Sam Jose, CA). For intracellular staining, all cells were fixed and permeabilized using the Foxp3 staining buffer kit (Ebioscience). All samples were run on a CyAn ADP Analyzer flow cytometer (Beckman Coulter, Inc., Fullerton, CA) and analyzed with FlowJo software (Treestar, Ashland, OR).

Statistical analysis

For all statistical analyses, JMP Statistical Software (SAS Institute, Cary, NC) was used. For parametric data, statistical significance was evaluated using a two-way ANOVA or a two-tailed unpaired Student *t* test. Nonparametric data was evaluated using the Wilcoxon signed rank test or Kruskal Wallis test. Mean values were considered statistically significant at $p \leq 0.05$. The log-rank test was used to compare percent survival.

Results

High fat and low fat diet fed mice are more susceptible to pH1N1 infection compared with chow fed mice

In studying diet-induced obesity in mice, careful consideration of the low fat control diet of lean mice is essential to limiting introduction of confounding factors. In diet-induced obesity models, a standard control for a HFD is a 10% kcal derived from fat, purified LFD, matched in every aspect except fat and carbohydrate content. However, standard CD are derived from unpurified plant constituents, often of variable types and quantities, resulting in the presence of dietary fiber, phytoestrogens and varying levels of micronutrients compared with the experimental high fat diet (66,69). However, purified LFD (69) or high sucrose diets (70) have been shown to induce metabolic disturbances and cause mild glucose intolerance. Therefore, in this study we used two dietary controls for lean mice, both the 10% kcal fat LFD and a standard CD.

Weanling, C57BL6/J mice were maintained on a HFD (60% kcal fat), a LFD (10% kcal fat) or a standard CD (14.3% kcal fat) for 15 wks. As expected, mice fed a HFD gain significantly more weight and become obese compared with LFD and CD fed mice (Figure 4.1A). Although LFD and CD mice exhibited relatively similar levels of weight gain in comparison with obese mice, LFD mice weighed significantly more than CD mice after 8 wks on the diet ($p<0.005$). Obesity induces a state of insulin resistance, resulting in hyperglycemia (1). Obese mice had elevated fasting blood glucose levels compared with LFD and CD mice, consistent with glucose intolerance (Figure 4.1B). Further, non-fasted serum triacylglycerol was elevated in obese mice compared with LFD mice (Figure 4.1C), and adiponectin concentration was lower in obese mice compared with CD mice (Figure 4.1D). Leptin is an anorexigenic and

immunomodulatory hormone primarily produced from adipocytes, and as adiposity increases, circulating leptin levels also increase. The serum leptin level of obese mice reached nearly 80ng/mL, LFD mice had an intermediate leptin concentration of 50ng/ml and CD mice had the lowest concentration of approximately 20ng/mL (Figure 4.1E). In summary, HFD mice exhibited prototypical characteristics of obesity, while LFD mice exhibited a slightly intermediate phenotype compared with HFD and CD mice.

Following the 15 wk dietary exposure, mice were infected with 5.8×10^2 $TCID_{50}$ of the 2009 pandemic strain, influenza A/Cal/07/09 (H1N1, pH1N1). Strikingly, while no CD mice succumbed to the pH1N1 infection, 40% of LFD mice and more than 80% of obese mice died by 10 dpi (Figure 4.1F). Obese mice exhibited a significantly higher mortality rate compared with both LFD and CD mice. Although it has been shown that obese mice are more susceptible to pH1N1 (67), it has never been demonstrated that LFD fed mice are also more likely to die from influenza infection compared with CD mice. Analysis of weight loss demonstrated that CD mice recover faster from the infection compared with obese and LFD mice (Figure 4.1G). Because obese mice weigh more compared with the lean groups, we also included total weight loss in our analysis, which revealed that obese mice lost greater absolute weight compared with both lean groups (Figure 4.1H).

Given that all CD mice survived the infection, we extended our analysis to determine if the discrepancy in pH1N1 mortality is maintained with a greater pH1N1 dose. All three dietary groups were infected with 1.3×10^3 $TCID_{50}$ (a 3.5 fold increase in dosage), and by 7 dpi 100% of obese mice died (Figure 4.1I). Further, 100% of LFD mice died by 8 dpi, and 80% of CD mice died by 9 dpi. Despite the enhanced death in all three groups compared with the previous dose, the mortality differences between the dietary groups were relatively maintained in that LFD and

obese mice were more susceptible compared with CD mice ($p<0.005$) and obese mice were nearly more susceptible compared with LFD mice ($p=0.08$). Of interest, obese mice displayed a significantly lower percent weight loss over the course of the more severe infection compared with LFD and CD mice (Figure 4.1J). However, this is because obese mice weighed nearly 40% compared with the lean groups; there were no differences in the total amount of weight lost (Figure 4.1K)

Obesity, independent of diet, increases pH1N1 susceptibility

It is apparent that obese mice exhibit greater pH1N1 infection severity. Unexpectedly, LFD mice also display greater mortality compared with CD mice, although not to the same extent as obese mice. This brings into question what the proper dietary control group is for infection comparisons, and if the differences in pH1N1 severity are mediated by obesity or diet (or perhaps both). Although it is intriguing that LFD mice exhibit greater pH1N1 mortality compared with CD mice, the focus of this study is to decipher mechanisms by which obesity enhances pH1N1 severity. One critical question that remains to be addressed thus far is whether obesity is responsible for the observed infection outcomes, or if the discrepancy in infection responses is simply due to modifying the diet of the mice.

To address the immunomodulatory impact of obesity on pH1N1 infection responses, independent of dietary changes, we utilized a genetic model of obesity in which excess adiposity is driven primarily by hyperphagia (all mice are fed a CD). It has previously been shown that *ob/ob* mice, a robust model of genetic obesity, are more susceptible to pH1N1 infection compared with wild type mice. However, utilization of the *ob/ob* mouse model has several limitations due to the global deficiency of leptin signaling. Leptin is critical for proper

physiology and immunity, and leptin deficiency can negatively impact host defenses, thus, confounding the effects of a obesity (14). Therefore, we used a tissue-specific model, previously characterized by Ring et al., in which disruption of leptin signaling is limited to hypothalamic neurons (the primary site of leptin-mediated appetite control) (221) to further address the impact of obesity on pH1N1 immunity.

Male and female $LepR^{H-/-}$ mice, lacking functional leptin receptors in hypothalamic neurons, rapidly gain excess body weight compared to lean $LepR^{Hfl/fl}$ and $LepR^{H+/-}$ mice (Figure 4.2A/2B). At 13-16 wks of age, $LepR^{H-/-}$, $LepR^{H+/-}$, and $LepR^{Hfl/fl}$ mice were infected with 5.8 x 10^2 $TCID_{50}$ pH1N1 (the identical dose utilized in Figure 4.1F). Following the infection, obese male and female $LepR^{H-/-}$ mice were significantly more susceptible compared with lean $LepR^{H+/-}$ and $LepR^{Hfl/fl}$ mice (Figure 4.2C/2D). Obese male and female $LepR^{H-/-}$ displayed a strikingly lower percentage of body weight lost compared with lean mice Figure (4.2E/3F). However, this is due to the greater pre-infection weight in $LepR^{H-/-}$ because the $LepR^{H-/-}$ mice lost a greater amount of weight compared with lean groups (Figure 4.2G/H). There were no differences in mortality between male and female $LepR^{H-/-}$ mice; therefore, for further analyses, male and female mice were combined. Also, there was no statistically significant difference in mortality between diet-induced obese mice and genetically obese mice.

Diet-induced obesity does not modulate lung pH1N1 viral burden

To assess potential mechanisms for the discrepancies in pH1N1 mortality between dietary groups, we first measured the level of viral burden in the lung airways of the three dietary groups CD, LFD and HFD (from Figure 4.1). There were no differences in viral titers among the three groups at 4 or 8 dpi (Figure 4.3A). While some studies report greater viral titers in obese

mice (80), others have shown obesity does not impact viral burden (67,77). We then assessed the level of cellular infiltration and lung pathology during the pH1N1 infection. HFD, LFD and CD mice exhibited similar levels of total bronchoalveolar lavage (BAL) cell numbers (Figure 4.3B) and total lung cell numbers (Figure 4.3C). Cytokine and chemokine production in the lung airways of the three dietary groups was also measured (Table 4.1 and Figure 4.3D). Figure 4.3D is a heat map demonstrating that while global changes in cytokine concentration over the course of infection are evident, the level of changes among the dietary groups within each dpi was relatively minimal. Obese mice had elevated levels of keratinocyte chemoattractant (KC or CXCL1) compared with LFD and CD mice at 8 dpi (Table 4.1). TNFα and MCP-1 were greater at 4 dpi in HFD mice compared with LFD, and IL-17A was greater at 8dpi in HFD mice compared with LFD mice. Although IFNγ was elevated in obese mice at 8 dpi, it was not significantly different from the lean groups. There were no differences in the level of IL-10, RANTES between the dietary groups, and IL-4 was below the level of detection. Taken together, obese mice exhibited minor differences in lung inflammatory responses, despite striking differences in infection mortality.

Diet-induced obesity enhances lung airway damage during pH1N1 infection

Total protein level in BALF is a classical measurement of damage to the alveolar-endothelial barrier. At 4 dpi, HFD mice exhibited a greater fold increase in BALF protein levels compared with LFD and CD mice (Figure 4.3E). Further, at 8 dpi, HFD mice displayed a greater fold increase in BALF protein compared with CD mice. Additionally, we measured BALF albumin concentration. Obese mice exhibited a greater fold increase in BALF albumin compared

with LFD and CD mice at 4 dpi (Figure 4.3F). Therefore, obesity enhances lung airway damage during pH1N1 infection.

We next addressed the impact of obesity on lung histopathology during pH1N1 infection. As expected, H&E stained lungs revealed that pH1N1 infection caused distinct pathological changes in the bronchioles of all three dietary groups (Figure 4.4A). At 4 dpi, partial bronchiole denuding and perivascular cuffing occurred in all three dietary groups compared with uninfected lungs. Additionally, the width of the bronchiole walls also increased compared with uninfected mice. By 8 dpi, the level of perivascular cuffing, bronchial denuding and immune cell infiltration increased in all three dietary groups compared with the day 4 time point. By 8 dpi, the total level of infiltration increased in all three groups, and LFD and HFD tended to have a greater level of diffuse infiltration in alveoli, but with minimal thickening of alveolar walls. Further, CD fed and LFD mice exhibited greater thickening of the bronchus wall at 8 dpi. Of interest, the bronchus wall in HFD mice appeared much thinner at 8 dpi compared with infected CD and LFD mice and with uninfected lean controls. Although we observed several interesting pathological features among the three dietary groups during pH1N1 infection, histopathology scores of total lung infiltration and inflammation revealed there were no significant differences among the three dietary groups (data not shown), consistent with no differences in total lung cell number.

Obese mice have fewer macrophages in the lung airways compared with lean mice.

In order to gain a better understanding for the greater lung damage in obese mice, we assessed the distribution of relevant innate immune cells in the lung airways of pH1N1 infected CD and HFD mice. We decided to focus on CD and HFD given the striking differences in mortality. Figure 4.5A is a representative flow cytometry gating scheme demonstrating how

macrophages, neutrophils and natural killer (NK) cells were identified. Figure 4.5B represents the percentage of F4/80$^+$ macrophages detected in the lung airways of CD and HFD mice at 4 and 8 dpi, and Figure 4.5C is the total number of macrophages. Unexpectedly, obese mice had significantly fewer BAL macrophages at 4 dpi. Figure 4.5D and E demonstrate that obesity did not alter BAL neutrophil percentage or number during the infection. Lastly, Figures 4.5F/G demonstrate that obese mice had a lower percentage of NK cells at 4 dpi, but not a statistically different number of NK cells at 4 dpi.

Obese mice have fewer Treg cells in the lung airways during pH1N1 infection.

We next assessed T cell responses in the lungs of CD and HFD mice. There were no differences in CD8$^+$ T cell numbers in the lung airways, but obese mice had fewer CD4$^+$ T cells at 8 dpi (Figures 4.6A/6B). Although CD8$^+$ T cells are classically considered to be primary mediators of controlling viral replication during influenza infection, effector CD4$^+$ T cells also facilitate viral clearance. However, we did not detect differences in viral replication between CD and HFD fed mice (Figure 4.3A).

Recently, CD4$^+$Foxp3$^+$ Tregs have been shown to modulate respiratory inflammatory responses to RSV and influenza virus infection in mice (205,216,222). Because we detected fewer CD4$^+$ T cells in obese mice, we also suspected fewer BAL Treg cells as well, perhaps contributing to heightened lung airway damage in obese mice. Figure 4.6C is a representative gating scheme for identification of BAL Tregs in CD and HFD mice. Consistent with fewer CD4$^+$ T cells at 8 dpi, obese mice also had less Treg cells at 8 dpi (Figure 4.6D). Additionally, we also assessed the level of Treg activation and found that obese mice had fewer CD103$^+$ Tregs as well (Figure 4.6E). Given the discrepancy in Treg number in the lung airways, we also

measured Treg distribution in the lung (Figure 4.6F/6G) and mediastinal lymph nodes (Figure 4.6H/I) of lean and obese mice during the course of the pH1N1 infection. We did not detect any differences in the percentage or number of Tregs or activated Tregs in these tissues. Due to the striking differences in the number of activated Tregs in the lung airways of HFD mice at 8 dpi, we also measured Treg distribution in $LepR^{H-/-}$ and $LepR^{Hfl/fl}$ mice at 8 dpi as well. Similarly, obese $LepR^{H-/-}$ mice also had fewer Tregs and a lower number of activated Tregs in the lung airways at 8 dpi (Figure 4.6J/K).

HFD-induced obese mice have elevated BALF leptin levels during pH1N1 infection

Leptin regulates the function of a number of immune cells, and it is well-established that a deficiency of leptin signaling impairs immune defenses (2). However, obese mice have greater levels of circulating leptin, and it is currently unclear if and how this greater concentration of leptin may alter immune defenses. It has recently been shown that leptin monoclonal antibody treatment during pH1N1 infection limits mortality in obese mice (82). Therefore, we measured circulating leptin levels during pH1N1 infection in HFD and CD mice. As expected, serum leptin levels were elevated prior to infection and at 8 dpi in HFD mice compared with CD mice (Figure 4.7A). Although leptin is elevated in circulation in obese mice, to our knowledge leptin levels in BALF during infection have not been measured. Of interest, obese mice had a greater concentration of leptin in the lung airways at 8 dpi infection compared with lean controls (Figure 4.7B). Interestingly, BALF leptin did not differ between uninfected lean and obese mice. Therefore, the elevated BALF leptin is dependent on the infection. The source of BALF leptin is unclear, as it could be derived from circulating leptin leaking into the BALF due to damaged epithelial barriers. However, there was an increase in BALF total protein from 0 to 8 dpi in CD

fed mice (Figure 4.3E), but we did not detect an increase in BALF leptin in CD fed mice from 0 to 8 dpi, suggesting that BALF leptin is not likely derived from impaired integrity of the lung epithelium. Additionally, serum leptin decreased in obese mice during the infection (likely due to reduced food intake). At this point the source of BALF leptin is unclear as other cell types in addition to adipocytes have been shown to secrete leptin, such as T cells (198). In summary, both serum and BALF leptin are elevated during a pH1N1 infection in diet-induced obese mice compared with lean, CD mice.

Disruption of leptin signaling in T cells does not prevent pH1N1 mortality in diet-induced obese mice

Leptin potentiates effector T cell responses and negatively regulates Treg proliferation (198). Therefore, perhaps excess leptin signaling is responsible for the reduced Treg number detected in the lung airways of obese mice. To investigate the impact of elevated leptin levels on T cell responses in obese mice during the context of influenza virus infection, we crossed leptin receptor floxed mice with LckCre mice, resulting in conditional disruption of leptin signaling in T cells. Weanling, male, littermate control $LepR^{Tfl/fl}$ and $LepR^{T-/-}$ mice were maintained on a HFD (60%) or CD for 15-17 wks. Figure 4.7C demonstrates that $LepR^{Tfl/fl}$ and $LepR^{T-/-}$ mice fed a HFD gained significantly more weight compared with CD mice, and there were no differences in weight gain between $LepR^{Tfl/fl}$ and $LepR^{T-/-}$ mice. Further, there were no differences in fasting glucose levels between obese $LepR^{Tfl/fl}$ or obese $LepR^{T-/-}$ mice. CD and HFD fed $LepR^{Tfl/fl}$ and $LepR^{T-/-}$ mice were infected with 5.8×10^2 $TCID_{50}$ pH1N1, and as expected HFD $LepR^{Tfl/fl}$ mice were more susceptible to pH1N1 mortality compared with CD $LepR^{Tfl/fl}$ mice (Figure 4.7E). Additionally, there were no differences in weight loss during the infection between dietary

groups or genotypes (Figure 4.7F). Therefore, leptin signaling in T cells does not likely mediate greater pH1N1 mortality observed in obese mice.

Discussion

In this study, we first demonstrated that both HFD fed obese and LFD fed lean mice are more susceptible to pH1N1 infection compared with lean CD mice. Currently, three studies have demonstrated that diet-induced obese mice are more susceptible to a primary pH1N1 infection (67,81,82). Two of these studies used a CD for the lean mouse group and a 45% or 60% kcal HFD for obese mice (67,82), and one study used a 60% kcal HFD compared with a nutrient matched, purified, 10% kcal low fat diet (81). In dietary studies, utilization of the proper control diet is critical for limiting introduction of confounding variables (69). Chow diets contain a variety of plant constituents that are not found in purified rodent diets, such as fiber and phytoestrogens (66,69). Dietary fiber and phytoestrogens can have profound metabolic and physiological effects, thereby complicating experimental results (66,69). Further, chow diets can have varying levels of ingredients from batch to batch, limiting experimental reproducibility. For these reasons, it is generally agreed that the most appropriate control for a high fat diet is a nutrient-matched, purified LFD differing only in carbohydrate and fat content (66,69). In this study, lean mice were fed either a CD or a LFD to compare to pH1N1 infection responses of obese mice. However, for the first time, we show that LFD fed mice are more susceptible than CD. This calls into question the most appropriate control diet for mouse models investigating the impact of obesity on immunity. Is the best control diet one that most closely matches the high fat diet, or one that results in the most "protective or effective" immune response? We propose that because CD mice were least susceptible to pH1N1 infection, they are the best control for

comparing infection responses to obese mice in this model. Further, although the LFD is matched in every aspect except for fat and carbohydrate content to the HFD, the fact that the levels of these two macronutrients are not identical may confound results. For example, perhaps elevated levels of sucrose in the LFD impact immune responses. It is unclear why LFD mice were more susceptible to pH1N1 infection compared with CD mice. LFD mice did have elevated levels of leptin compared with CD, so perhaps this contributed to greater mortality. Given these complications of utilizing a diet model of obesity, we also included a genetic model of obesity whereby the effects of diet could be eliminated.

Ob/ob mice are a classic model of genetically-induced obesity in which lack of leptin satiety cues result in hyperphagia and obesity (65,223). O'brien et al. has previously demonstrated that *ob/ob* obese mice are more susceptible to pH1N1 mortality (67). Although this is informative and helps to address the complications of dietary models discussed above, a global deficiency of leptin signaling can cause physiologic complications that are not necessarily characteristic of obesity (65). Therefore, we utilized a genetic model of obesity in which leptin signaling is only disrupted in hypothalamic neurons. Although this model limits the introduction of confounding effects caused by a global disruption of leptin signaling, there is some evidence of Nkx2.1 expression in the lung, esophagus and during development (221).

At this point, the two most well-defined mechanisms contributing to greater pH1N1 severity in obese mice during a primary infection appear to be impaired lung wound healing (67) and hyperleptinemia (80). In addressing the consequences of hyperleptinemia on pH1N1 outcomes in obese mice, we first set out to investigate if leptin was also elevated in the lung airways of obese mice. For the first time, we report that obese mice have greater leptin concentration in the lung airways during pH1N1 infection. The source of this greater BALF

leptin is unclear. It is unlikely that it is completely derived from serum leptin leaking into the lung for two reasons: 1) There is already leptin in the BALF prior to the infection. 2) BALF leptin decreases in lean mice during infection, despite greater lung airway damage (and without changes in circulating leptin level). Perhaps the elevated leptin in the BALF of obese mice is derived from infiltrating immune cells.

Leptin can enhance effector T cell inflammation and proliferation, and conversely is a potent inhibitor of Treg proliferation (198). Given that we detected greater lung damage in obese mice and fewer Tregs in the lung airways, we tested if disruption of leptin signaling in T cells ameliorates pH1N1 severity in obese mice. However, obese $LepR^{T-/-}$ and $LepR^{Tfl/fl}$ mice did not exhibit differences in pH1N1 susceptibility. The lack of differences in infection severity is likely explained by the fact that greater pH1N1 mortality in obese mice is driven by an array of factors and not simply leptin signaling in T cells. Although we did not detect differences in mortality between obese $LepR^{T-/-}$ and $LepR^{Tfl/fl}$ mice, further investigation of this model could be useful in eliminating plausible mechanisms. For example, if Treg number is enhanced in obese $LepR^{T-/-}$ compared with obese $LepR^{Tfl/fl}$ mice, this would indicate that the reduced Treg number is likely not responsible for the differences in mortality between lean and obese mice. We detected fewer Tregs in both diet and genetic models of obesity, and we hypothesize this is due to impaired proliferation due to excess leptin. Further, investigation of other infection parameters such as lung damage will reveal interesting information regarding the role of T cell leptin signaling in obesity-induced pH1N1 severity.

We detected fewer BAL macrophages in the lung airways at 4 dpi in obese mice compared with CD mice, but there were no differences in neutrophils or NK cell number. This is surprising given that obesity enhances inflammatory macrophage polarization and the greater

lung damage observed in pH1N1 infected obese mice. However, we only assessed macrophage number by F4/80 staining. Utilization of other macrophage markers and macrophage subset (alveolar macrophage, M1, M2 etc.) markers would reveal information regarding the actual polarization/inflammatory status of these BAL macrophages in lean and obese mice.

Obese mice had greater lung airway damage without major differences in lung infiltration or inflammation. Further, we did not detect differences in lung viral titers between lean and obese mice. It is unclear if the greater lung damage observed in obese mice is responsible for the enhanced mortality. Because we did not detect robust differences in lung inflammation or histopathology, this would suggest that greater damage to the lung epithelium may only be partially responsible for greater mortality in obese mice. Obesity also results in fatty liver and can impact heart and kidneys (224-226). Therefore, perhaps greater pH1N1 mortality is caused by synergistic effects of greater lung damage and other systemic consequences of obesity during influenza infection.

Tables and Figures

Table 4.1 BALF cytokine concentrations during a primary pH1N1 infection

Cytokine/Chemokine	Diet Group	Day 0 (pg/mL)	Day 4 (pg/mL)	Day 8 (pg/mL)
IFNγ	CD	1.5 ± 0.4	13.8 ± 4.7	130.1 ± 29.7
	LFD	1.9 ± 0.4	5.6 ± 0.8	96.7 ± 25.7
	HFD	1.6 ± 0.3	7.4 ± 0.9	478.6 ± 210.2
KC	CD	3.4 ± 0.6	200.0 ± 19.2	115.8 ± 17.1
	LFD	3.6 ± 1.0	216.2 ± 19.6	95.6 ±15.3
	HFD	3.0 ± 0.4	251.2 ± 15.3	237.7 ± 47.2*****$^{\#}$
IL-10	CD	6.9 ± 1.6	4.0 ± 1.0	47.7 ± 12.7
	LFD	5.9 ± 1.1	4.0 ± 0.9	38.1 ± 6.4
	HFD	3.8 ± 1.1	4.1 ± 0.9	71.4 ± 25.2
IL-17A	CD	2.2 ± 0.4	2.7 ± 0.3	5.1 ± 0.8
	LFD	2.2 ± 0.4	1.5 ± 0.1	4.1 ± 0.9
	HFD	1.9 ± 0.2	2.1 ± 0.2	7.8 ± 1.9
TNFα	CD	380.0 ± 54.6	521.3 ± 21.5	422.1 ± 24.4
	LFD	469.2 ± 27.3	510.1 ± 9.5	248.9 ± 29.1^
	HFD	438.2 ± 12.4	466.0 ± 21.7	435.3 ± 22.0$^{\#}$
MCP-1	CD	27.8 ± 7.5	2972.0 ± 579.6	4006.7 ± 1782.9
	LFD	24.9 ± 5.1	2559.6 ± 455.1	2682.5 ± 375.8
	HFD	14.3 ± 4.7	4588.9 ± 697.1$^{\#}$	8271.5 ± 2890.0
RANTES	CD	2.1 ± 0.5	103.2 ± 9.7	106.2 ± 20.9
	LFD	3.3 ± 0.6	89.6 ± 12.0	100.4 ± 15.8
	HFD	3.3 ± 0.3	81.5 ± 11.3	100.0 ± 12.8

Table 4.1: Values represent mean concentration ± SEM (n=5-8), *p<0.05 HFD compared CD within same infection day, #p<0.05 HFD compared with LFD within same infection day, ^p<0.05 LFD compared with CD within same infection day. IL-4 was below the limit of detection.

Figure 4.1 Diet-induced obesity results in greater pH1N1 infection mortality in mice

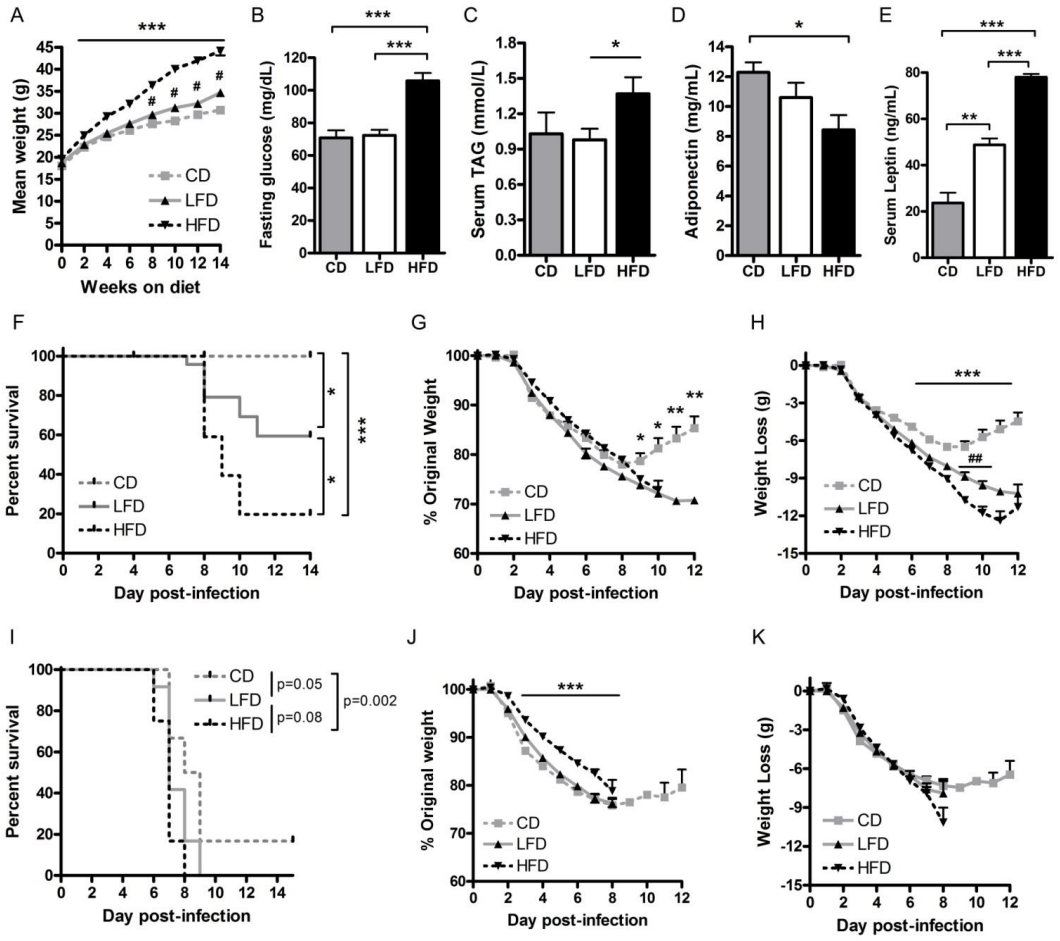

Figure 4.1: A, Weanling, male, C57BL6/J mice were randomly placed on a high fat (60% kcal fat), low fat (10% kcal fat) or chow diet for 14 wks (n>30). B, Mice were fasted overnight and blood glucose was measured (n=8). C-E, Non-fasted serum TAG (C), adiponectin (D) and leptin (E) were measured via ELISA (n=6-7). F, After 15 wks of dietary exposure, mice were infected intranasally with 5.8 x 10^2 $TCID_{50}$ pH1N1 and monitored for death (n≥21). G, Percent weight loss over the course of the pH1N1 (n≥21). H, Total weight loss during the infection (n≥21). I, After 14 wks of dietary exposure, mice were infected with 1.3 x 10^3 $TCID_{50}$ and death was monitored (n=12). J, Percent weight loss during the infection (n=12). K, Total weight loss during the infection (n=12). Each bar or data point represents mean ± SEM. *p<0.05, **p<0.005, ***p<0.0005. In Figure 1A, ***p<0.0005 comparing HFD with both LFD and CD mice, and #p<0.05 comparing CD and LFD mice. For Figures 1G, 1H, 1J, *p<0.05, **p<0.005, ***p<0.0005 comparing HFD mice with CD and LFD mice.

Figure 4.2 Genetically obese mice are more susceptible to pH1N1 mortality

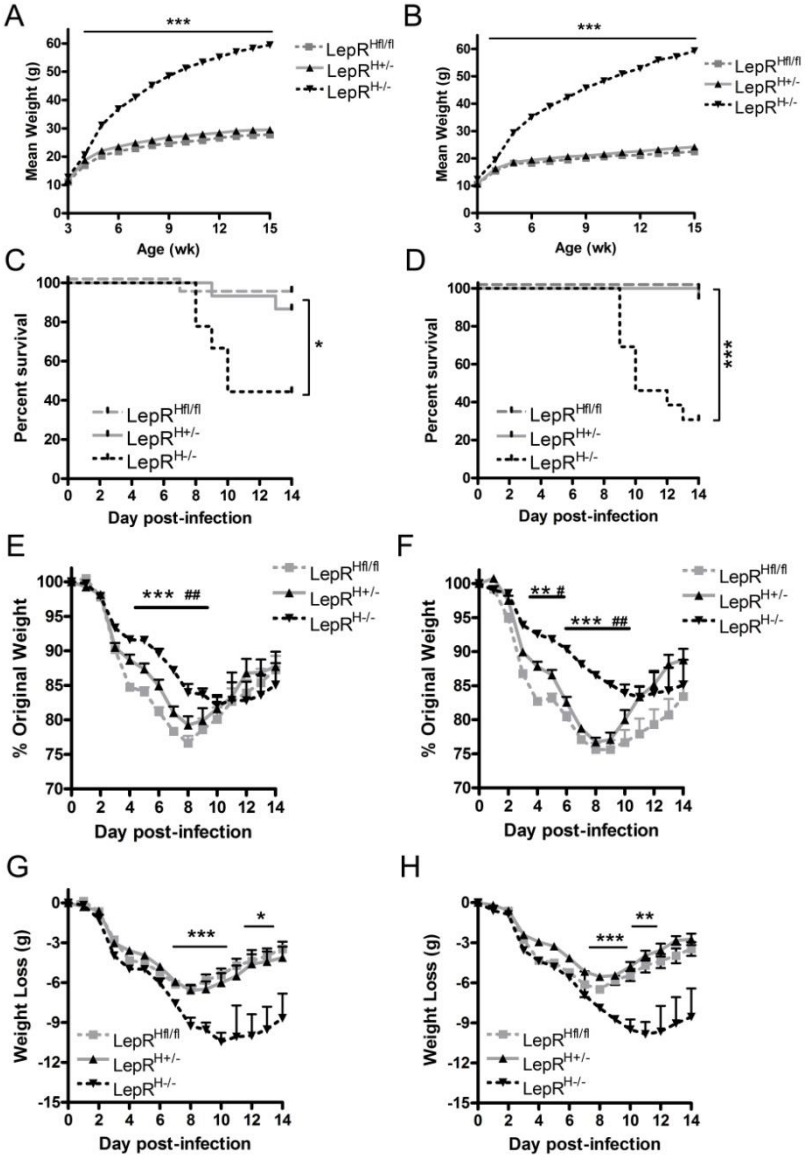

Figure 4.2: A&B, Weight gain of male (A) and female (B) mice lacking leptin receptor signaling in hypothalamic neurons $LepR^{H-/-}$, heterozygous mice $Lep^{H+/-}$ and fully floxed $LepR^{Hfl/fl}$ mice (n≥9). C&D, Mortality curves for male (C) and female (D) mice after infection with 5.8 x 10^2 $TCID_{50}$ pH1N1 at 13-17 wk of age (n≥9). E&F, Percent weight loss for male (E) and female (F) mice after pH1N1 infection (n≥9). G&H, Total weight loss for male (G) and female (H) mice after pH1N1 infection (n≥9). Each bar or data point represents mean ± SEM. *p<0.05, **p<0.005, ***p<0.0005. In Figures 1A-D, *p<0.05 or ***p<0.0005 comparing $LepR^{H-/-}$ with both $LepR^{H-/-}$ and $LepR^{H+/-}$ mice. For Figures 1 D-E, **p<0.05 or ***p<0.0005 comparing $LepR^{H-/-}$ with $LepR^{H-/-}$ mice and $^{\#}$p<0.05 or $^{\#\#}$p<0.005 comparing $LepR^{H-/-}$ with $LepR^{H+/-}$ mice. For Figure F&G, *p<0.05, ***p<0.0005 comparing $LepR^{H-/-}$ with both $LepR^{H-/-}$ and $LepR^{H+/-}$ mice.

Figure 4.3 Obese mice exhibit greater lung damage during pH1N1 infection

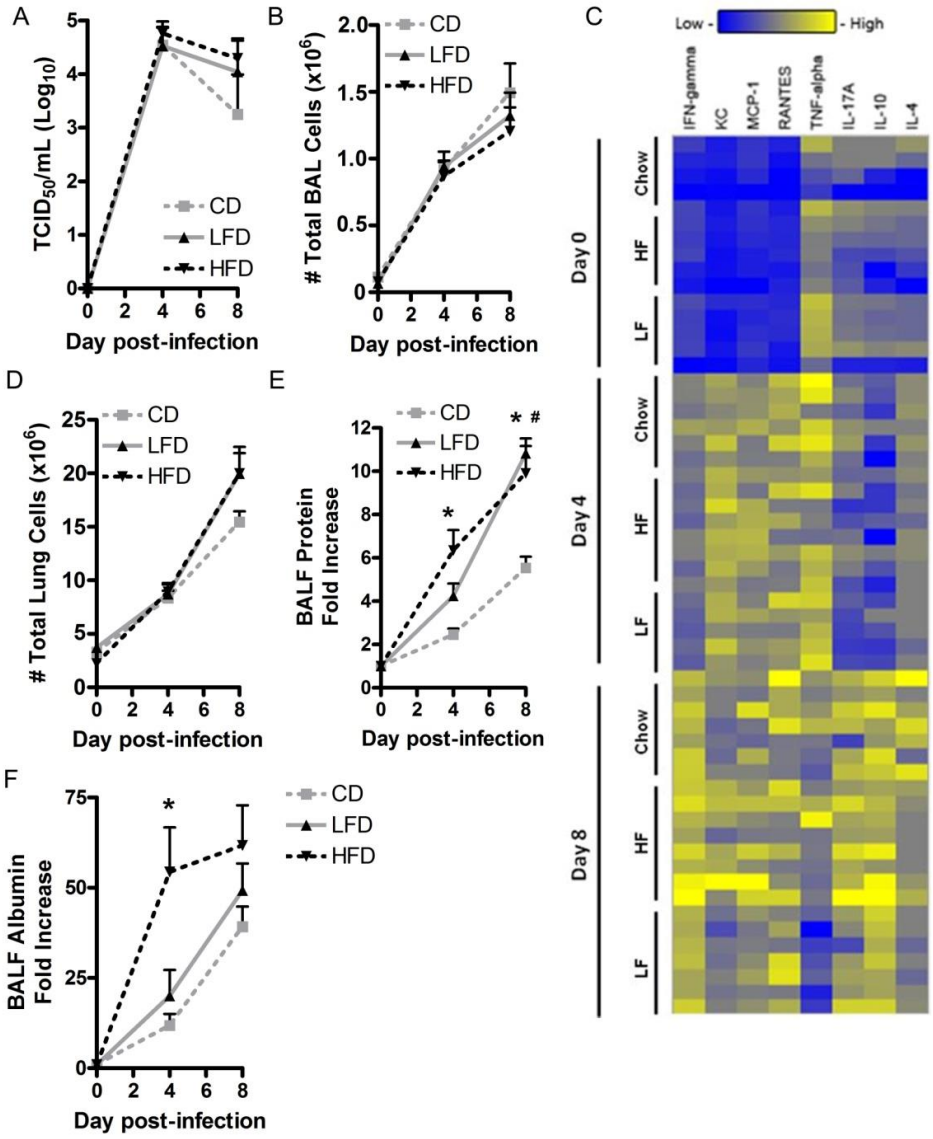

Figure 4.3: A, BALF viral titers during pH1N1 infection, (n=4 for uninfected mice and n=7-8 at 4 and 8 dpi). B, Total number of BAL cells (n≥8).C, Heat map demonstrating relative differences in fold increase of BALF cytokine concentration between CD, LFD and HFD mice determined from a multiplex assay (n=5-8). D, Total number of lung cells (n≥8). E, Fold increase of BALF protein during infection. Fold increase normalized to uninfected mice within each dietary group (n=6-10). F, Fold increase in BALF albumin. Fold increase normalized to uninfected mice within each dietary group (n=5-7). Each bar or data point represents mean ± SEM. In Figure 4.3E&F, *p<0.05 comparing HFD with LFD and CD mice at 4 dpi. In Figure 4.3E, at 8 dpi *p<0.05 comparing HFD with CD mice and $^{\#}$p<0.05 comparing LFD and CD mice.

Figure 4.4 Obese mice did not exhibit differences in lung pathology during pH1N1 infection

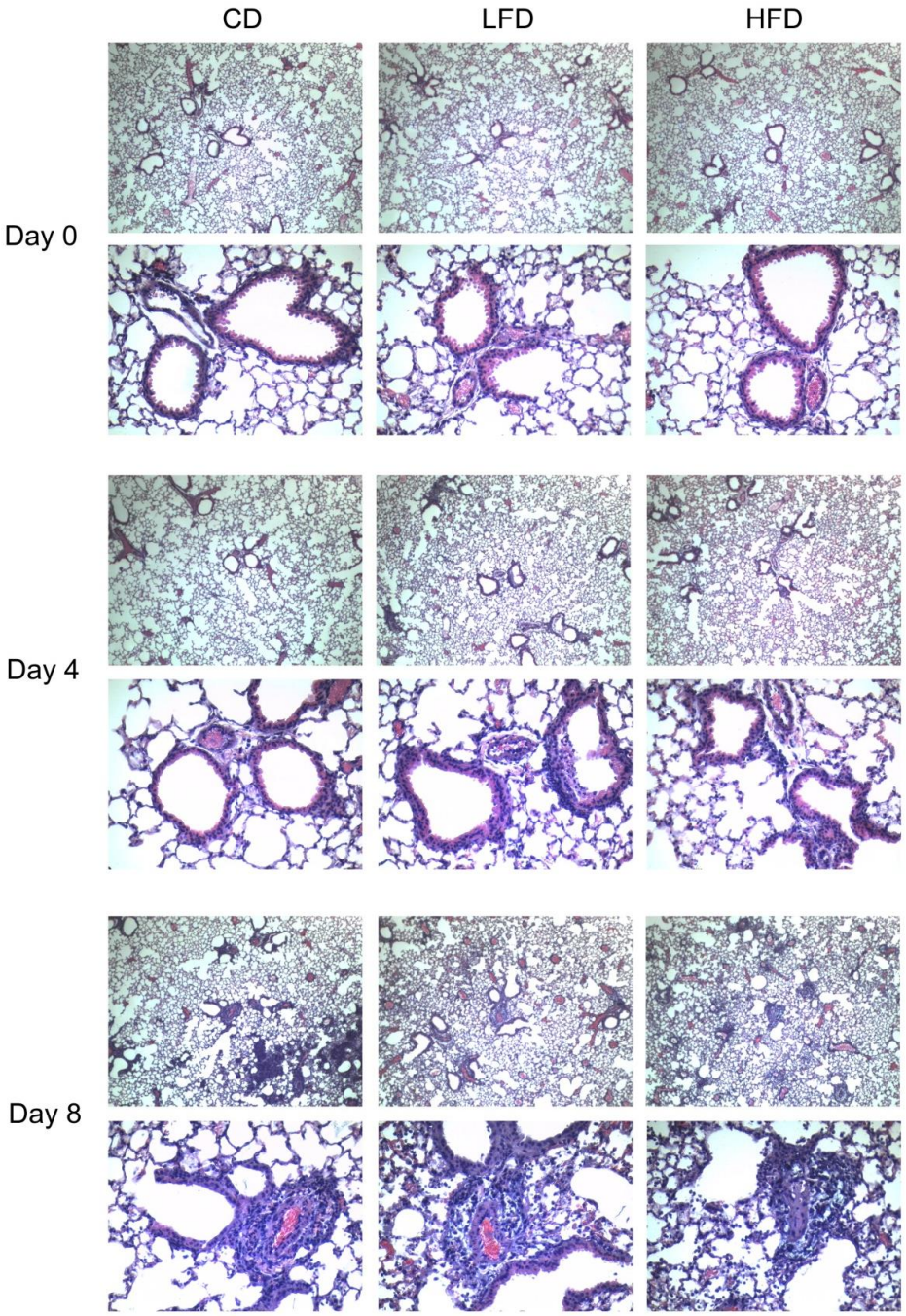

Figure 4.4: H&E stained lung pathology slides from CD, LFD and HFD mice. The top panel of histology slides for each dpi is 10x magnification and the bottom panel is 40x magnification of the same slide. n=6-8.

Figure 4.5 Obese mice have fewer BAL macrophage during pH1N1 infection

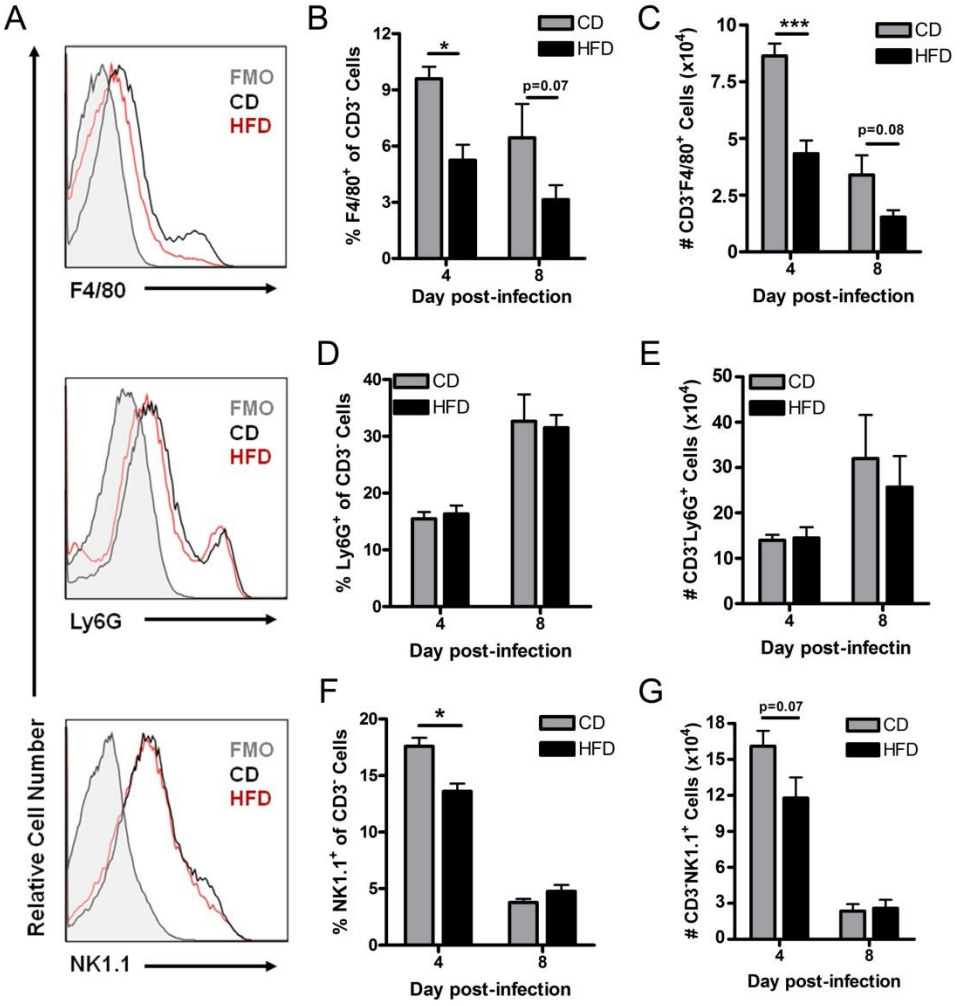

Figure 4.5: A, Representative flow cytometry gating scheme comparing CD and HFD mice at 4 dpi. Fluorescence minus one (FMO) staining controls were included for gating purposes. B, Percentage of $F4/80^+$ cells of total $CD3^-$ cells. C, Total number of $CD3^-F4/80^+$ cells (n=7-9). D, Percentage of $Ly6G^+$ cells of total $CD3^-$ cells. E, Total number of $CD3^-Ly6G^+$ cells (n=7-9). F, Percentage of $NK1.1^+$ cells of total $CD3^-$ cells. G, Total number of $CD3^-F4/80^+$ cells (n=7-9). Each bar or data point represents mean $\pm$ SEM. *p<0.05, ***p<0.0005.

Figure 4.6 Diet- and genetic-induced obese mice have fewer BAL Tregs at 8 dpi

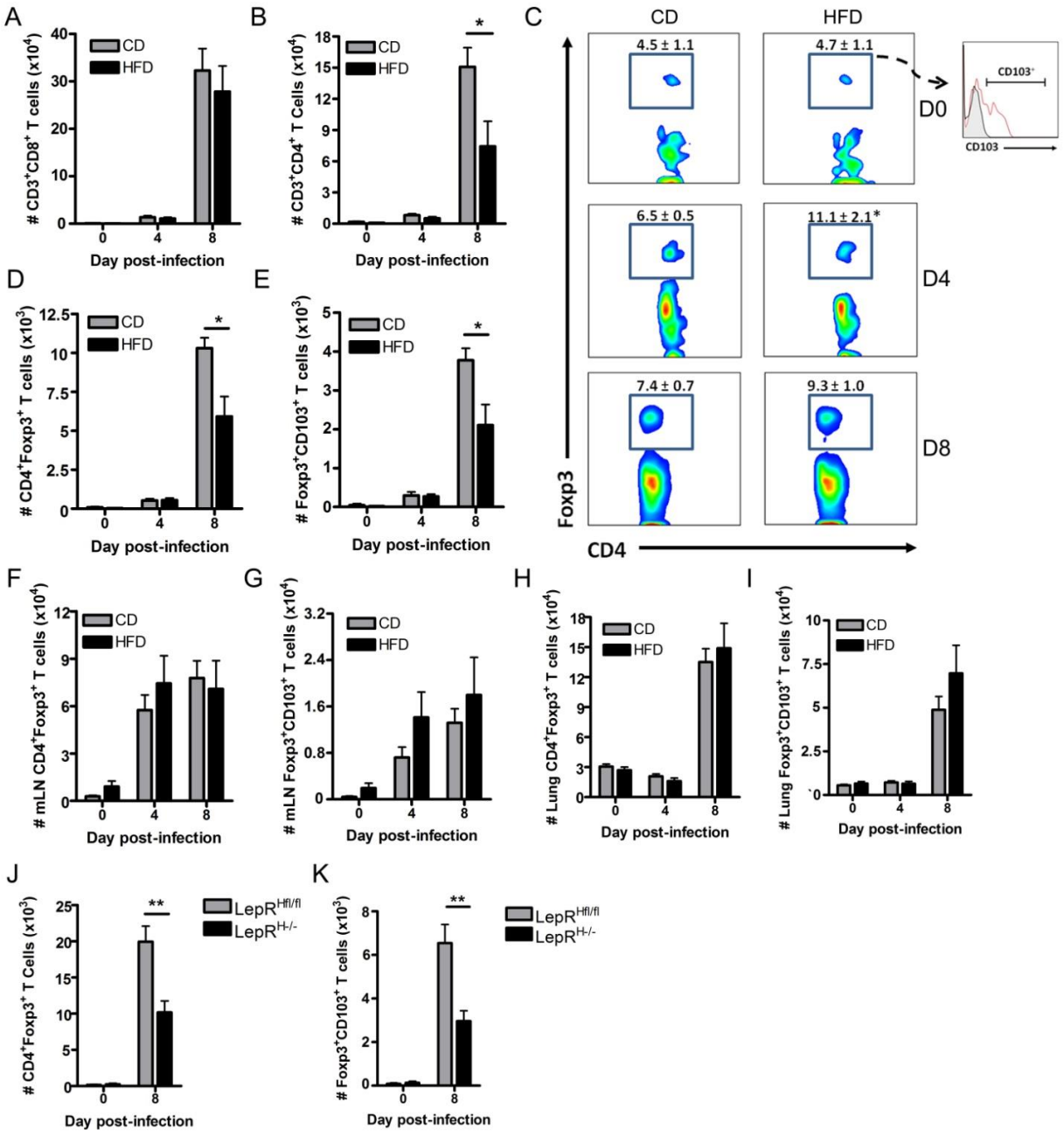

Figure 4.6: A, Total number of BAL $CD8^+$ T cells (n=3 at day 0 and n=7-9 at 4 and 8 dpi). B, Total number of BAL $CD4^+$ T cells (n=3 at day 0 and n=7-9 at 4 and 8 dpi). *p<0.05. C, Representative flow cytometry gating scheme of BAL Tregs including mean percentage and standard error. *p<0.05 comparing HFD and CD mice at 4 dpi (n=3 at day 0 and n=7-9 at 4 and 8 dpi). D&E, Total number of BAL Tregs (D) and activated Tregs (E) (n=3 at day 0 and n=7-9 at 4 and 8 dpi). *p<0.05. F&G, Total number of mLN Tregs (F) and activated mLN Tregs (G) (n=8-10). H&I, Total number of Lung Tregs (H) and activated lung Tregs (I) (n=8-10). J&K, Total number of BAL Tregs (J) and activated BAL Tregs (K) from $LepR^{Hfl/fl}$ and $LepR^{H-/-}$ mice (n=4-5 at 0 dpi and n=7-8 at 8 dpi. **p<0.05. Each bar represents mean ± SEM.

Figure 4.7 Leptin signaling in T cells does not mediate pH1N1 mortality in obese mice

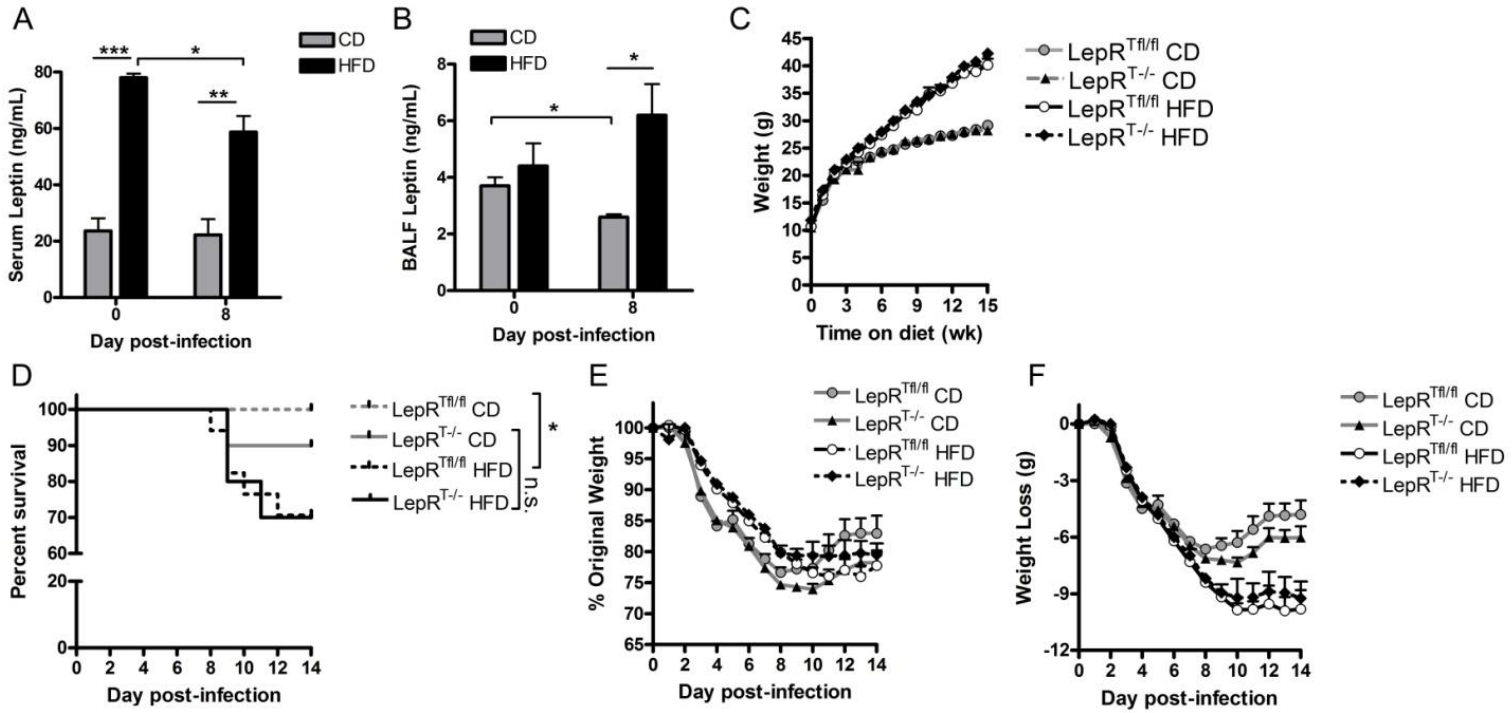

Figure 4.7: Serum leptin concentration in uninfected and at 8 dpi in CD and HFD mice (n=5-7). B, BALF leptin in uninfected and 8 dpi infected CD and HFD mice (n=4-6). $LepRT^{fl/fl}$ and $LepR^{T-/-}$ littermate controls were randomly placed on a HFD (60% kcal fat) or CD (14.02% kcal fat) for 15 weeks and weight gain was measured weekly (n≥9). D, After 15-17 wks of dietary exposure, mice were infected with 5.8 x 10^2 $TCID_{50}$ pH1N1 and percent survival was measured (n≥10). E&F, Percent weight loss (E) and total weight lost (F) during the pH1N1 infection (n≥6). There were no differences in % original body weight between genotypes or dietary groups. There were no differences in total weight lost between genotypes within each dietary group. Each bar represents mean ± SEM. *p<0.05, ***p<0.0005.

CHAPTER V: H NMR-BASED PROFILING REVEALS DIFFERENTIAL IMMUNE-METABOLIC NETWORKS DURING INFLUENZA VIRUS INFECTION IN OBESE MICE[2]

Introduction

Obesity has reached epidemic proportions (8). Global approximations report that two out of every three individuals are clinically overweight (BMI≥25-29.9) or obese (BMI≥30) (3). The pathological complications of obesity are diverse and include co-morbidities such as cardiovascular disease, type 2 diabetes, and hypertension, to name a few (1,227). Obese individuals are also more susceptible to viral and bacterial infections (2). In 2009, the Centers for Disease Control and Prevention reported a high prevalence of obesity among intensive care patients with confirmed 2009 pandemic H1N1 influenza (pH1N1) infection (4). Several investigations have since established obesity as an independent risk factor for enhanced pH1N1 (4-7,228) and seasonal influenza infection severity (17,229,230). Given that seasonal influenza epidemics result in 250,000 to 500,000 deaths globally (9) and future pandemics are likely imminent (10), understanding how obesity enhances influenza severity is a global public health concern.

We have previously shown that obese individuals exhibit impaired cellular and humoral immune responses to influenza vaccination (12). Further, mouse models of obesity have extensively demonstrated that obesity enhances influenza infection mortality

[2]This chapter was published in *PLoS One:*
Milner J.J., Wang J., Sheridan P.A., Ebbels T., Beck M.A.*, Saric, J.* 2014. [1]H NMR-based profiling reveals differential immune-metabolic networks during influenza infection in obese mice. *PLoS One*. In Press. *Co-last authors

(14,67,68,78,79,81,82). Both innate and adaptive influenza immune defenses are altered by obesity, but elucidation of the underlying mechanisms driving greater influenza severity in obese mice is currently lacking (2,14,78,79,231). Further, obesity is inherently a metabolic disease, and thus far, no studies have considered how dynamic changes in metabolism during influenza may impact immunity and infection outcome in the obese.

Metabolic profiling, combining ^{1}H nuclear magnetic resonance (NMR) spectroscopy and multivariate statistical data analysis, has found wide application in metabolic syndrome related diseases and has also gained significant momentum in infectious diseases for discovery of predictive and diagnostic biomarkers (232-236). In more recent years, the approach has evolved towards a more systemic assessment of host response, and integrating immune measures has become established in particular (237,238). The purpose of this study was to develop a global view of the impact of obesity on metabolism and immunity during influenza infection and to generate data which can serve as the basis for the formation of new mechanistic hypotheses and perhaps new prognostic or diagnostic methodology.

In the present study, lean and obese mice were infected with a mild dose of influenza A/PR/8/34 (H1N1) and subsequently tissues and biofluids were harvested for metabolic profiling. ^{1}H NMR-based profiling revealed distinct metabolic signatures between infected lean and obese mice. Interestingly, we identified unique metabolic signatures in urine and fecal samples that allowed for discrimination of infection status and distinguished uninfected and infected lean and obese mice. Further, the metabolic analysis was extended to include lung tissue, bronchoalveolar lavage fluid (BALF), serum, mesenteric white adipose tissue (WAT), and liver from infected lean and obese mice. We detected significant alterations in ketone body, lipid, choline, nucleotide, vitamin, amino acid and carbohydrate metabolic pathways in influenza

infected obese mice. We also analyzed T cell populations from lean and obese infected mice to identify immune-metabolic correlation structures, and several interactions between a variety of metabolites and BAL and draining lymph node T cell populations were uncovered. Identification of differential metabolic signatures and immune-metabolic structures in lean and obese mice facilitates the establishment of metabolic profiling as a useful tool for characterizing influenza infection responses and advances the current understanding of potential factors contributing to impaired influenza protection in obese mice.

Materials and methods

Ethics Statement

Animal experiments were conducted at the University of North Carolina at Chapel Hill Animal Facility, which is fully accredited by the American Association for Accreditation of Laboratory Animal Care. All mouse-related procedures were approved by the University of North Carolina at Chapel Hill Institutional Animal Care and Use Committee.

Animal housing and maintenance

Weanling, male, C57BL/6J mice (Jackson Laboratory, Bar Harbor, ME) were housed under pathogen free conditions and fed a high fat (45% kcal fat, Research Diets D12451) or low fat, control diet (10% kcal fat, Research Diets D12450B, New Brunswick, NJ) for 20 weeks.

Reagents

Phosphate buffer for ^{1}H NMR acquisition of urine and extracts was made at a D_2O:H_2O ratio of 1:1 at a pH of 7.4 containing Na_2HPO_4 and NaH_2PO_4 (Sigma-Aldrich). D_2O served as a field frequency lock and sodium 3- (trimethylsilyl) [2,2,3,3-2H4] propionate (Sigma-Aldrich) at 0.01% was added as a chemical shift reference represented at δ 0.0. For ^{1}H NMR acquisition of serum 0.9% saline was equally made up in 50% D_2O (Sigma-Aldrich). HPLC-grade water, chloroform, and methanol, for tissue extractions were obtained from VWR International Ltd.

Influenza infection and sample collection

Influenza A/Puerto Rico/8/1934 (H1N1, PR/8), (ATCC, Manassas, VA), was propagated in embryonated chicken eggs as described previously (14,78). For influenza inoculations, mice were lightly anesthetized via isoflurane inhalation, and infected with $1.1x10^2$ 50% tissue culture infective dose ($TCID_{50}$) PR/8 in 50 µL of phosphate buffered saline via non-invasive oropharyngeal aspiration, as similarly reported (14,193,194).

Urine and fecal samples for metabolic profiling were obtained at three different time points: one day prior to infection (D-1), 2 and 6 dpi (Figure 1). Details regarding fecal/urine sample collection are described elsewhere (234). At 9 dpi, liver, lungs, mesenteric (visceral) white adipose tissue (WAT), bronchoalveolar lavage fluid (BALF) and mediastinal lymph nodes (mLN) were harvested and further processed for flow cytometry or were flash frozen in liquid nitrogen. Collection of BALF was performed as previously described (14,78). Urine, serum, fecal pellets, BALF, liver, lung and WAT samples were shipped to Imperial College London on dry ice for ^{1}H NMR data acquisition and analysis.

Flow cytometry

BAL and mLN cells were processed and stained for flow cytometry as previously described (14,78) with the following antibodies: CD16/32 (Fc blocker), CD4 (FITC), CD25 (PE-Cy7), and Foxp3 (APC) from eBioscience (San Diego, CA); CD3 (APC/Cy7) and CD8 (PerCP) from BioLegend (San Diego, CA). The MHC class I tetramer (PE) specific for H-2Db-resricted epitope of the influenza nucleoprotein (NP, D_bNP_{366-74}) of PR/8 was obtained from the NIH Tetramer Core Facility (Atlanta, GA). Stained cells were subsequently analyzed on a CyAn ADP Analyzer flow cytometer (Beckman Coulter, Inc., Fullerton, CA), and all flow cytometry data were analyzed via FlowJo Software (TreeStar, Ashland, OR). All flow cytometry analysis of T cells consisted of a doublet exclusion gate followed by gating of $CD3^+$ cells for further analysis of $CD4^+$ and $CD8^+$ T cell populations.

Sample preparation and acquisition of ^{1}H NMR spectral data

Urine, feces, serum, and tissue samples were prepared according to previously published protocols (234,239). Individual BALF samples (200 μl) were mixed with phosphate buffer (400 μl) and 550 μl of the mixture was subsequently transferred into 5 mm diameter standard NMR tubes for data acquisition (Bruker Biospin, Rheinstetten). All biological samples were analyzed using a 600 MHz Avance DRX NMR spectrometer (Bruker; Rheinstetten), employing a standard one dimensional (1D) ^{1}H NMR Noesypr1d pulse sequence with water suppression (recycle delay (rd)-90°-t1-90°-tm-90°-acquisition time) for all samples. Recycle delay (rd) and mixing time (tm) were set to 2 s and 100 ms respectively. For obtaining more comprehensive information on the serum samples, two additional pulse programs were utilized namely Carr-Purcell-Meiboom-Gill (cpmgpr) and diffusion edited spectroscopy (ledbipolpr) (239). The numbers of scans were

adjusted for each biological matrix, whereby urine and serum were analyzed in 256 and extracts in 128 scans to obtain maximum signal output. Data from each sample was accumulated into 32 k data points within a spectral width of 20 ppm.

Pre-processing of spectral data

Topspin 3.1 (Bruker Biospin) was utilized for partially pre-processing of the raw spectra, including manual phasing, baseline correction and calibration of the chemical shifts to the TSP signal at δ 0.00 or to the lactate doublet at 1.33 representing the CH_3 signal, for serum samples. Spectra were subsequently imported into a MATLAB interface (Mathworks Inc., USA) where regions containing ethanol, methanol, urea, and water resonances were cut out from the whole spectra. Selected regions were δ 1.049-1.232, δ 3.599-3.7 (ethanol) for BALF spectra, δ 4.704-6.318 (H_2O and urea) for urine, δ 3.332-3.443 (methanol), δ 4.598-5.001 (H_2O) for serum, δ 4.216-5.556 (H_2O) for feces, δ 4.723-5.012 (H_2O) for liver, δ 4.713-5.075 (H_2O) for lung, and δ 4.675-5.093 (H_2O) for WAT. All remaining spectral regions were aligned and normalized to the median spectrum according to an in-house developed MATLAB script (Dr. Kirill Veselkov) (240).

Multi- and uni-variate data treatment

Processed spectral data were exported to SIMCA-P software (Umetrics, Sweden) for Principal component analysis (PCA) and projection to latent structure discriminant analysis (PLS-DA) for obtaining an overview on the data distribution and presence of class differences (241,242). For identification of the discriminatory metabolites, orthogonal PLS-DA (O-PLS-DA) was applied using an in-house developed script in MATLAB including a 7-fold cross validation

(243). Metabolites that are related to a certain class are represented by yellow to red colors in the color code included in the O-PLS-DA plots, whereby the exact correlation value can be extracted from the main plot in MATLAB. Here, only candidate biomarkers above a correlation threshold corresponding to $p \leq 0.05$ were selected as significant.

In order to explore correlation structures between metabolic data and T cell populations, an additional correlation analysis was conducted. The spectral information which built the X-matrix was therefore integrated with a second Y-matrix that contained the flow cytometry data. The Pearson-based correlation script further contained a peak picking algorithm to reduce inclusion of noise, and a 10,000 fold permutation resulting in display of correlations with $p \leq 0.05$ only. Identity of peaks was confirmed by using in-house NMR chemical shift database, Chenomx NMR suite profiler software (Chenomx Inc, USA), and published ^{1}H NMR assignments (234,244,245). Identities were further confirmed by using statistical total correlation spectroscopy (STOCSY) in a MATLAB environment (243).

Results

Metabolic profiling uncovers distinct metabolic perturbations in influenza infected obese mice

Weanling, male C57BL/6J mice were maintained on a high fat (45% kcal fat) or a low fat, control diet (10% kcal fat) for 20 weeks. Following the dietary exposure, obese mice weighed 33% more than lean mice (Figure 5.1A). Figure 5.1B is a representative timeline for collection of samples processed for immune-metabolic characterization, and all samples were obtained from the same cohort of lean and obese mice. Following the 20 wk dietary exposure, mice were infected with $1.1x10^{2}$ $TCID_{50}$ of PR/8. Although obese mice lost more absolute

weight compared with lean mice (Figure 5.1C), there were no differences detected in percent weight loss between the two groups (Figure 5.1D). It is well established that obese mice are more likely to die from influenza if given a sufficient viral dose (67,68,78,79,81). However, we utilized a relatively mild infection dose, as only 10% of lean and obese mice succumbed to the infection. We chose a mild infection for this model in order ensure that we captured metabolic changes induced by obesity during infection rather than secondary responses caused by lethal infection conditions.

We first set out to determine if metabolic profiling could distinguish urine and fecal samples from uninfected and infected lean and obese mice. We chose urine and feces because these are biosamples that could easily be tested in humans. Further, we chose to sample urine and feces at 2 dpi and 6 dpi to capture metabolic changes during early and late infection responses. Figure 5.2 represents a PCA scores plot showing clear separation of naïve (D-1) urine samples from early infection (D2) and later infection (D6) time points for lean (Figure 5.2A) and obese mice (Figure. 5.2B). Pre-infection and 6 dpi samples were furthermore combined in a PLS-DA analysis in order to capture whether obesity status or infection state was the predominant influence to the murine metabolic profile (Figure 5.2C). Of interest, all infection-dietary groups displayed metabolically distinct urinary profiles.

Analysis of urinary and fecal metabolites differentially altered in lean and obese mice during the infection revealed mixed effects in a variety of metabolic processes, including perturbations in nucleotide, vitamin, ketone body, amino acid, carbohydrate, choline and lipid metabolism (Table 5.1). Reflective of impaired glucose tolerance, characteristic of obesity, obese mice had greater urinary glucose levels prior to infection and throughout the course of the infection (246,247). Further, uninfected obese mice had significantly higher concentrations of

urinary taurine, ureidopropanoate, 1-methylnicotinamide, several unknown metabolites and lower levels of trimethylamine. At 2 dpi ascorbate, ureidopropanoate and acetylcarnitine were detected in the urine of obese mice, whereas trimethylamine levels were greater in lean mice at -1 and 2 dpi. Urinary 3-hydroxybutyrate concentration was greater at 6 dpi in obese mice as well as several lipid metabolites in fecal extracts at 2 dpi.

The metabolic analysis was also extended to include assessments of BALF, lung tissue, serum, liver and mesenteric WAT from lean and obese mice at 9 dpi (Table 5.2). To limit variation within dietary groups, due to intra-individual differences between mice, all samples used for profiling were obtained from the same cohort of mice. Although this is an inherent strength in our model, it limited the analysis to one time period for harvesting terminal samples (serum, WAT, BALF, lung and livers). We specifically chose BALF and lung to examine local changes at the site of infection, and we included peripheral tissues and serum to enhance understanding of the systemic and global consequences of obesity during influenza. Analyses of tissues at 9 dpi revealed that WAT showed the greatest number of altered metabolites, whereby the majority of changes were linked to amino acid metabolism (Table 5.2). Additionally, serum showed a high degree of metabolic change between lean and obese mice, including relatively higher general lipid levels in the obese mice (Figure 5.6, Table 5.2). However, lean mice had greater levels of serum acetone, 3-hydroxybutryate and acetate. Lung and BALF did not show any significant differences between lean and obese mice at 9 dpi.

Differential immune-metabolic correlations in influenza infected lean and obese mice

Metabolic profiling has previously been used to explore immune regulatory systems during infections by applying multivariate statistical methods to uncover metabolic-immune

interactions (238,248). To further assess the co-variation between tissue/biofluid metabolites and immune parameters in our model, a correlation analysis was conducted between T cell population numbers and ^{1}H NMR data for lean and obese statuses separately in order to characterize the systemic background metabolism linked to T cell responses. Although a variety of cellular defenses are altered by obesity, we chose to focus our analysis on T cell populations because this cell type is consistently altered by obesity during influenza infection (14,67,78,213,231). We have previously detected perturbations in antigen specific $CD8^{+}$ T cell and regulatory T cell (Tregs) responses during influenza infection in obese mice (14,78,79,213); therefore, we focused our immune-metabolic integration on these cell types in particular. For influenza-specific $CD8^{+}$ T cells, we utilized an MHC class I tetramer specific for H-2Db-resricted epitope of the influenza nucleoprotein (NP, D_bNP_{366-74}) of PR/8, and Tregs were identified as $CD4^{+}Foxp3^{+}CD25^{+}$ cells.

The ^{1}H NMR data from each biological compartment (i.e. lung, liver, WAT, feces, BALF, serum, and urine) were correlated with BAL and mLN T cell populations at 9 dpi. Urine (6 dpi), lung (Tables 5.3 and 5.4) and liver presented the highest amount of T cell-metabolite correlations in both lean and obese mice. Interestingly the correlations were not restricted to the corresponding cellular compartment but showed systemic links. For example, 3-hydroxybutyrate in serum negatively correlated with BAL $CD4^{+}$ T cells in lean mice, whereas urinary 3-hydroxybutyrate positively correlated with BAL $CD4^{+}$ T cells in obese mice (Table 5.5). A relatively similar pattern of correlations was detected for BAL Tregs ($CD4^{+}CD25^{+}Foxp3^{+}$), but 3-hydroxybutyrate in the lungs of obese mice positively correlated with BAL Tregs (Table 5.3, Figure 5.4). Further, 3-hydroxybutrate in several compartments correlated with various mLN and BAL $CD8^{+}$ T cell populations in lean and obese mice. Other metabolites, such as choline, taurine

and creatine from a variety of tissues/biofluids were found to be significantly associated with several T cell populations in the lung airways and mLN. A detailed list of correlative metabolic markers is provided in Tables 5.3/4 and Supplementary Table 5.1. Significant correlations among metabolites and T cell populations may result from co-variation without indication of a mechanistic link, but it is also possible that detected correlations reveal underlying mechanisms directly or indirectly affecting T cell distribution and function in lean and obese mice.

Discussion

Globally, 500 million adults are clinically obese, and the number of pathophysiological complications and identified health risks of excess adiposity continue to mount (3). Although a number of innate and adaptive immune defenses are altered by obesity during influenza infection, explanatory mechanisms remain relatively undefined. Through metabolic assessment of urine and feces, we demonstrated that metabolic profiling can successfully distinguish uninfected lean and obese mice, naïve and infected mice, and lean and obese mice infected with influenza. Metabolic analysis of serum, WAT and livers also revealed differences in a variety of metabolic pathways in obese mice during the peak of influenza immune responses. Lastly, statistical relationships between T cell responses and tissue/biofluid metabolites were uncovered allowing for a thorough differential immune-metabolic characterization.

Metabolic profiling of urine and feces revealed greater levels of urinary taurine, ureidopropanoate, 1-methylnicotinamide, glucose and fecal choline in uninfected obese mice. Metabolic changes detected in the urine and feces may reflect local changes in the kidneys or gastrointestinal system, as well as systemic alterations in metabolism. To our knowledge, there are currently no reports defining how influenza infection alters metabolite profiles in the urine

and feces of mice. During infection, acetylcarnitine, ascorbate, glucose and 3-hydroxybutyrate were elevated in the urine of obese mice. Of interest, a variety of lipid metabolites and propionate (a short chain fatty acid) (249) were detected at greater concentrations in the feces of obese mice at 2 dpi. Because these changes were not observed prior to infection, the increased levels of these metabolites are specific to the infection in obese mice (and not simply due to diet or obesity status). This finding may yield new hypotheses related to obesity and influenza infection, such as: Are there local changes in the gastrointestinal system of obese mice during influenza that may impact infection outcome? Does obesity induce alterations in the gut microbiota during influenza, potentially impacting infection responses (propionate can be produced by gut microbiota) (249)? Further, acetylcarnitine was detected at higher levels in the urine of obese mice at 6 dpi. Acetylcarnitine is the acetylated form of carnitine, which is utilized in fatty acid transport into mitochondria for subsequent β-oxidation. Therefore, various metabolites related to lipid metabolism were significantly altered in the feces and urine of obese mice, perhaps suggesting alterations in lipid metabolism contributes to differential infection responses in obese mice.

Ascorbate (vitamin C) was significantly higher in the urine of obese mice at 2 dpi. Excess levels of ascorbate in mice are controlled, in part, through urinary excretion (250,251). Unlike humans, mice have the ability to synthesize endogenous ascorbate (252,253). Further, during times of stress, mammals upregulate ascorbate biosynthesis (254). Ascorbate fulfills a variety of physiological functions, including regulation of oxidative stress (253,255). Elevated ascorbate in the urine may be indicative of greater levels of oxidative stress in infected obese mice. Oxidative stress and vitamin C deficiency in mice can increase influenza infection pathology and mortality (178,253,256). Further, influenza infection and obesity are independently associated with greater

levels of oxidative stress (177,257). Therefore, it is likely that obesity exacerbates oxidative stress conditions during influenza infections, ultimately affecting infection outcome. Further, if vitamin C requirements are increased during infection in the obese, perhaps obese humans require greater ascorbate intake during influenza infection and should supplement during influenza seasons. It is interesting that ascorbate was detected at greater levels in the urine of obese mice, but it is unclear why elevated levels weren't detected in the serum or the liver (primary site of synthesis). Perhaps, at 9 dpi, when serum and livers were harvested, ascorbate in obese mice returned to similar levels as in lean mice.

Another interesting finding revealed by metabolic profiling was that glucose was significantly elevated in the urine of obese mice prior to infection, and at 2 and 6 dpi. Glucose intolerance often results in glucosuria (246,258). Further, obese mice had greater levels of glucose in the serum and liver at 9 dpi compared with lean mice. It has been extensively demonstrated that diet-induced and genetic obese mice exhibit elevated blood glucose levels (65,242). However, tissue and circulating glucose levels in obese mice have never been measured during the context of an influenza infection. Chronically elevated glucose can have a variety of pathological effects, including glycation products, oxidants, hyperosmolarity and perturbations in cell signaling pathways (259). Therefore, it would be interesting to investigate influenza severity in a model in which obese mice have normalized insulin sensitivity and glucose tolerance (235).

In recent years, an abundance of research has focused on how metabolism is a critical regulator of immune cell function (260). Manipulation of nutrient availability in culture or genetic manipulation of genes that regulate metabolic pathways can have a profound impact on immune activity and disease outcome (1,260). However, it is relatively unclear how metabolites

and nutrients in the immune cell microenvironment may alter cellular metabolism, distribution and function during the context of an infection. Therefore, we took advantage of this comprehensive metabolic analysis and assessed significant interactions between T cell populations and metabolites. A number of immune-metabolic correlations were uncovered. For example, lung choline and phosphocholine were positively associated with BAL Tregs and other $CD4^+$ T cell populations in lean mice but not in obese mice. Perhaps, perturbations in choline/phosphocholine metabolism may impact T cell responses in obese mice. These findings could be indicative of direct or indirect T cell-metabolite interactions, although it is also possible that these associations are biologically insignificant. Nonetheless, identification of BAL and mLN T cell-metabolite correlates provides a more dynamic and global assessment of the consequences of obesity during influenza infection.

The urinary and fecal data are particularly interesting given the non-invasive nature of these bio-samples and the high degree of separation detected between naïve and infected, lean and obese mice. Numerous reports have established metabolic profiling of urine can identify biomarkers and metabolic matrices that can distinguish disease states, with the capability of ultimately guiding treatment (80,261,262). At 2 dpi, prior to significant weight loss and any obvious signs of sickness, we identified a unique metabolic fingerprint in the urine and feces of influenza infected obese mice, consisting of perturbations in lipid, nucleotide, carbohydrate, microbial, and vitamin metabolism. Given the rapidity of influenza transmission during epidemics and pandemics and the sudden onset of severe symptoms in infected individuals (9), identification of a metabolic profile unique to an early infection time point holds widespread implications for personal and public health. We have identified a metabolic signature that could be used to predict influenza infection status even prior to any obvious signs of illness. Further

testing can determine if this signature is unique to influenza infection rather than a generalized response to an infection or inflammation.

Taken together, this investigation establishes metabolic profiling as a useful tool for characterizing infection responses during influenza and identifying potential pathways and mechanisms contributing to altered immunity in obese mice. Teasing apart differential responses during influenza infection is key to understanding the mechanisms driving greater disease severity in obese mice compared with lean mice. Further utilization of metabolic profiling as a complimentary tool to immunological measures of infection outcome could help advance the current knowledge of the response to influenza infection in other rodent research models and may have potential applications in clinical and research settings.

Tables and Figures

Table 5.1. Metabolic biomarkers recovered from urine and fecal extracts during influenza infection in lean and obese mice

Metabolic Pathway	Metabolite	Day -1	Day 2	Day 6
Ketone Body Metabolism	3 hydroxybutyrate			**Urine**
Lipid Metabolism	acetylcarnitine		**Urine**	
	(CH2)n		**Feces**	
	CH2CH2CO		**Feces**	
	CH2**CH2**CO		**Feces**	
	propionate		**Feces**	
	taurine	**Urine**		
Choline Metabolism	choline	**Feces**		
Microbial Metabolism	trimethylamine	Urine	Urine	
Nucleotide Metabolism	ureidopropanoate	**Urine**	**Urine**	
Vitamin Metabolism	ascorbate		**Urine**	
	1-methylnicotinamide	**Urine**		
Carbohydrate Metabolism	glucose	**Urine**	**Urine**	**Urine**
UK1	2.458(s)		**Feces**	
UK2	8.54(d), 8.33(d), 6.7(d), 6.67(d), 3.65(s)	**Urine**	**Urine**	**Urine**

Table 5.1: Bolded and underlined urine and feces indicates that metabolite was significantly higher in obese mice, and metabolites in normal font were significantly lower in obese mice. UK: unknown metabolite. n=8-9.

Table 5.2 Discriminatory metabolites between lean and obese mice at 9 days post-infection in liver, serum and white adipose tissue samples

Metabolic Pathway	Metabolite	Liver	Serum	WAT
Amino acid Metabolism	alanine			+
	glutamate			+
	isoleucine			+
	leucine			+
	lysine			+
	methionine			+
	phenylacetylglycine			+
	tyrosine			+
	valine			+
Biosynthesis of Secondary Metabolism	*scyllo*-inositol			-
Carbohydrate Metabolism	glucose	+	+	
Ketone Body Metabolism	acetone		-	
	3 hydroxybutyrate		-	
Lipid Metabolism	glycerophosphocholine		+	
	LDL (=CH-CH2-)		+	
	LDL (-CH=CH-CH2-CH=CH-)		+	
	LDL (CH3)		+	
Pyruvate Metabolism	acetate		-	

Table 5.2: Metabolites that were detected at a significantly greater level in obese mice are indicated by +, whereas – represents metabolites detected at lower levels in obese mice compared with lean mice, n=8-9.

Table 5.3 Lung metabolite correlation patterns with BAL T cell populations

BAL Cells	Lean	Obese
Total BAL cell number	**creatine, glycerol, taurine**	
$CD4^+$ T cells	**creatine, glycerol, phosphocholine, taurine**	
$CD4^+CD25^+$ T cells	**3-hydroxybutyrate, acetate, alanine, creatine, glycerol, lactate, phosphocholine, taurine**	
$CD4^+CD25^+FoxP3^-$ T cells	**3-hydroxybutyrate, creatine, glycerol, lactate, phosphocholine, taurine**	
$CD4^+CD25^+Foxp3^+$ T cells	**3-hydroxybutyrate, acetate, choline, creatine, glycerol, lactate, phosphocholine, taurine**	**3-hydroxybutyrate**
$CD4^+FoxP3^+$ T cells	**3-hydroxybutyrate, acetate, choline, creatine, glycerol, lactate, phosphocholine, taurine**	**3-hydroxybutyrate**
$CD4^+FoxP3^{hi}$ T cells	**3-hydroxybutyrate, acetate, choline, creatine, glycerol, lactate, phosphocholine, taurine**	
$CD8^+CD25^+$ T cells	**3-hydroxybutyrate, creatine**	
$CD8^+D_bNP_{366\text{-}74}{}^+$ T cells		**choline, glycerol**
$CD8^+CD25^+D_bNP_{366\text{-}74}{}^+$ T cells		**acetate, alanine, choline, creatine, glucose, glycerol, lactate, leucine, methionine, phosphocholine, taurine, valine**

Table 5.3: Underlined metabolites represent a significant negative correlation, and text without an underline indicates a significant positive association. Correlation analysis is based on a Pearson correlation matrix validated by 10,000 permutations. n=8-9.

Table 5.4 Lung metabolite correlation patterns with mLN T cell populations

mLN Cells	Lean	Obese
Total mLN cell number		glucose
$CD4^+$ T cells		glucose, glycerol
$CD4^+CD25^+Foxp3^+$ T cells	alanine, leucine, valine	glucose
$CD4^+Foxp3^+$ T cells	leucine, valine	
$CD4^+Foxp3^{hi}$ T cells		glucose
$CD8^+$ T cells		3-hydroxybutyrate, glucose, glycerol
$CD8^+D_bNP_{366\text{-}74}{}^+$ T cells		3-hydroxybutyrate, acetate, alanine, choline, creatine, glucose, glycerol, lactate, leucine, methionine, phosphocholine, valine
$CD8^+CD25^+D_bNP_{366\text{-}74}{}^+$ T cells		3-hydroxybutyrate, acetate, alanine, choline, creatine, glucose, glycerol, lactate, leucine, methionine, taurine, valine phosphocholine

Table 5.4: Underlined text represents a significant negative correlation, and text without an underline indicates a significant positive association. Correlation analysis is based on a Pearson correlation matrix validated by 10,000 permutations. n=8-9.

Table 5.5 Correlation patterns between ^{1}H NMR data and BAL or mLN T cell populations

Liver NMR		**Lean**	**Obese**
BAL cells	**Total BAL cell number**	**glucose, leucine**	
	$CD4^+$ T cells	**acetate, alanine, glucose, lactate, leucine**	**acetate, glucose, glutamine, isoleucine**
	$CD4^+CD25^+$ T cells	**acetate, alanine, glucose, glycerol, lactate, leucine**	
	$CD4^+CD25^+FoxP3^-$ T cells	**acetate, alanine, choline, glucose, glycerol, lactate, leucine**	
	$CD4^+FoxP3^+$ T cells	**glucose**	
	$CD4^+FoxP3^{hi}$ T cells	**glucose**	
	$CD4^+CD25^+Foxp3^+$ T cells	**glucose**	
	$CD8^+CD25^+$ T cells	**glucose**	**acetate, choline, glucose, glutamine, isoleucine, lactate**
	$CD8^+CD25^+D_bNP_{366\text{-}74}{}^+$ T cells		**alanine, aspartate, choline, glucose, glutamate, glycerol**

mLN cells	$CD4^+$ T cells	choline	
	$CD4^+CD25^+$ T cells	**acetate, choline**	
	$CD4^+CD25^+Foxp3^+$ T cells	**acetate, choline**	
	$CD4^+Foxp3^+$ T cells	**choline**	
	$CD4^+Foxp3^{hi}$ T cells	**choline**	
	$CD4^+CD25^+Foxp3^-$ T cells	**acetate, choline**	
	$CD3^+CD8^+$ T cells	**choline**	
	$CD8^+D_bNP_{366\text{-}74}{}^+$ T cells		**choline, glucose**
	$CD8^+CD25^+D_bNP_{366\text{-}74}{}^+$ T cells		**choline, glucose, glutamate**
WAT NMR		**Lean**	**Obese**
BAL cells	**$CD4^+$ T cells**		**choline, lactate, phosphocholine, taurine**

	$CD4^+Foxp3^+$ T cells		phosphocholine
	$CD4^+FoxP3^{hi}$ T cells		**choline, phosphocholine, taurine**
	$CD8^+CD25^+$ T cells		**alanine, glycerol, leucine**
mLN cells	**Total mLN cells**	**taurine**	
	$CD3^+CD4^+$ T cells	**glycerol, lactate, taurine**	
	$CD4^+CD25^+Foxp3^-$ T cells		**leucine**
	$CD3^+CD8^+$ T cells	**glycerol, lactate, taurine**	
Feces NMR		**Lean**	**Obese**
BAL cells	**Total BAL cell number**		**deoxycholic acid**
	$CD4^+CD25^+$ T cells		**deoxycholic acid**
	$CD4^+CD25^+FoxP3^-$ T cells		**deoxycholic acid**

	$CD4^+CD25^+Foxp3^+$ T cells		deoxycholic acid
	$CD4^+FoxP3^+$ T cells		**deoxycholic acid**
	$CD4^+FoxP3^{hi}$ T cells		**deoxycholic acid**
	$CD8^+CD25^+$ T cells		**deoxycholic acid**
	$CD8^+CD25^+D_bNP_{366\text{-}74}{}^+$ T cells	**acetate**	
	$CD8^+D_bNP_{366\text{-}74}{}^+$ T cells	**acetate**	
mLN cells	**$CD3^+CD4^+$ T cells**	**deoxycholic acid**	
	$CD4^+CD25^+Foxp3^-$ T cells		**deoxycholic acid**
	$CD3^+CD8^+$ T cells	**deoxycholic acid**	**deoxycholic acid**
BALF NMR		**Lean**	**Obese**

mLN cells	$CD8^+D_bNP_{366-74}{}^+$ T cells	lactate	
	$CD8^+CD25^+D_bNP_{366-74}{}^+$ T cells	**lactate**	
Serum NMR		**Lean**	**Obese**
BAL cells	**$CD3^+CD4^+$ T cells**	**3-hydroxybutyrate, acetone**	
	$CD4^+CD25^+$ T cells	**3-hydroxybutyrate, acetone**	
	$CD4^+CD25^+Foxp3^+$ T cells		**3-hydroxybutyrate**
	$CD4^+CD25^+FoxP3^-$ T cells	**3-hydroxybutyrate, acetone**	
	$CD4^+FoxP3^+$ T cells		**3-hydroxybutyrate**
	$CD4^+FoxP3^{hi}$ T cells		**3-hydroxybutyrate**
	$CD3^+CD8^+$ T cells	**3-hydroxybutyrate, acetone**	

	$CD8^+CD25^+$ T cells	3-hydroxybutyrate, acetone	
mLN cells	**$CD4^+CD25^+Foxp3^-$ T cells**	**acetone**	
Urine NMR		**Lean**	**Obese**
BAL cells	**Total BALF cell number**	***N*-acetyl glycoprotein**	**glucose**
	$CD3^+CD4^+$ T cells	***N*-methylnicotinamide**	**3-hydroxybutyrate, glucose, *N*-acetyl glycoprotein, taurine**
	$CD4^+CD25^+$ T cells	***N*-methylnicotinamide, trimethylamine**	**2-oxovalerate, ascorbate, creatine, creatinine, glucose**
	$CD4^+CD25^+FoxP3^-$ T cells	**guanidinoacetate, *N*-methylnicotinamide, trimethylamine**	**2-oxovalerate, ascorbate, creatine, creatinine**
	$CD4^+CD25^+Foxp3^+$ T cells		**2-oxovalerate, ascorbate, creatinine**
	$CD4^+FoxP3^+$ T cells		**glucose**
	$CD4^+FoxP3^{hi}$ T cells		**2-oxovalerate**

	$CD3^+CD8^+$ T cells	3-hydroxybutyrate	glucose
	$CD8^+CD25^+$ T cells	**3-hydroxybutyrate**	
	$CD8^+D_bNP_{366-74}{}^+$ T cells	**creatine, creatinine, indoxylsulfate, *N*-acetyl glycoprotein, phenoacetylglycine, taurine**	**glucose**
	$CD8^+CD25^+D_bNP_{366-74}{}^+$ T cells	**ascorbate, creatine, creatinine, indoxylsulfate, *N*-acetyl glycoprotein, phenoacetylglycine, taurine**	**glucose, guanidinoacetate, indoxylsulfate, *p* cresol glucuronide, phenoacetylglycine**
mLN cells	**mLN cell number**		**2-oxovalerate, creatinine**
	$CD3^+CD4^+$ T cells	***N*-methylnicotinamide, trimethylamine**	**2-oxovalerate, creatinine, glucose**
	$CD4^+CD25^+$ T cells		**2-oxovalerate, ascorbate, creatinine, dimethylamine, glucose, *N*-methylnicotinamide**
	$CD4^+CD25^+Foxp3^-$ T cells	**indoxylsulfate**	**2-oxovalerate, ascorbate, creatinine**
	$CD4^+CD25^+Foxp3^+$ T cells		**2-oxovalerate ascorbate, creatinine, dimethylamine, glucose, *N*-methylnicotinamide**

	$CD4^+Foxp3^+$ T cells		2-oxovalerate, ascorbate, creatinine, dimethylamine, glucose, *N*-methylnicotinamide
	$CD4^+Foxp3^{hi}$ T cells	**indoxylsulfate**	**Ascorbate, creatinine, dimethylamine, glucose, *N*-methylnicotinamide**
	$CD3^+CD8^+$ T cells	***N*-methylnicotinamide, trimethylamine**	**2-oxovalerate, creatinine, glucose, phenoacetylglycine**
	$CD8^+D_bNP_{366-74}{}^+$ T cells	**<u>3-hydroxybutyrate</u>**	**guanidinoacetate, indoxylsulfate, *p* cresol glucuronide, phenoacetylglycine**
	$CD8^+CD25^+D_bNP_{366-74}{}^+$ T cells		**guanidinoacetate, indoxylsulfate, *p* cresol glucuronide, phenoacetylglycine**

Table 5.5: Underlined text represents a significant negative correlation, and text without an underline indicates a significant positive association. All ^{1}H NMR data are from tissues harvested at 9 dpi or urine and feces harvested at 6 dpi. Correlation analysis is based on a Pearson correlation matrix validated by 10,000 permutations. n=8-9.

Figure 5.1 Summary of influenza infection and metabolic profiling model

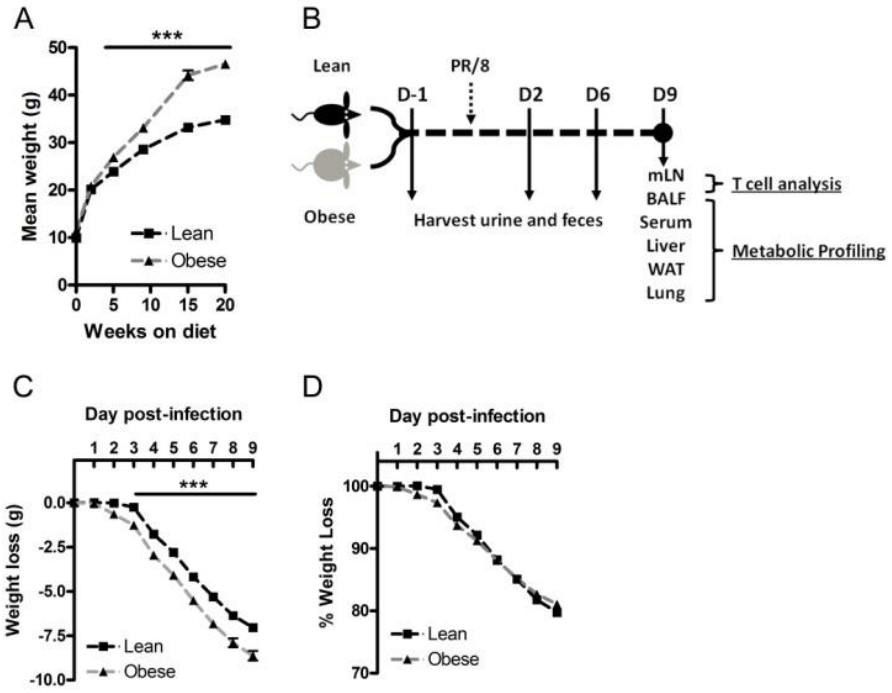

Figure 5.1. A, Weanling, male C57BL6/J mice were maintained on a high fat (45% kcal fat) or low fat control diet (10% kcal fat) for 20 wks, n≥9. B) Timeline of samples harvested for metabolic profiling. Lean and obese mice were infected with $1.1x10^2$ $TCID_{50}$ of influenza A/PR/8/34, and urine and feces were collected at -1 (uninfected mice), 2 and 6 dpi. Terminal samples (mLN, BALF, serum, liver, WAT and lungs) were collected from the same cohort of mice at 9 dpi. Flow cytometry was used to enumerate BAL and mLN T cell populations for immune-metabolic integration, n=8-9. C) Absolute weight loss in lean and obese mice following PR/8 infection, n≥9. D) Percent weight loss normalized to pre-infection body weight, n≥9. Values represent mean ± SEM, ***p<0.0005 compared with lean mice.

Figure 5.2 Metabolic profiling can distinguish urine samples from both uninfected and infected lean and obese mice

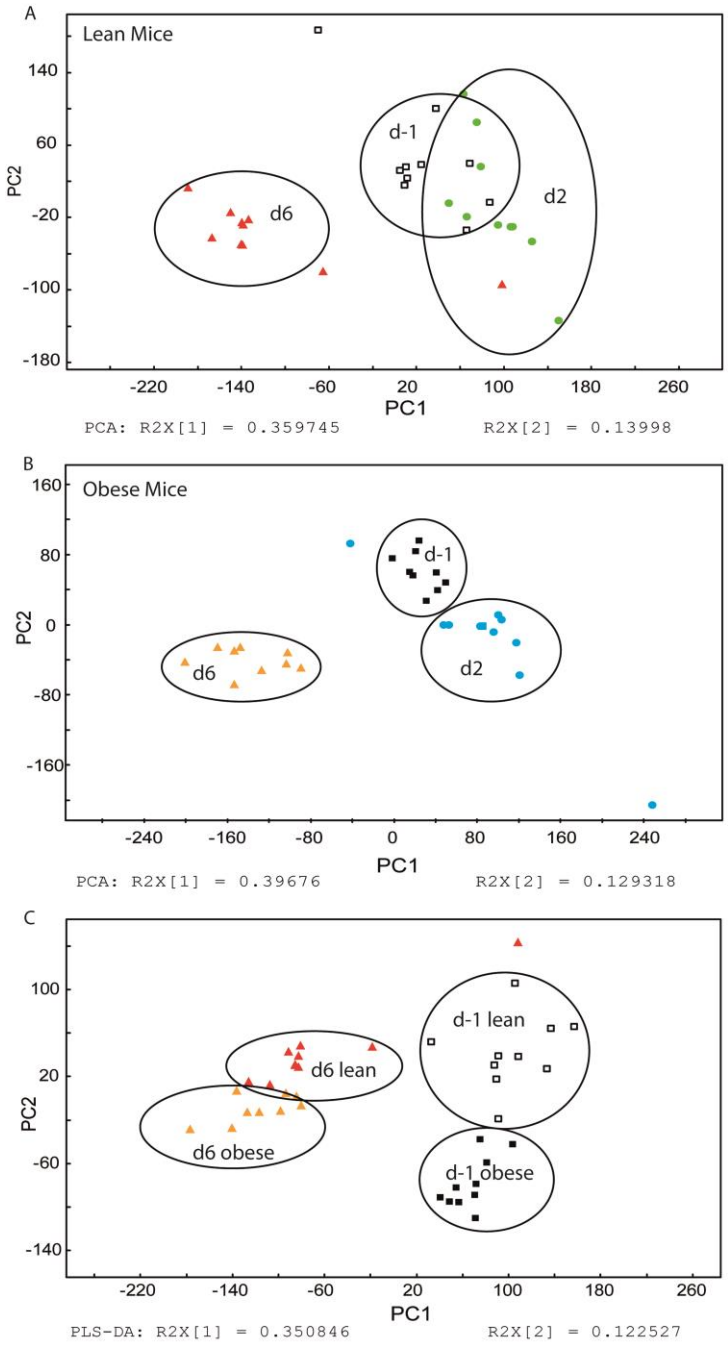

Figure 5.2. Pre-processed ^{1}H NMR urine spectra were analyzed using PCA and PLS-DA. Urine spectra from lean and obese mice were collected one day prior to infection and at 2 and 6 dpi. A&B The urine spectra from lean mice (A) and obese mice (B) showed clear separation according to time, in a PCA analysis. C, PLS-DA analysis showed additional separation between lean and obese mice for two selected time points (i.e. -1 dpi and 6 dpi). n=8-9.

Figure 5.3 Representative analysis of serum samples from infected lean and obese mice

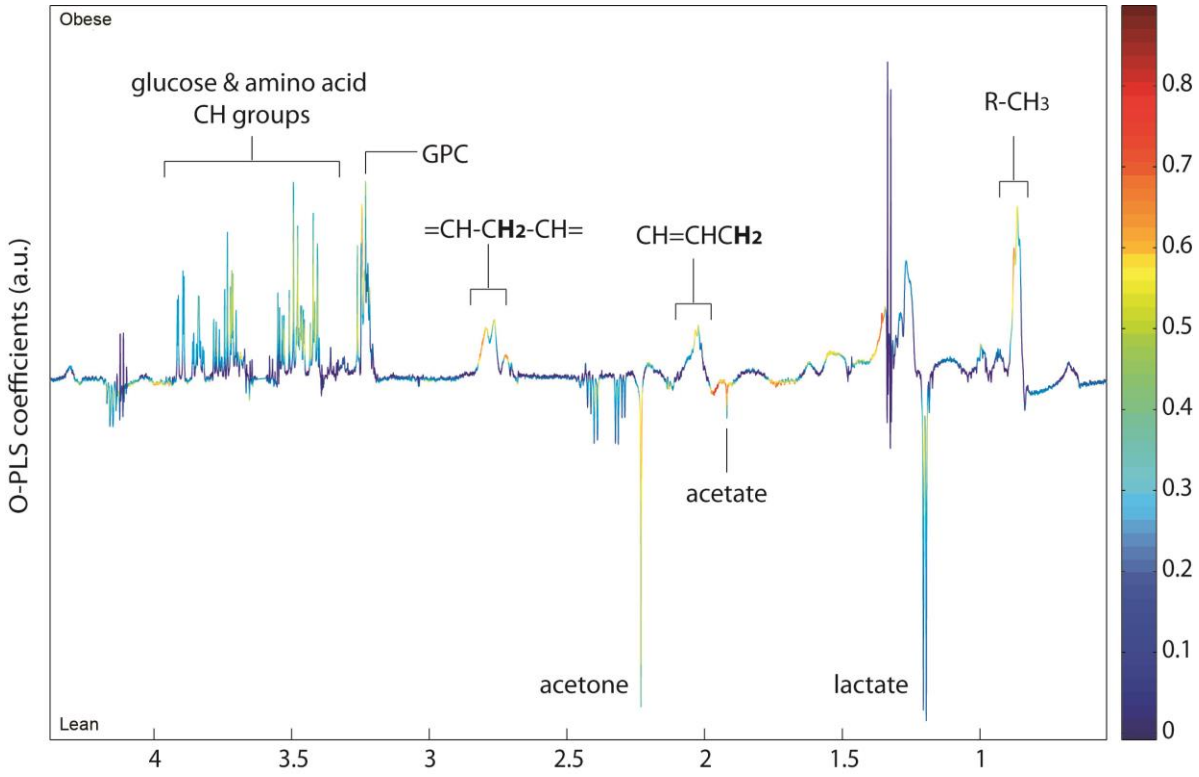

Figure 5.3. O-PLS-DA analysis comparing serum ^{1}H NMR spectra of lean and obese mice at 9 dpi. n=8-9.

Figure 5.4 Correlation analysis of lung analytes and lung and mLN T cell populations

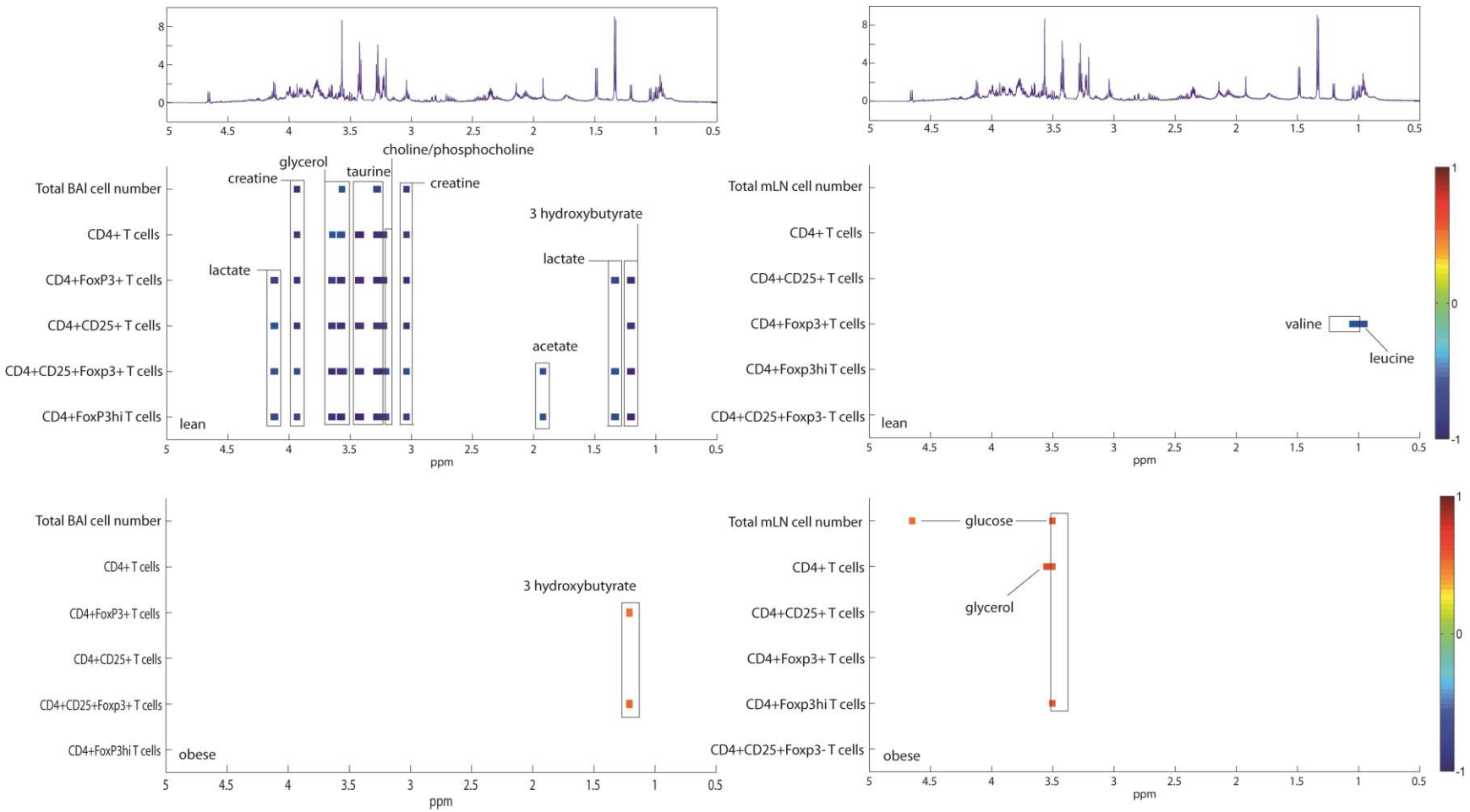

Figure 5.4. A&B, Correlation analysis of lung ^{1}H NMR data and T cell populations in BALF (A) and mLN (B) reveals differential correlation patterns between lean and obese mice. n=8-9.

CHAPTER VI: SYNTHESIS

Overview of research findings

This doctoral dissertation demonstrates that obesity results in greater lung damage during primary and secondary pH1N1 infections in mice. The first aim of this proposal was to investigate the impact of obesity on the cross-reactive immune response to a secondary pH1N1 influenza virus infection. In this model, obese mice unexpectedly had lower levels of cross-reactive non-neutralizing NP antibodies following a primary PR8 infection, which likely contributed to greater viral burden in the lungs of obese mice. Additionally, obese mice had greater lung damage, lung inflammation and heightened cross-reactive $CD8^+$ T cell responses during the secondary pH1N1 influenza infection. To address the discrepancy in lung damage and inflammation during this secondary challenge, we also investigated the impact of obesity on Treg distribution and function. Although Treg number was elevated in the lung airways of obese mice during the secondary challenge, Tregs isolated from obese mice were 40% less suppressive than Tregs isolated from lean mice. Taken together, excess viral titers and impaired Treg function likely contributed to greater lung damage during a secondary pH1N1 infection in obese mice (Figure 6.1). This data may help to explain why obese humans were at greater risk for severe pH1N1 infections. Perhaps infected obese individuals weren't able to properly control antiviral immune responses, ultimately resulting in excessive inflammatory responses and collateral lung damage.

To further address the consequences of obesity on lung damage during pH1N1 infection, we utilized a primary pH1N1 infection model in diet- and genetically-induced obese mice (Table 6.1 summarizes the diets used in this dissertation). Both models of obesity exhibited significantly greater mortality following pH1N1 infection compared with lean control mice. Unexpectedly, obese mice did not display any differences in lung viral titers, lung inflammation or lung pathology scores. However, obese mice exhibited significantly higher damage to the lung epithelium. Because we demonstrated Tregs isolated from obese mice had impaired function in Aim 1, we then measured Treg distribution during this primary infection. Diet- and genetic-induced obese mice had fewer total Tregs and fewer activated Tregs in the lung airways.

Leptin is a critical regulator of immune responses; however, obesity is characterized by hyperleptinemia. During the context of a pH1N1 infection, we demonstrated that obese mice have greater leptin levels in circulation and in the lung airways. While a deficiency of leptin is associated with an immunodeficient state, the consequences of excess leptin signaling remain unclear (2). We hypothesized that disruption of leptin signaling in T cells would ameliorate pH1N1 severity in obese mice. Therefore, we generated mice with conditional disruption of leptin signaling in T cells. Obese $LepR^{T-/-}$ gained a similar level of weight compared with obese $LepR^{Tfl/fl}$ mice. However, disruption of leptin signaling did not limit pH1N1 infection severity in obese mice. Therefore, leptin signaling in T cells is likely not a mediator of infection severity in obese mice.

Although we addressed a possible mechanism of leptin signaling in T cells mediating pH1N1 severity in obese mice, focusing on one specific signaling pathway in one cell type is likely not the most informative approach given the complexity of other potential mechanisms contributing to differential infection outcomes. Therefore, we extended our analysis of the

consequences of obesity to include a metabolomics approach. ^{1}H NMR based metabolic profiling revealed that obesity caused distinct perturbations in a number of metabolic pathways and metabolites in the lung and in peripheral biofluids. Not only did we identify unique biomarkers altered by obesity that could be used to generate hypotheses for the consequences of obesity on infection, but we also demonstrated that metabolic profiling of urine could be used to predict infection status or infection severity. Therefore, we established metabolic profiling as a useful methodology for uncovering explanatory mechanisms for greater influenza pathogenesis in obese mice and as useful tool for predicting influenza infection status and severity.

How does obesity alter pH1N1 immunity?

Understanding the impact of obesity on immunity is difficult for a variety of reasons. Like most diseases in which the immune system plays a role in pathogenesis (autoimmune, cancer, CVD etc.), a complex array of factors could contribute to alterations in immune cell function. Mouse models are useful for addressing this problem and dissecting possible mechanisms, whereby the effects of a certain enzyme, hormone, signaling pathway etc. can be genetically or pharmaceutically manipulated. However, the pathogenesis and consequences of obesity are complex. Molecular manipulation of enzymes or hormones in attempt to understand how obesity is associated with greater susceptibility of a certain disease state may affect weight gain and other characteristics or features of obesity, thereby confounding results. Ideally, manipulation of a suspected mechanism would not affect any of the characteristics of obesity (hyperleptinemia, chronic inflammation, insulin resistance etc.), and this would allow one to address the isolated effects of a proposed mechanism (without the secondary consequences of

affecting obesity). However, the immune system greatly influences obesity and the associated consequences (1).

Although, an abundance of research has begun to focus on the consequences of obesity on immunity, the complexity of this research continues to grow. It is clear that obesity affects the function of immune cells in different ways; obesity does not cause a global impairment in all immune cells, but rather, it appears that obesity may differentially affect the function of each type of immune cell (and each subtype) (2). For example, leptin impairs Treg proliferation but enhances effector T cell proliferation (198). Further, obesity may only impact certain functions of immune cells, making it even more difficult to determine what experimental readouts to use.

Does hyperleptinemia underlie the consequences of obesity on pH1N1 immunity?

The molecular mechanisms for a number of findings from this dissertation remain unknown. For example, in obese mice we detected heightened $CD8^+$ T cell responses during a secondary infection, impaired Treg function, impaired antibody responses and greater lung damage. As mentioned, a number of factors may interact to cause these outcomes. Leptin is a critical modulator of immunity, and obese mice exhibit chronic hyperleptinemia. It is possible that elevated leptin levels are responsible for all of the differential outcomes we observed. Leptin enhances $CD8^+$ T cell proliferation, regulates Treg and B cell function, and could alter the function of a variety of cells involved in propagating greater lung damage in influenza infected obese mice. Hyperleptinemia could alter immune cell function through excess leptin signaling or may induce a state of leptin resistance. We favor a mechanism by which excess leptin signaling is responsible for the altered immune responses observed.

Central leptin resistance is a fairly well accepted phenomenon of obesity, whereby neurons become resistant to the effects of leptin signaling (2,263). Further, central leptin resistance has been shown to be caused by hyperleptinemia (264). Excess leptin signaling upregulates Jak/Stat signaling pathways resulting in up regulation of a number of STAT3 responsive genes, such as SOCS3 (2,263). SOCS3 impairs JAK2 and LepR phosphorylation, critical steps of leptin signaling (2,263). Whether obesity induces a state of leptin resistance in immune cells is less clear. Some arguments against a role for leptin resistance in immune cells contributing to greater pH1N1 severity are:

1. Leptin is an acute phase inflammatory cytokine (2). It has been hypothesized that prolonged leptin signaling induces a state of resistance in immune cells. However, negative feedback mechanisms are in place for every inflammatory cytokine. Obesity also induces a state of low-grade, chronic inflammation. Yet, there are currently no proposed mechanisms whereby immune cells become resistant to TNFα or IL-6 signaling in an obese state. Further, during the context of an influenza infection, expression of some inflammatory cytokines are increased 100-1000 fold (significantly greater than fold increase in leptin levels which is typically in the range of 2-10 times greater) (78,79).
2. Leptin enhances T cell proliferation and activation (2). However, most mouse models demonstrate that obese mice exhibit greater T cell activation and inflammation during pH1N1 infection. Similarly, obese mice tend to exhibit excessive inflammatory responses during pH1N1 infection, which would not be expected if immune cells were leptin resistant (2,14).
3. Two studies have demonstrated that immune cells from obese rodents exhibit resistance to leptin signaling (265,266). However, these studies would have been strengthened by

including assessments of signaling activation of other inflammatory molecules. Perhaps these studies weren't demonstrating selective leptin resistance, but rather a general impaired responsiveness to an inflammatory signal. Additionally, these studies did not link impaired leptin signaling to any functional readout, such as reduced proliferation or inflammatory function.

4. We demonstrated that lean mice lacking leptin signaling in T cells were not more susceptible to pH1N1 infection. Although this is an isolated effect in T cells and does not assess other immune cells, this demonstrates that complete disruption of leptin signaling in T cells (which in theory would mimic a state of leptin resistance) does not increase pH1N1 susceptibility.

Therefore, we hypothesize that hyperleptinemia alters immune defenses through excess leptin signaling rather than inducing a state of leptin resistance.

Mechanisms of greater lung damage during pH1N1 infection

Enhanced infection mortality is not simply due to an inability to control infectious virus in obese mice, as a number of studies have demonstrated greater influenza mortality despite a lack of differences in viral titers (2). Further, several investigations have demonstrated that obesity impairs the function of a variety of immune cells, of both innate and adaptive arms of immunity (2). However, there have been no studies clearly demonstrating a direct role for how impaired function of a specific immune cell contributes to greater mortality. Further, because differences in viral titers aren't typically reported during primary influenza infections, it is unlikely that impaired antiviral immune cell responses are responsible for the discrepancy in infection severity (unless perhaps it's an inability to respond to homeostatic signals that function

to control immune responses). In asking why obese mice are more susceptible to influenza infection, the first question to address is what is the cause of death in pH1N1 infected obese mice?

The most concrete findings, regarding greater pH1N1 mortality in obese mice, which have been uncovered thus far, are 1) obese mice exhibit impaired lung healing during pH1N1 infection (67), and 2) treatment with leptin monoclonal antibody ameliorates infection severity in obese mice (82). However, these findings are only suggestive of possible mechanisms, as neither study demonstrated a direct link or mechanism between these findings and pH1N1 mortality. Our findings also demonstrate that obese mice exhibit greater lung damage during primary and secondary pH1N1 infection. Therefore, perhaps greater lung damage is responsible for greater pH1N1 mortality.

To address differences in lung pathology and damage during a primary pH1N1 infection between lean and obese mice, we scored H&E stained lung pathology slides, measured immune cell infiltration, inflammatory cytokine responses, and assayed damage to the lung epithelium. Despite significant differences in damage to the lung epithelium, we did not detect differences in lung pathology scores (which is a measurement of immune cell infiltration into bronchioles and alveoli), total BAL cell number, total lung number, nor did we detect striking differences in inflammatory cytokine responses in obese mice. This would suggest that lung damage is not mediated by inflammatory immune cells, but is likely due to impaired healing responses of epithelial cells. With that said, immune cells, such as M2 macrophages and Tregs, can mediate wound healing. Perhaps M2 macrophage healing is impaired in obese mice (studies to address this mechanism are currently in progress). However, there is very little known of the negative effects of obesity on alveolar/bronchial epithelial cell function. Future investigations should

address the impact of obesity on the function, healing capacity, and antiviral responses of lung epithelial cells to influenza infection.

Although, it is likely that greater lung damage is responsible for the greater mortality of influenza infected obese mice, there are no studies demonstrating a direct role for excess lung damage in mediating mortality. Theoretically, impaired wound healing would impair gas exchange at alveolar-endothelial spaces, thus impairing breathing, lowering circulating levels of oxygen and ultimately leading to suffocation. However, there have been no studies to directly investigate whether obesity impairs gas exchange during influenza infection or if dying mice are suffocating. However, several studies have demonstrated that obese mice exhibit heightened airway hyperresponsiveness (AHR) (267,268). Although, there are differences in influenza infection models and AHR models, understanding the impact of obesity on lung physiology and lung inflammation is critical area of research that must be further investigated.

As mentioned, a direct link between greater lung damage and pH1N1 mortality has not been established. Therefore, perhaps systemic consequences are at play or synergism between lung damage and other obesity-associated pathologies. This is where metabolomics or other systems biology approaches may be useful for generating hypotheses. For example, we identified greater levels of vitamin C in the urine of influenza infected obese mice (compared with uninfected obese mice and infected lean mice). Vitamin C is endogenously produced in mice and can be upregulated during pro-oxidant conditions (253, 256). Additionally we also uncovered perturbations in lipid metabolism in a variety of tissues and biofluids of obese mice. Therefore, perhaps greater levels of oxidative stress and altered lipid metabolism work together to enhance influenza severity in obese mice.

Recommendations for future research

There are two key outcomes from this dissertation that should be addressed in future experiments:

1) Greater damage to the lung epithelium of obese mice during a primary pH1N1 infection
2) Impaired antibody responses following a primary, sublethal PR8 infection

In addressing mechanisms for greater damage to the lung epithelium, this also has implications for understanding why obese mice are also more susceptible to death from pH1N1 infection. As discussed, it is possible that impairments in epithelial cell responses to pH1N1 infection underlie greater mortality in obese mice. Further, there are multiple mouse and human lung epithelial cell lines that would facilitate identification of a molecular mechanism. One important question to address is the impact of leptin on epithelial cell function in obese mice. An interesting model would be to cross LepR floxed mice with Surfactant protein C (SPC)-Cre mice, resulting in disruption of leptin signaling in Type II respiratory epithelial cells. This would help to determine if leptin signaling in epithelial cells drives greater pH1N1 severity.

One striking finding from Aim I, is we demonstrated that obese mice exhibited impaired maintenance of influenza antibodies following a sublethal PR8 infection (14). This is interesting because we have also demonstrated that obese humans exhibit impaired maintenance of influenza antibodies following TIV vaccination (12). One critical aspect of obesity that should be further address is how the bone marrow microenvironment impacts the trafficking and maintenance of long lived plasma cells to the bone marrow. It has previously been shown that obesity causes dramatic changes to the bone marrow microenvironment including deposition of adipocytes and increased expression of leptin. Therefore, it would also be interesting to

determine if excess leptin signaling alters plasma cell trafficking, maintenance or function. By crossing LepR floxed mice with CD19-Cre mice, this could be achieved.

Therefore, future investigations should focus on the role of leptin signaling, and the use of conditional knockout mice will facilitate this. Additionally, we have demonstrated that metabolic profiling can provide a more global perspective of the consequences of obesity on pH1N1 immunity. Therefore, this methodology could be integrated into future immunological assays to determine how complex changes in metabolism interact with alterations in the immune system.

Tables and Figures

Table 6.1 Comparison of diets used in this dissertation

Diet	Fat Kcal%	Carbohydrate Kcal %	Protein Kcal %	Primary Carbohydrate Source	Primary Fat Source	Fiber	Phytoestrogens?	Purified Ingredients?	Micro-nutrient Content Matched
Research Diets D12450B	10	70	20	Sucrose (35% Kcal)	Soybean Oil (6% Kcal)	Low (cellulose)	No	Yes	Yes
Research Diets D12451	45	35	20	Sucrose (17% Kcal)	Lard (39% Kcal)	Low (cellulose)	No	Yes	Yes
Research Diets D12492	60	20	20	Maltodextrin 10 (12% Kcal)	Lard (54% Kcal)	Low (cellulose)	No	Yes	Yes
ProLab 3000 Chow	14.3	59.7	26	Starch (32.6%)	Acid hydrolysis	Hi (various sources)	Yes	No	No

Figure 6.1 Summary of heterologous infection data

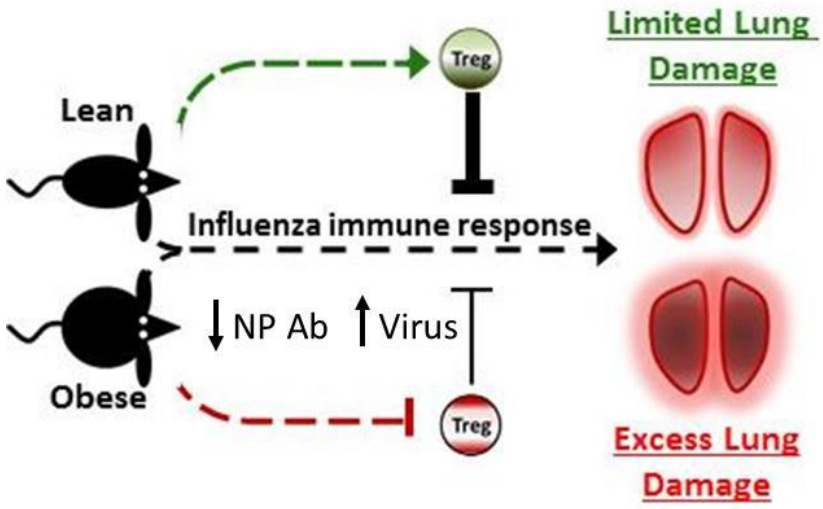

Figure 6.1. Obesity mice had fewer cross-reactive, non-neutralizing nucleoprotein antibodies during a secondary pH1N1 challenge. This likely contributed to greater levels of infectious virus, which subsequently triggered overactive immune responses and excess lung damage. Further, obese mice exhibited impaired Treg function, which likely further propagated this excess lung damage in obese mice.

REFERENCES

1. Johnson AR, Milner JJ, Makowski L (2012) The inflammation highway: metabolism accelerates inflammatory traffic in obesity. *Immunol Rev* **249**(1), 218-238.

2. Milner JJ, Beck MA (2012) The impact of obesity on the immune response to infection. *Proc Nutr Soc* **71**(02), 298-306.

3. World Health Organization. Obesity and overweight. Available at: http://www.who.int/mediacentre/factsheets/fs311/en/index.html. Accessed 20 September 2013.

4. Anonymous (2009) Intensive-care patients with severe novel influenza A (H1N1) virus infection-Michigan, June 2009. *Morb Mortal Wkly Rep* **58**(27), 749-752.

5. Louie JK, Acosta M, Samuel MC, Schechter R, Vugia DJ, Harriman K, Matyas BT (2011) A novel risk factor for a novel virus: obesity and 2009 pandemic influenza A (H1N1). *Clin Infect Dis* **52**(3), 301-312.

6. Morgan OW, Bramley A, Fowlkes A, Freedman DS, Taylor TH, Gargiullo P, Belay B, Jain S, Cox C, Kamimoto L (2010) Morbid obesity as a risk factor for hospitalization and death due to 2009 pandemic influenza A (H1N1) disease. *PLoS One* **5**(3), e9694.

7. Jain S, Kamimoto L, Bramley AM, Schmitz AM, Benoit SR, Louie J, Sugerman DE, Druckenmiller JK, Ritger KA, Chugh R (2009) Hospitalized patients with 2009 H1N1 influenza in the United States, April–June 2009. *N Engl J Med* **361**(20), 1935-1944.

8. Caballero B (2007) The global epidemic of obesity: an overview. *Epidemiol Rev* **29**(1), 1-5.

9. World Health Organization. (2009) Influenza (Seasonal). Available at: http://www.who.int/mediacentre/factsheets/fs211/en/index.html. Accessed 20 September 2013.

10. Imai M, Watanabe T, Hatta M, Das SC, Ozawa M, Shinya K, Zhong G, Hanson A, Katsura H, Watanabe S (2012) Experimental adaptation of an influenza H5 HA confers respiratory droplet transmission to a reassortant H5 HA/H1N1 virus in ferrets. *Nature* **486**(7403), 420-428.

11. Paich HA, Sheridan PA, Handy J, Karlsson EA, Schultz-Cherry S, Hudgens MG, Noah TL, Weir SS, Beck MA (2013) Overweight and obese adult humans have a defective cellular immune response to pandemic H1N1 influenza A virus. *Obesity (Silver Spring)* **21**, 2377-2386.

12. Sheridan P, Paich H, Handy J, Karlsson E, Hudgens M, et al. (2011) Obesity is associated with impaired immune response to influenza vaccination in humans. Int J Obes (Lond) 36: 1072 1077.

13. Presanis AM, De Angelis D, Hagy A, Reed C, Riley S, Cooper BS, Finelli L, Biedrzycki P, Lipsitch M (2009) The severity of pandemic H1N1 influenza in the United States, from April to July 2009: a Bayesian analysis. *PLoS Med* **6**(12), e1000207.

14. Milner JJ, Sheridan PA, Karlsson EA, Schultz-Cherry S, Shi Q, Beck MA (2013) Diet-induced obese mice exhibit altered heterologous immunity during a secondary 2009 pandemic H1N1 infection. *J Immunol* **191**, 2474-2485.

15. Anonymous. (2009) Update: novel influenza A (H1N1) virus infection-Mexico, March-May 2009. *Morb Mortal Weekly Rep* **58**(21), 585-589.

16. Centers for Disease Control and Prevention. 2009 H1N1: Overveiw of a Pandemic. Available at: http://www.cdc.gov/h1n1flu/yearinreview/yir5.htm. Accessed 20 September 2013.

17. Mertz D, Kim TH, Johnstone J, Lam P, Kuster SP, Fadel SA, Tran D, Fernandez E, Bhatnagar N, Loeb M (2013) Populations at risk for severe or complicated influenza illness: systematic review and meta-analysis. *BMJ* **347**, f5061.

18. Flier JS & Maratos-Flier E (2008) Biology of obesity. *Harrison's principle of internal medicine* **17**, 262-263.

19. Dossett LA, Heffernan D, Lightfoot M, Collier B, Diaz JJ, Sawyer RG, May AK (2008) Obesity and pulmonary complications in critically injured adults. *Chest* **134**(5), 974-980.

20. Bochicchio GV, Joshi M, Bochicchio K, Nehman S, Tracy JK, Scalea TM (2006) Impact of obesity in the critically ill trauma patient: A prospective study. *J Am Coll Surg* **203**(4), 533-538.

21. Pi-Sunyer FX (2002) The medical risks of obesity. *Obesity Surg* **12**(Supplement 1), 6-11.

22. Bercault N, Boulain T, Kuteifan K, Wolf M, Runge I, Fleury JC (2004) Obesity-related excess mortality rate in an adult intensive care unit: A risk-adjusted matched cohort study*. *Crit Care Med* **32**(4), 998.

23. Falagas ME & Kompoti M (2006) Obesity and infection. *Lancet Infect Dis* **6**(7), 438-446.

24. Olsen MA, Nepple JJ, Riew KD, Lenke LG, Bridwell KH, Mayfield J, Fraser VJ (2008) Risk factors for surgical site infection following orthopaedic spinal operations. *J Bone Joint Surg Am* **90**(1), 62-69.

25. Löfgren M, Poromaa IS, Stjerndahl JH, Renström B (2004) Postoperative infections and antibiotic prophylaxis for hysterectomy in Sweden: a study by the Swedish National Register for Gynecologic Surgery. *Acta Obstet Gynecol Scand* **83**(12), 1202-1207.

26. Cantürk Z, Cantürk NZ, Çetinarslan B, Utkan NZ, Tarkun I (2003) Nosocomial infections and obesity in surgical patients. *Obesity* **11**(6), 769-775.

27. Dowsey MM & Choong PFM (2008) Obesity is a major risk factor for prosthetic infection after primary hip arthroplasty. *Clinical Orthopaedics and Related Research*® **466**(1), 153-158.

28. Potapov EV, Loebe M, Anker S, Stein J, Bondy S, Nasseri BA, Sodian R, Hausmann H, Hetzer R (2003) Impact of body mass index on outcome in patients after coronary artery bypass grafting with and without valve surgery. *Eur Heart J* **24**(21), 1933.

29. Newell MA, Bard MR, Goettler CE, Toschlog EA, Schenarts PJ, Sagraves SG, Holbert D, Pories WJ, Rotondo MF (2007) Body mass index and outcomes in critically injured blunt trauma patients: weighing the impact. *J Am Coll Surg* **204**(5), 1056-1061.

30. Lillenfeld DE, Vlahov D, Tenney JH, McLaughlin JS (1988) Obesity and diabetes as risk factors for postoperative wound infections after cardiac surgery. *Am J Infect Control* **16**(1), 3-6.

31. Knight RJ, Bodian C, Rodriguez-Laiz G, Guy SR, Fishbein TM (2000) Risk factors for intra-abdominal infection after pancreas transplantation. *Am J Surg* **179**(2), 99-102.

32. Davenport DL, Xenos ES, Hosokawa P, Radford J, Henderson WG, Endean ED (2009) The influence of body mass index obesity status on vascular surgery 30-day morbidity and mortality. *J Vasc Surg* **49**(1), 140-147. e1.

33. Dowsey MM & Choong PFM (2009) Obese diabetic patients are at substantial risk for deep infection after primary TKA. *Clin Orthop Relat Res* **467**(6), 1577-1581.

34. Swenne C, Lindholm C, Borowiec J, Carlsson M (2004) Surgical-site infections within 60 days of coronary artery by-pass graft surgery. *J Hosp Infect* **57**(1), 14-24.

35. Dossett LA, Dageforde LA, Swenson BR, Metzger R, Bonatti H, Sawyer RG, May AK (2009) Obesity and Site-Specific Nosocomial Infection Risk in the Intensive Care Unit*. *Surg infect* **10**(2), 137-142.

36. Mathison CJ (2003) Skin and wound care challenges in the hospitalized morbidly obese patient. *J Wound Ostomy Continence Nurs* **30**(2), 78.

37. Hanley MJ, Abernethy DR, Greenblatt DJ (2010) Effect of obesity on the pharmacokinetics of drugs in humans. *Clin Pharmacokinet* **49**(2), 71.

38. Ylöstalo P, Suominen-Taipale L, Reunanen A, Knuuttila M (2008) Association between body weight and periodontal infection. *J Clin Periodontol* **35**(4), 297-304.

39. Herwaldt LA, Cullen JJ, French P, Hu J, Pfaller MA, Wenzel RP, Perl TM (2004) Preoperative risk factors for nasal carriage of Staphylococcus aureus. *Infect Control Hosp Epidemiol* , 481-484.

40. Perdichizzi G, Bottari M, Pallio S, Fera M, Carbone M, Barresi G (1996) Gastric infection by Helicobacter pylori and antral gastritis in hyperglycermic obese and in diabetic subjects. *The New microbiol* **19**(2), 149-154.

41. Karjala Z, Neal D, Rohrer J (2011) Association between HSV1 Seropositivity and Obesity: Data from the National Health and Nutritional Examination Survey, 2007–2008. *PloS one* **6**(5), e19092.

42. Bearden DT & Rodvold KA (2000) Dosage adjustments for antibacterials in obese patients: applying clinical pharmacokinetics. *Clin Pharmacokinet* **38**(5), 415-426.

43. Bauer L, Black D, Lill J (1998) Vancomycin dosing in morbidly obese patients. *Eur J Clin Pharmacol* **54**(8), 621-625.

44. Stein GE, Schooley SL, Peloquin CA, Kak V, Havlichek DH, Citron DM, Tyrrell KL, Goldstein EJC (2005) Pharmacokinetics and pharmacodynamics of linezolid in obese patients with cellulitis. *Ann Pharmacother* **39**(3), 427.

45. Mancuso P (2010) Obesity and lung inflammation. *J Appl Physiol* **108**(3), 722.

46. Akiyama N, Segawa T, Ida H, Mezawa H, Noya M, Tamez S, Urashima M (2011) Bimodal Effects of Obesity Ratio on Disease Duration of Respiratory Syncytial Virus Infection in Children. *Allergol Int.*

47. Jedrychowski W, Maugeri U, Flak E, Mroz E, Bianchi I (1998) Predisposition to acute respiratory infections among overweight preadolescent children: an epidemiologic study in Poland. *Public Health* **112**(3), 189-195.

48. Brandt M, Harder K, Walluscheck KP, Schöttler J, Rahimi A, Möller F, Cremer J (2001) Severe obesity does not adversely affect perioperative mortality and morbidity in coronary artery bypass surgery* 1. *European journal of cardio-thoracic surgery* **19**(5), 662-666.

49. McClean K, Kee F, Young I, Elborn J (2008) Obesity and the lung: 1· Epidemiology. *Thorax* **63**(7), 649.

50. Nishina PM, Lowe S, Wang J, Paigen B (1994) Characterization of plasma lipids in genetically obese mice: the mutants obese, diabetes, fat, tubby, and lethal yellow. *Metab Clin Exp* **43**(5), 549-553.

51. Pelleymounter MA, Cullen MJ, Baker MB, Hecht R, Winters D, Boone T, Collins F (1995) Effects of the obese gene product on body weight regulation in ob/ob mice. *Science* **269**(5223), 540.

52. La Cava A & Matarese G (2004) The weight of leptin in immunity. *Nat Rev Immunol* **4**(5), 371-379.

53. Mancuso P, Gottschalk A, Phare SM, Peters-Golden M, Lukacs NW, Huffnagle GB (2002) Leptin-deficient mice exhibit impaired host defense in Gram-negative pneumonia. *J Immunol* **168**(8), 4018.

54. Hsu A, Aronoff D, Phipps J, Goel D, Mancuso P (2007) Leptin improves pulmonary bacterial clearance and survival in ob/ob mice during pneumococcal pneumonia. *Clin Exp Immunol* **150**(2), 332-339.

55. Wieland CW, Florquin S, Chan ED, Leemans JC, Weijer S, Verbon A, Fantuzzi G, Van Der Poll T (2005) Pulmonary Mycobacterium tuberculosis infection in leptin-deficient ob/ob mice. *Int Immunol* **17**(11), 1399.

56. Ordway D, Henao-Tamayo M, Smith E, Shanley C, Harton M, Troudt JL, Bai X, Basaraba RJ, Orme IM, Chan ED (2008) Animal model of Mycobacterium abscessus lung infection. *J Leukoc Biol* **83**(6), 1502.

57. Park S, Rich J, Hanses F, Lee JC (2009) Defects in innate immunity predispose C57BL/6J-Leprdb/Leprdb mice to infection by Staphylococcus aureus. *Infect Immun* **77**(3), 1008.

58. Ikejima S, Sasaki S, Sashinami H, Mori F, Ogawa Y, Nakamura T, Abe Y, Wakabayashi K, Suda T, Nakane A (2005) Impairment of host resistance to Listeria monocytogenes infection in liver of db/db and ob/ob mice. *Diabetes* **54**(1), 182.

59. Plotkin B, Paulson D, Chelich A, Jurak D, Cole J, Kasimos J, Burdick J, Casteel N (1996) Immune responsiveness in a rat model for type II diabetes (Zucker rat, fa/fa): susceptibility to Candida albicans infection and leucocyte function. *J Med Microbiol* **44**(4), 277.

60. Smith AG, Sheridan PA, Harp JB, Beck MA (2007) Diet-induced obese mice have increased mortality and altered immune responses when infected with influenza virus. *J Nutr* **137**(5), 1236-1243.

61. Karlsson EA, Sheridan PA, Beck MA (2010) Diet-induced obesity impairs the T cell memory response to influenza virus infection. *J Immunol* **184**(6), 3127.

62. Shamshiev AT, Ampenberger F, Ernst B, Rohrer L, Marsland BJ, Kopf M (2007) Dyslipidemia inhibits Toll-like receptor–induced activation of CD8α-negative dendritic cells and protective Th1 type immunity. *J Exp Med* **204**(2), 441-452.

63. Verwaerde C, Delanoye A, Macia L, Tailleux A, Wolowczuk I (2006) Influence of High-Fat Feeding on Both Naive and Antigen-Experienced T-Cell Immune Response in DO10. 11 Mice. *Scand J Immunol* **64**(5), 457-466.

64. Huszar D, Lynch CA, Fairchild-Huntress V, Dunmore JH, Fang Q, Berkemeier LR, Gu W, Kesterson RA, Boston BA, Cone RD (1997) Targeted disruption of the melanocortin-4 receptor results in obesity in mice. *Cell* **88**(1), 131-141.

65. Kennedy AJ, Ellacott KL, King VL, Hasty AH (2010) Mouse models of the metabolic syndrome. *Dis Model Mech* **3**(3-4), 156-166.

66. Warden CCH (2008) Comparisons of Diets Used in Animal Models of High-Fat Feeding. *Cell Metab* **7**(4), 277.

67. O'Brien KB, Vogel P, Duan S, Govorkova EA, Webby RJ, McCullers JA, Schultz-Cherry S (2012) Impaired Wound Healing Predisposes Obese Mice to Severe Influenza Virus Infection. *J Infect Dis* **205**(2), 252-261.

68. Kim YH, Kim JK, Kim DJ, Nam JH, Shim SM, Choi YK, Lee CH, Poo H (2012) Diet-induced obesity dramatically reduces the efficacy of a 2009 pandemic H1N1 vaccine in a mouse model. *J Infect Dis* **205**(2), 244-251.

69. Benoit B, Plaisancié P, Awada M, Géloën A, Estienne M, Capel F, Malpuech-Brugère C, Debard C, Pesenti S, Morio B (2013) High-fat diet action on adiposity, inflammation, and insulin sensitivity depends on the control low-fat diet. *Nutr Res* **33**(11), 952-960.

70. Sumiyoshi M, Sakanaka M, Kimura Y (2006) Chronic intake of high-fat and high-sucrose diets differentially affects glucose intolerance in mice. *J Nutr* **136**(3), 582-587.

71. Jain S & Chaves SS (2011) Obesity and Influenza. *Clin Infect Dis* **53**(5), 422-424.

72. Hanslik T, Boelle PY, Flahault A (2010) Preliminary estimation of risk factors for admission to intensive care units and for death in patients infected with A (H1N1) 2009 influenza virus, France, 2009-2010. *PLoS Currents* **2**.

73. Louie JK, Acosta M, Samuel MC, Schechter R, Vugia DJ, Harriman K, Matyas BT, the California Pandemic (H1N1) Working Group (2011) A Novel Risk Factor for a Novel Virus: Obesity and 2009 Pandemic Influenza A (H1N1). *Clin Infect Dis*.

74. Santa-Olalla Peralta P, Cortes-Garcia M, Vicente-Herrero M, Castrillo-Villamandos C, Arias-Bohigas P, Pachon-del Amo I, Sierra-Moros MJ, Surveillance Group for New Influenza A(H1N1) Virus Investigation and Control Team in Spain (2010) Risk factors for disease severity among hospitalised patients with 2009 pandemic influenza A (H1N1) in Spain, April - December 2009. *Euro Surveill* **15**(38), 19667.

75. Morgan OW, Bramley A, Fowlkes A, Freedman DS, Taylor TH, Gargiullo P, Belay B, Jain S, Cox C, Kamimoto L (2010) Morbid obesity as a risk factor for hospitalization and death due to 2009 pandemic influenza A (H1N1) disease. *PLoS One* **5**(3), e9694.

76. Díaz E, Rodríguez A, Martin-Loeches I, Lorente L, del Mar Martín M, Pozo JC, Montejo JC, Estella A, Arenzana Á, Rello J (2011) Impact of obesity in patients infected with 2009 influenza A (H1N1). *Chest* **139**(2), 382.

77. Kwong JC, Campitelli MA, Rosella LC (2011) Obesity and Respiratory Hospitalizations During Influenza Seasons in Ontario, Canada: A Cohort Study. *Clin Infect Dis* **53**(5), 413-421.

78. Karlsson EA, Sheridan PA, Beck MA (2010) Diet-Induced Obesity Impairs the T Cell Memory Response to Influenza Virus Infection. *J Immunol* **184**(6), 3127-3133.

79. Smith AG, Sheridan PA, Harp JB, Beck MA (2007) Diet-induced obese mice have increased mortality and altered immune responses when infected with influenza virus. *J Nutr* **137**(5), 1236-1243.

80. Zhang A, Sun H, Han Y, Yan G, Wang X (2013) Urinary Metabolic Biomarker and Pathway Study of Hepatitis B Virus Infected Patients Based on UPLC-MS System. *PloS one* **8**(5), e64381.

81. Easterbrook JD, Dunfee RL, Schwartzman LM, Jagger BW, Sandouk A, Kash JC, Memoli MJ, Taubenberger JK (2011) Obese mice have increased morbidity and mortality compared to non-obese mice during infection with the 2009 pandemic H1N1 influenza virus. *Influenza other respi viruses* **5**(6), 418-425.

82. Zhang AJ, To KK, Li C, Lau CC, Poon VK, Chan CC, Zheng B, Hung IF, Lam KS, Xu A (2013) Leptin mediates the pathogenesis of severe 2009 pandemic influenza A (H1N1) infection associated with cytokine dysregulation in mice with diet-induced obesity. *J Infect Dis* **207**(8), 1270-1280.

83. Bouvier NM & Palese P (2008) The biology of influenza viruses. *Vaccine* **26**, D49-D53.

84. Krumbholz A, Philipps A, Oehring H, Schwarzer K, Eitner A, Wutzler P, Zell R (2011) Current knowledge on PB1-F2 of influenza A viruses. *Med Microbiol Immunol (Berl)* **200**(2), 69-75.

85. Liu J, Xiao H, Lei F, Zhu Q, Qin K, Zhang XW, Zhang XL, Zhao D, Wang G, Feng Y, Ma J, Liu W, Wang J, Gao GF (2005) Highly pathogenic H5N1 influenza virus infection in migratory birds. *Science* **309**(5738), 1206.

86. Webster RG & Rott R (1987) Influenza virus A pathogenicity: the pivotal role of hemagglutinin. *Cell* **50**(5), 665-666.

87. Tong S, Li Y, Rivailler P, Conrardy C, Castillo DA, Chen LM, Recuenco S, Ellison JA, Davis CT, York IA, Turmelle AS, Moran D, Rogers S, Shi M, Tao Y, Weil MR, Tang K, Rowe LA, Sammons S, Xu X, Frace M, Lindblade KA, Cox NJ, Anderson LJ, Rupprecht CE, Donis RO (2012) A distinct lineage of influenza A virus from bats. *Proc Natl Acad Sci U S A* **109**(11), 4269-4274.

88. Fodor E (2013) The RNA polymerase of influenza a virus: mechanisms of viral transcription and replication. *Acta Virol* **57**(2), 113-122.

89. Treanor J (2004) Influenza vaccine—outmaneuvering antigenic shift and drift. *N Engl J Med* **350**(3), 218-220.

90. Morens DM, Taubenberger JK, Fauci AS (2010) The 2009 H1N1 pandemic influenza virus: what next? *MBio* **1**(4), 10.1128/mBio.00211-10.

91. Peiris JS, de Jong MD, Guan Y (2007) Avian influenza virus (H5N1): a threat to human health. *Clin Microbiol Rev* **20**(2), 243-267.

92. Bertram S, Glowacka I, Steffen I, Kühl A, Pöhlmann S (2010) Novel insights into proteolytic cleavage of influenza virus hemagglutinin. *Rev Med Virol* **20**(5), 298-310.

93. Beigel J, Farrar J, Han A, Hayden F, Hyer R, De Jong M (2005) Avian influenza A (H5N1) infection in humans. *N Engl J Med* **353**(1374-1385).

94. Lam TT, Wang J, Shen Y, Zhou B, Duan L, Cheung C, Ma C, Lycett SJ, Leung CY, Chen X (2013) The genesis and source of the H7N9 influenza viruses causing human infections in China. *Nature* **502**(7470), 241-244.

95. Otte A, Sauter M, Alleva L, Baumgarte S, Klingel K, Gabriel G (2011) Differential Host Determinants Contribute to the Pathogenesis of 2009 Pandemic H1N1 and Human H5N1 Influenza A Viruses in Experimental Mouse Models. *Am J Pathol* **179**(1), 230-239.

96. Itoh Y, Shinya K, Kiso M, Watanabe T, Sakoda Y, Hatta M, Muramoto Y, Tamura D, Sakai-Tagawa Y, Noda T (2009) In vitro and in vivo characterization of new swine-origin H1N1 influenza viruses. *Nature* **460**(7258), 1021-1025.

97. Maines TR, Jayaraman A, Belser JA, Wadford DA, Pappas C, Zeng H, Gustin KM, Pearce MB, Viswanathan K, Shriver ZH (2009) Transmission and pathogenesis of swine-origin 2009 A (H1N1) influenza viruses in ferrets and mice. *Science* **325**(5939), 484-487.

98. Munster VJ, De Wit E, van den Brand JMA, Herfst S, Schrauwen EJA, Bestebroer TM, Van De Vijver D, Boucher CA, Koopmans M, Rimmelzwaan GF (2009) Pathogenesis and transmission of swine-origin 2009 A (H1N1) influenza virus in ferrets. *Science* **325**(5939), 481-483.

99. Kelly HA (2010) A pandemic response to a disease of predominantly seasonal intensity. *Med J Aust* **192**(2), 81-83.

100. Girard MP, Tam JS, Assossou OM, Kieny MP (2010) The 2009 A (H1N1) influenza virus pandemic: A review. *Vaccine* **28**(31), 4895-4902.

101. Writing Committe of the WHO Consultation (2010) Clinical Aspects of Pandemic 2009 Influenza A (H1N1) Virus Infection. *N Engl J Med* **362**(18), 1708-1719.

102. Hancock K, Veguilla V, Lu X, Zhong W, Butler EN, Sun H, Liu F, Dong L, DeVos JR, Gargiullo PM (2009) Cross-reactive antibody responses to the 2009 pandemic H1N1 influenza virus. *N Engl J Med* **361**(20), 1945-1952.

103. Ikonen N, Strengell M, Kinnunen L, Osterlund P, Pirhonen J, Broman M, Davidkin I, Ziegler T, Julkunen I (2010) High frequency of cross-reacting antibodies against 2009 pandemic influenza A (H1N1) virus among the elderly in Finland. *Euro Surveill* **15**(5), 19478.

104. Anonymous (2009) Serum cross-reactive antibody response to a novel influenza A (H1N1) virus after vaccination with seasonal influenza vaccine. *Morb Mortal Weekly Rep* **58**(19), 521-524.

105. Lee VJ, Tay JK, Chen MIC, Phoon M, Xie M, Wu Y, Lee CXX, Yap J, Sakharkar K, Sakharkar M (2010) Inactivated trivalent seasonal influenza vaccine induces limited cross-reactive neutralizing antibody responses against 2009 pandemic and 1934 PR8 H1N1 strains. *Vaccine* **28**(42), 6852-6857.

106. Iorio A, Camilloni B, Lepri E, Neri M, Basileo M, Azzi A (2011) Induction of Cross-Reactive Antibodies to 2009 Pandemic H1N1 Influenza Virus (pH1N1) After Seasonal Vaccination (Winters 2003/04 and 2007/08). *Procedia Vaccinol* **4**, 50-58.

107. Iorio AM, Bistoni O, Galdiero M, Lepri E, Camilloni B, Russano AM, Neri M, Basileo M, Spinozzi F (2012) Influenza viruses and cross-reactivity in healthy adults: Humoral and cellular immunity induced by seasonal 2007/2008 influenza vaccination against vaccine antigens and 2009 A (H1N1) pandemic influenza virus. *Vaccine* **30**(9), 1617-1623.

108. Tripathi S, White MR, Hartshorn KL (2013) The amazing innate immune response to influenza A virus infection. *Innate Immun* .

109. Wilkins C & Gale Jr M (2010) Recognition of viruses by cytoplasmic sensors. *Curr Opin Immunol* **22**(1), 41-47.

110. Fukuyama S & Kawaoka Y (2011) The pathogenesis of influenza virus infections: the contributions of virus and host factors. *Curr Opin Immunol* **23**(4), 481-486.

111. McGill J, Heusel JW, Legge KL (2009) Innate immune control and regulation of influenza virus infections. *J Leukoc Biol* **86**(4), 803-812.

112. Miao H, Hollenbaugh JA, Zand MS, Holden-Wiltse J, Mosmann TR, Perelson AS, Wu H, Topham DJ (2010) Quantifying the early immune response and adaptive immune response kinetics in mice infected with influenza A virus. *J Virol* **84**(13), 6687-6698.

113. Thomas PG, Keating R, Hulse-Post DJ, Doherty PC (2006) Cell-mediated protection in influenza infection. *Emerg Infect Dis* **12**(1), 48-54.

114. Aoshi T, Koyama S, Kobiyama K, Akira S, Ishii KJ (2011) Innate and adaptive immune responses to viral infection and vaccination. *Curr Opin Virol* **1**(4), 226-232.

115. Kim TS, Sun J, Braciale TJ (2011) T cell responses during influenza infection: getting and keeping control. *Trends Immunol* **32**(5), 225-231.

116. Román E, Miller E, Harmsen A, Wiley J, von Andrian UH, Huston G, Swain SL (2002) CD4 effector T cell subsets in the response to influenza: heterogeneity, migration, and function. *J Exp Med* **196**(7), 957-968.

117. Flynn KJ, Belz GT, Altman JD, Ahmed R, Woodland DL, Doherty PC (1998) Virus-Specific CD8< sup> </sup> T Cells in Primary and Secondary Influenza Pneumonia. *Immunity* **8**(6), 683-691.

118. Swain SL, Dutton RW, Woodland DL (2004) T cell responses to influenza virus infection: effector and memory cells. *Viral Immunol* **17**(2), 197-209.

119. Pearce EL, Walsh MC, Cejas PJ, Harms GM, Shen H, Wang L, Jones RG, Choi Y (2009) Enhancing CD8 T-cell memory by modulating fatty acid metabolism. *Nature* **460**(7251), 103-107.

120. Waffarn EE & Baumgarth N (2011) Protective B cell responses to flu--no fluke! *J Immunol* **186**(7), 3823-3829.

121. Wolf AI, Mozdzanowska K, Quinn WJ,3rd, Metzgar M, Williams KL, Caton AJ, Meffre E, Bram RJ, Erickson LD, Allman D, Cancro MP, Erikson J (2011) Protective antiviral antibody responses in a mouse model of influenza virus infection require TACI. *J Clin Invest* **121**(10), 3954-3964.

122. Osterholm MT, Kelley NS, Sommer A, Belongia EA (2012) Efficacy and effectiveness of influenza vaccines: a systematic review and meta-analysis. *Lancet Infect Dis* **12**(1), 36-44.

123. Tinoco JC, Pavia-Ruz N, Cruz-Valdez A, Doniz CA, Chandrasekaran V, Dewé W, Liu A, Innis BL, Jain VK (2014) Immunogenicity, reactogenicity, and safety of inactivated quadrivalent influenza vaccine candidate versus inactivated trivalent influenza vaccine in healthy adults aged≥ 18 years: A phase III, randomized trial. *Vaccine* .

124. Ambrose CS, Levin MJ, Belshe RB (2011) The relative efficacy of trivalent live attenuated and inactivated influenza vaccines in children and adults. *Influenza other respi viruses* **5**(2), 67-75.

125. Weber DJ, Rutala WA, Samsa GP, Santimaw JE, Lemon SM (1985) Obesity as a predictor of poor antibody response to hepatitis B plasma vaccine. *JAMA: The Journal of the American Medical Association* **254**(22), 3187.

126. Weber DJ, Rutala WA, Samsa GP, Bradshaw SE, Lemon SM (1986) Impaired immunogenicity of hepatitis B vaccine in obese persons. *N Engl J Med* **314**(21), 1393-1393.

127. Eliakim A, Swindt C, Zaldivar F, Casali P, Cooper DM (2006) Reduced tetanus antibody titers in overweight children. *Autoimmunity* **39**(2), 137-141.

128. Middleman AB, Anding R, Tung C (2010) Effect of needle length when immunizing obese adolescents with Hepatitis B vaccine. *Pediatrics* **125**(3), e508.

129. Valkenburg SA, Rutigliano JA, Ellebedy AH, Doherty PC, Thomas PG, Kedzierska K (2011) Immunity to seasonal and pandemic influenza A viruses. *Microb Infect* **13**, 489-501.

130. Ge X, Tan V, Bollyky PL, Standifer NE, James EA, Kwok WW (2010) Assessment of seasonal influenza A virus-specific CD4 T-cell responses to 2009 pandemic H1N1 swine-origin influenza A virus. *J Virol* **84**(7), 3312-3319.

131. Tu W, Mao H, Zheng J, Liu Y, Chiu SS, Qin G, Chan PL, Lam KT, Guan J, Zhang L, Guan Y, Yuen K, Peiris J, Lau Y (2010) Cytotoxic T lymphocytes established by seasonal human influenza cross-react against 2009 pandemic H1N1 influenza virus. *J Virol* **84**(13), 6527-6535.

132. Subbramanian RA, Basha S, Shata MT, Brady RC, Bernstein DI (2010) Pandemic and seasonal H1N1 influenza hemagglutinin-specific T cell responses elicited by seasonal influenza vaccination. *Vaccine* **28**(52), 8258-8267.

133. Guo H, Santiago F, Lambert K, Takimoto T, Topham DJ (2011) T cell-mediated protection against lethal 2009 pandemic H1N1 influenza virus infection in a mouse model. *J Virol* **85**(1), 448-455.

134. Greenbaum JA, Kotturi MF, Kim Y, Oseroff C, Vaughan K, Salimi N, Vita R, Ponomarenko J, Scheuermann RH, Sette A (2009) Pre-existing immunity against swine-origin H1N1 influenza viruses in the general human population. *Proc Natl Acad Sci U S A* **106**(48), 20365-20370.

135. Xing Z & Cardona CJ (2009) Preexisting immunity to pandemic (H1N1) 2009. *Emerg Infect Dis* **15**(11), 1847-1549.

136. Skountzou I, Koutsonanos DG, Kim JH, Powers R, Satyabhama L, Masseoud F, Weldon WC, del Pilar Martin M, Mittler RS, Compans R, Jacob J (2010) Immunity to pre-1950 H1N1 influenza viruses confers cross-protection against the pandemic swine-origin 2009 A (H1N1) influenza virus. *J Immunol* **185**(3), 1642-1649.

137. Alam S & Sant AJ (2011) Infection with Seasonal Influenza Virus Elicits CD4 T Cells Specific for Genetically Conserved Epitopes That Can Be Rapidly Mobilized for Protective Immunity to Pandemic H1N1 Influenza Virus. *J Virol* **85**(24), 13310-13321.

138. Hillaire MLB, van Trierum SE, Kreijtz JHCM, Bodewes R, Geelhoed-Mieras MM, Nieuwkoop NJ, Fouchier RAM, Kuiken T, Osterhaus ADME, Rimmelzwaan GF (2011) Cross-protective immunity to influenza pH1N1 2009 viruses induced by seasonal A (H3N2) virus is mediated by virus-specific T cells. *J Gen Virol* **92**, 2339-2349.

139. Sun K, Ye J, Perez DR, Metzger DW (2011) Seasonal FluMist vaccination induces cross-reactive T cell immunity against H1N1 (2009) influenza and secondary bacterial infections. *J Immunol* **186**(2), 987-993.

140. Couch RB, Atmar RL, Franco LM, Quarles JM, Niño D, Wells JM, Arden N, Cheung S, Belmont JW (2012) Prior infections with seasonal influenza A/H1N1 virus reduced the illness severity and epidemic intensity of pandemic H1N1 influenza in healthy adults. *Clin Infect Dis* **54**(3), 311-317.

141. LaMere MW, Lam HT, Moquin A, Haynes L, Lund FE, Randall TD, Kaminski DA (2011) Contributions of antinucleoprotein IgG to heterosubtypic immunity against influenza virus. *J Immunol* **186**(7), 4331-4339.

142. Fang Y, Banner D, Kelvin AA, Huang SSH, Paige CJ, Corfe SA, Kane KP, Bleackley RC, Rowe T, Leon AJ (2012) Seasonal H1N1 Influenza Virus Infection Induces Cross-Protective Pandemic H1N1 Virus Immunity through a CD8-Independent, B Cell-Dependent Mechanism. *J Virol* **86**(4), 2229-2238.

143. Bulló M, García-Lorda P, Megias I, Salas-Salvadó J (2003) Systemic inflammation, adipose tissue tumor necrosis factor, and leptin expression. *Obesity* **11**(4), 525-531.

144. Fantuzzi G (2005) Adipose tissue, adipokines, and inflammation. *J Allergy Clin Immunol* **115**(5), 911-919.

145. Tilg H & Moschen AR (2006) Adipocytokines: mediators linking adipose tissue, inflammation and immunity. *Nat Rev Immunol* **6**(10), 772-783.

146. Fenton J, Nunez N, Yakar S, Perkins S, Hord N, Hursting S (2009) Diet-induced adiposity alters the serum profile of inflammation in C57BL/6N mice as measured by antibody array. *Diabetes Obes and Metab* **11**(4), 343-354.

147. Defronzo RA, Soman V, Sherwin RS, Hendler R, Felig P (1978) Insulin binding to monocytes and insulin action in human obesity, starvation, and refeeding. *J Clin Invest* **62**(1), 204.

148. ROBERT A, GRUNBERGER G, CARPENTIER JL, DAYER JM, ORCI L, GORDEN P (1984) The insulin receptor of a human monocyte-like cell line: characterization and function. *Endocrinology* **114**(1), 247.

149. Trischitta V, Brunetti A, Chiavetta A, Benzi L, Papa V, Vigneri R (1989) Defects in insulin-receptor internalization and processing in monocytes of obese subjects and obese NIDDM patients. *Diabetes* **38**(12), 1579.

150. Liang CP, Han S, Okamoto H, Garnemolla R, Tabas I, Accili D, Tall AR (2004) Increased CD36 protein as a response to defective insulin signaling in macrophages. *J Clin Invest* **113**(5), 764-773.

151. Stentz FB & Kitabchi AE (2003) Activated T lymphocytes in type 2 diabetes: implications from in vitro studies. *Curr Drug Targets* **4**(6), 493-503.

152. Viardot A, Grey ST, Mackay F, Chisholm D (2007) Potential antiinflammatory role of insulin via the preferential polarization of effector T cells toward a T helper 2 phenotype. *Endocrinology* **148**(1), 346.

153. Helderman J (1981) Role of insulin in the intermediary metabolism of the activated thymic-derived lymphocyte. *J Clin Invest* **67**(6), 1636.

154. MacIver NJ, Jacobs SR, Wieman HL, Wofford JA, Coloff JL, Rathmell JC (2008) Glucose metabolism in lymphocytes is a regulated process with significant effects on immune cell function and survival. *J Leukoc Biol* **84**(4), 949.

155. Koerner A (2005) Adipocytokines: leptin--the classical, resistin--the controversical, adiponectin--the promising, and more to come. *Best Pract Res Clin Endocrino Metab* **19**(4), 525-546.

156. Wolf AM, Wolf D, Rumpold H, Enrich B, Tilg H (2004) Adiponectin induces the anti-inflammatory cytokines IL-10 and IL-1RA in human leukocytes. *Biochem Biophys Res Commun* **323**(2), 630-635.

157. Kim K, Kim JK, Han SH, Lim JS, Kim KI, Cho DH, Lee MS, Lee JH, Yoon DY, Yoon SR (2006) Adiponectin is a negative regulator of NK cell cytotoxicity. *J Immunol* **176**(10), 5958.

158. Ziegler-Heitbrock H, Wedel A, Schraut W, Ströbel M, Wendelgass P, Sternsdorf T, Bäuerle P, Haas JG, Riethmüller G (1994) Tolerance to lipopolysaccharide involves mobilization of nuclear factor kappa B with predominance of p50 homodimers. *J Biol Chem* **269**(25), 17001.

159. Lord GM, Matarese G, Howard JK, Baker RJ, Bloom SR, Lechler RI (1998) Leptin modulates the T-cell immune response and reverses starvation-induced immunosuppression. *Nature* **394**(6696), 897-900.

160. Zarkesh-Esfahani H, Pockley G, Metcalfe RA, Bidlingmaier M, Wu Z, Ajami A, Weetman AP, Strasburger CJ, Ross RJM (2001) High-dose leptin activates human leukocytes via receptor expression on monocytes. *J Immunol* **167**(8), 4593.

161. Zhao Y, Sun R, You L, Gao C, Tian Z (2003) Expression of leptin receptors and response to leptin stimulation of human natural killer cell lines. *Biochem Biophys Res Commun* **300**(2), 247-252.

162. Papathanassoglou E, El-Haschimi K, Li XC, Matarese G, Strom T, Mantzoros C (2006) Leptin receptor expression and signaling in lymphocytes: kinetics during lymphocyte activation, role in lymphocyte survival, and response to high fat diet in mice. *J Immunol* **176**(12), 7745-7752.

163. Caldefie-Chezet F, Poulin A, Tridon A, Sion B, Vasson M (2001) Leptin: a potential regulator of polymorphonuclear neutrophil bactericidal action? *J Leukoc Biol* **69**(3), 414.

164. Loffreda S, Yang S, Lin H, Karp C, Brengman M, Wang D, Klein A, Bulkley G, Bao C, Noble P (1998) Leptin regulates proinflammatory immune responses. *The FASEB journal* **12**(1), 57.

165. Gainsford T, Willson TA, Metcalf D, Handman E, McFarlane C, Ng A, Nicola NA, Alexander WS, Hilton DJ (1996) Leptin can induce proliferation, differentiation, and functional activation of hemopoietic cells. *Proc Natl Acad Sci U S A* **93**(25), 14564.

166. Caldefie-Chezet F, Poulin A, Vasson MP (2003) Leptin regulates functional capacities of polymorphonuclear neutrophils. *Free Radic Res* **37**(8), 809-814.

167. Montecucco F, Bianchi G, Gnerre P, Bertolotto M, Dallegri F, Ottonello L (2006) Induction of Neutrophil Chemotaxis by Leptin. *Ann N Y Acad Sci* **1069**(1), 463-471.

168. Tian Z, Sun R, Wei H, Gao B (2002) Impaired natural killer (NK) cell activity in leptin receptor deficient mice: leptin as a critical regulator in NK cell development and activation. *Biochem Biophys Res Commun* **298**(3), 297-302.

169. Howard JK, Lord GM, Matarese G, Vendetti S, Ghatei MA, Ritter MA, Lechler RI, Bloom SR (1999) Leptin protects mice from starvation-induced lymphoid atrophy and increases thymic cellularity in ob/ob mice. *J Clin Invest* **104**, 1051-1059.

170. Claycombe K, King LE, Fraker PJ (2008) A role for leptin in sustaining lymphopoiesis and myelopoiesis. *Proc Natl Acad Sci U S A* **105**(6), 2017.

171. Martín-Romero C, Santos-Alvarez J, Goberna R, Sanchez-Margalet V (2000) Human leptin enhances activation and proliferation of human circulating T lymphocytes. *Cell Immunol* **199**(1), 15-24.

172. Matarese G, Moschos S, Mantzoros CS (2005) Leptin in immunology. *J Immunol* **174**(6), 3137-42

173. Nave H, Mueller G, Siegmund B, Jacobs R, Stroh T, Schueler U, Hopfe M, Behrendt P, Buchenauer T, Pabst R (2008) Resistance of Janus kinase-2 dependent leptin signaling in natural killer (NK) cells: a novel mechanism of NK cell dysfunction in diet-induced obesity. *Endocrinology* **149**(7), 3370.

174. Bjørbæk C, Elmquist JK, Frantz JD, Shoelson SE, Flier JS (1998) Identification of SOCS-3 as a potential mediator of central leptin resistance. *Mol Cell* **1**(4), 619-625.

175. Sahu A (2002) Resistance to the satiety action of leptin following chronic central leptin infusion is associated with the development of leptin resistance in neuropeptide Y neurones. *J Neuroendocrinol* **14**(10), 796-804.

176. Munzberg H & Myers MG (2005) Molecular and anatomical determinants of central leptin resistance. *Nat Neurosci* **8**(5), 566-570.

177. Furukawa S, Fujita T, Shimabukuro M, Iwaki M, Yamada Y, Nakajima Y, Nakayama O, Makishima M, Matsuda M, Shimomura I (2004) Increased oxidative stress in obesity and its impact on metabolic syndrome. *J Clin Invest* **114**(12), 1752-1761.

178. Imai Y, Kuba K, Neely GG, Yaghubian-Malhami R, Perkmann T, van Loo G, Ermolaeva M, Veldhuizen R, Leung Y, Wang H (2008) Identification of oxidative stress and Toll-like receptor 4 signaling as a key pathway of acute lung injury. *Cell* **133**(2), 235-249.

179. Turnbaugh PJ, Ley RE, Mahowald MA, Magrini V, Mardis ER, Gordon JI (2006) An obesity-associated gut microbiome with increased capacity for energy harvest. *Nature* **444**(7122), 1027-1131.

180. Ichinohe T, Pang IK, Kumamoto Y, Peaper DR, Ho JH, Murray TS, Iwasaki A (2011) Microbiota regulates immune defense against respiratory tract influenza A virus infection. *Proc Natl Acad Sci U S A* **108**(13), 5354-5359.

181. Pacchiarotta T, Deelder AM, Mayboroda OA (2012) Metabolomic investigations of human infections. *Bioanalysis* **4**(8), 919-925.

182. Li JV, Holmes E, Saric J, Keiser J, Dirnhofer S, Utzinger J, Wang Y (2009) Metabolic profiling of a< i> Schistosoma mansoni</i> infection in mouse tissues using magic angle spinning-nuclear magnetic resonance spectroscopy. *Int J Parasitol* **39**(5), 547-558.

183. Saric J, Li JV, Wang Y, Keiser J, Veselkov K, Dirnhofer S, Yap IK, Nicholson JK, Holmes E, Utzinger J (2009) Panorganismal metabolic response modeling of an experimental Echinostoma caproni infection in the mouse. *J Proteome Res* **8**(8), 3899-3911.

184. Zhou L, Ding L, Yin P, Lu X, Wang X, Niu J, Gao P, Xu G (2012) Serum Metabolic Profiling Study of Hepatocellular Carcinoma Infected with Hepatitis B or Hepatitis C Virus by Using Liquid Chromatography-Mass Spectrometry. *J Proteome Res* **11**, 5433-5442.

185. Godoy M, Lopes E, Silva R, Hallwass F, Koury L, Moura I, Gonçalves S, Simas A (2010) Hepatitis C virus infection diagnosis using metabonomics. *J Viral Hepat* **17**(12), 854-858.

186. Shin J, Yang J, Jeon B, Yoon YJ, Cho S, Kang Y, Ryu DH, Hwang G (2011) 1H NMR-based metabolomic profiling in mice infected with Mycobacterium tuberculosis. *J Proteome Res* **10**(5), 2238-2247.

187. Fabisiak JP, Medvedovic M, Alexander DC, McDunn JE, Concel VJ, Bein K, Jang AS, Berndt A, Vuga LJ, Brant KA (2011) Integrative metabolome and transcriptome profiling reveals discordant energetic stress between mouse strains with differential sensitivity to acrolein-induced acute lung injury. *Mol Nutr Food Res* **55**(9), 1423-1434.

188. Hu JZ, Rommereim DN, Minard KR, Woodstock A, Harrer BJ, Wind RA, Phipps RP, Sime PJ (2008) Metabolomics in Lung Inflammation: A High-Resolution 1H NMR Study of Mice Exposedto Silica Dust. *Toxicol Mech Methods* **18**(5), 385-398.

189. Leikauf GD, Pope-Varsalona H, Concel VJ, Liu P, Bein K, Berndt A, Martin TM, Ganguly K, Jang AS, Brant KA, Dopico RA,Jr, Upadhyay S, Di YP, Li Q, Hu Z, Vuga LJ, Medvedovic M, Kaminski N, You M, Alexander DC, McDunn JE, Prows DR, Knoell DL, Fabisiak JP (2012) Integrative assessment of chlorine-induced acute lung injury in mice. *Am J Respir Cell Mol Biol* **47**(2), 234-244.

190. Van Kerkhove MD, Vandemaele KAH, Shinde V, Jaramillo-Gutierrez G, Koukounari A, Donnelly CA, Carlino LO, Owen R, Paterson B, Pelletier L, Vachon J, Gonzalez C, Hongjie Y, Zijian F, Chuang SK, Au A, Buda S, Krause G, Haas W, Bonmarin I, Taniguichi K, Nakajima K, Shobayashi T, Takayama Y, Sunagawa T, Heraud JM, Orelle A, Palacios E, van der Sande MA, Wielders CC, Hunt D, Cutter J, Lee VJ, Thomas J, Santa-Olalla P, Sierra-Moros MJ, Hanshaoworakul W, Ungchusak K, Pebody R, Jain S, Mounts AW, WHO Working Group for Risk Factors for Severe H1N1pdm Infection (2011) Risk factors for severe outcomes following 2009 influenza A (H1N1) infection: a global pooled analysis. *PLoS Med* **8**(7), e1001053.

191. Gianazza E, Sensi C, Eberini I, Gilardi F, Giudici M, Crestani M (2012) Inflammatory serum proteome pattern in mice fed a high-fat diet. *Amino Acids* .

192. Reed LJ & Muench H (1938) A simple method of estimating fifty per cent endpoints. *Am J Epidemiol* **27**(3), 493-497.

193. Wortham BW, Eppert BL, Motz GT, Flury JL, Orozco-Levi M, Hoebe K, Panos RJ, Maxfield M, Glasser SW, Senft AP, Raulet DH, Borchers MT (2012) NKG2D Mediates NK Cell Hyperresponsiveness and Influenza-Induced Pathologies in a Mouse Model of Chronic Obstructive Pulmonary Disease. *J Immunol* **188**(9), 4468-4475.

194. Glasser SW, Witt TL, Senft AP, Baatz JE, Folger D, Maxfield MD, Akinbi HT, Newton DA, Prows DR, Korfhagen TR (2009) Surfactant protein C-deficient mice are susceptible to respiratory syncytial virus infection. *Am J Phsiol Lung Cell Mol Physiol* **297**(1), L64-L72.

195. Snell LM, McPherson AJ, Lin GHY, Sakaguchi S, Pandolfi PP, Riccardi C, Watts TH (2010) CD8 T cell-intrinsic GITR is required for T cell clonal expansion and mouse survival following severe influenza infection. *J Immunol* **185**(12), 7223-7234.

196. Farag-Mahmod FI, Wyde PR, Rosborough JP, Six HR (1988) Immunogenicity and efficacy of orally administered inactivated influenza virus vaccine in mice. *Vaccine* **6**(3), 262-268.

197. World Health Organization. Serological diagnosis of influenza by microneutralization assay. Available at: http://www.who.int/influenza/gisrs_laboratory/2010_12_06_serological_diagnosis_of_influenza_by_microneutralization_assay.pdf. Accessed 20 September 2013.

198. De Rosa V, Procaccini C, Calì G, Pirozzi G, Fontana S, Zappacosta S, La Cava A, Matarese G (2007) A key role of leptin in the control of regulatory T cell proliferation. *Immunity* **26**(2), 241-255.

199. Carragher DM, Kaminski DA, Moquin A, Hartson L, Randall TD (2008) A novel role for non-neutralizing antibodies against nucleoprotein in facilitating resistance to influenza virus. *J Immunol* **181**(6), 4168-4176.

200. LaMere MW, Moquin A, Lee FE, Misra RS, Blair PJ, Haynes L, Randall TD, Lund FE, Kaminski DA (2011) Regulation of antinucleoprotein IgG by systemic vaccination and its effect on influenza virus clearance. *J Virol* **85**(10), 5027-5035.

201. Flynn KJ, Belz GT, Altman JD, Ahmed R, Woodland DL, Doherty PC (1998) Virus-specific CD8 T cells in primary and secondary influenza pneumonia. *Immunity* **8**(6), 683-691.

202. Effros RB, Doherty PC, Gerhard W, Bennink J (1977) Generation of both cross-reactive and virus-specific T-cell populations after immunization with serologically distinct influenza A viruses. *J Exp Med* **145**(3), 557-568.

203. Sallusto F, Lenig D, Förster R, Lipp M, Lanzavecchia A (1999) Two subsets of memory T lymphocytes with distinct homing potentials and effector functions. *Nature* **401**, 708-712.

204. Loebbermann J, Thornton H, Durant L, Sparwasser T, Webster KE, Sprent J, Culley FJ, Johansson C, Openshaw PJ (2012) Regulatory T cells expressing granzyme B play a critical role in controlling lung inflammation during acute viral infection. *Mucosal Immunol* **5**(2), 161-172.

205. Fulton RB, Meyerholz DK, Varga SM (2010) Foxp3+ CD4 Regulatory T Cells Limit Pulmonary Immunopathology by Modulating the CD8 T Cell Response during Respiratory Syncytial Virus Infection. *J Immunol* **185**(4), 2382-2392.

206. Deiuliis J, Shah Z, Shah N, Needleman B, Mikami D, Narula V, Perry K, Hazey J, Kampfrath T, Kollengode M (2011) Visceral adipose inflammation in obesity is associated with critical alterations in t regulatory cell numbers. *PloS one* **6**(1), e16376.

207. Ma X, Hua J, Mohamood AR, Hamad ARA, Ravi R, Li Z (2007) A high-fat diet and regulatory T cells influence susceptibility to endotoxin-induced liver injury. *Hepatology* **46**(5), 1519-1529.

208. Betts RJ, Ho AWS, Kemeny DM (2011) Partial Depletion of Natural CD4 CD25 Regulatory T Cells with Anti-CD25 Antibody Does Not Alter the Course of Acute Influenza A Virus Infection. *PloS one* **6**(11), e27849.

209. Betts RJ, Prabhu N, Ho AWS, Lew FC, Hutchinson PE, Rotzschke O, Macary PA, Kemeny DM (2012) Influenza A Virus Infection Results in a Robust, Antigen-Responsive, and Widely Disseminated Foxp3 Regulatory T Cell Response. *J Virol* **86**(5), 2817-2825.

210. Sehrawat S & Rouse BT (2011) Tregs and infections: on the potential value of modifying their function. *J Leukoc Biol* **90**(6), 1079-1087.

211. Wan YY & Flavell RA (2007) Regulatory T-cell functions are subverted and converted owing to attenuated Foxp3 expression. *Nature* **445**(7129), 766-770.

212. Josefowicz SZ, Lu LF, Rudensky AY (2012) Regulatory T cells: mechanisms of differentiation and function. *Annu Rev Immunol* **30**, 531-564.

213. Karlsson EA, Sheridan PA, Beck MA (2010) Diet-induced obesity in mice reduces the maintenance of influenza-specific CD8 memory T cells. *J Nutr* **140**(9), 1691-1697.

214. Damjanovic D, Small C, Jeyananthan M, McCormick S, Xing Z (2012) Immunopathology in influenza virus infection: Uncoupling the friend from foe. *Clin Immunol* **144**(1), 57-69.

215. Mauad T, Hajjar LA, Callegari GD, da Silva LFF, Schout D, Galas FRBG, Alves VAF, Malheiros DMAC, Auler JOC, Ferreira AF, Borsato MRL, Bezerra SM, Gutierrez PS, Caldini ETEG, Pasqualucci CA, Dolhnikoff M, Saldiva PHN (2010) Lung Pathology in Fatal Novel Human Influenza A (H1N1) Infection. *Am J Respir Crit Care Med* **181**(1), 72-79.

216. Lee DCP, Harker JAE, Tregoning JS, Atabani SF, Johansson C, Schwarze J, Openshaw PJM (September 1, 2010) CD25+ Natural Regulatory T Cells Are Critical in Limiting Innate and Adaptive Immunity and Resolving Disease following Respiratory Syncytial Virus Infection. *J Virol* **84**(17), 8790-8798.

217. Brincks EL, Roberts AD, Cookenham T, Sell S, Kohlmeier JE, Blackman MA, Woodland DL (2013) Antigen-Specific Memory Regulatory CD4 Foxp3 T Cells Control Memory Responses to Influenza Virus Infection. *J Immunol* **190**, 3438-3446.

218. Centers for Disease Control and Prevention. Interim Estimates of 2013-2014 Seasonal Influenza Vaccine Effectiveness - United States, February 2014. Available at: http://www.cdc.gov/mmwr/preview/mmwrhtml/mm6307a1.htm. Accessed 17 March 2014.

219. Centers for Disease Control and Prevention: Key Facts About Seasonal Flu Vaccine. Available at: http://www.cdc.gov/flu/protect/keyfacts.htm. Accessed 20 September 2013.

220. Carbone F, La Rocca C, Matarese G (2012) Immunological functions of leptin and adiponectin. *Biochimie* **94**(10), 2082-2088.

221. Ring LE & Zeltser LM (2010) Disruption of hypothalamic leptin signaling in mice leads to early-onset obesity, but physiological adaptations in mature animals stabilize adiposity levels. *J Clin Invest* **120**(8), 2931-2941.

222. Bedoya F, Cheng GS, Leibow A, Zakhary N, Weissler K, Garcia V, Aitken M, Kropf E, Garlick DS, Wherry EJ, Erikson J, Caton AJ (2013) Viral antigen induces differentiation of

Foxp3+ natural regulatory T cells in influenza virus-infected mice. *J Immunol* **190**(12), 6115-6125.

223. Klebanov S, Astle CM, DeSimone O, Ablamunits V, Harrison DE (2005) Adipose tissue transplantation protects ob/ob mice from obesity, normalizes insulin sensitivity and restores fertility. *J Endocrinol* **186**(1), 203-211.

224. Ge F, Hu C, Hyodo E, Arai K, Zhou S, Lobdell H,4th, Walewski JL, Homma S, Berk PD (2012) Cardiomyocyte triglyceride accumulation and reduced ventricular function in mice with obesity reflect increased long chain Fatty Acid uptake and de novo Fatty Acid synthesis. *J Obes* **2012**, 205648.

225. Jiang T, Wang Z, Proctor G, Moskowitz S, Liebman SE, Rogers T, Lucia MS, Li J, Levi M (2005) Diet-induced obesity in C57BL/6J mice causes increased renal lipid accumulation and glomerulosclerosis via a sterol regulatory element-binding protein-1c-dependent pathway. *J Biol Chem* **280**(37), 32317-32325.

226. Wahba IM & Mak RH (2007) Obesity and obesity-initiated metabolic syndrome: mechanistic links to chronic kidney disease. *Clin J Am Soc Nephrol* **2**(3), 550-562.

227. Poirier P, Giles TD, Bray GA, Hong Y, Stern JS, Pi-Sunyer FX, Eckel RH (2006) Obesity and cardiovascular disease pathophysiology, evaluation, and effect of weight loss. *Arterioscler Thromb Vasc Biol* **26**(5), 968-976.

228. Ren Y, Yin Y, Li W, Lin Y, Liu T, Wang S, Zhang S, Li Z, Wang X, Bi Z (2013) Risk factors associated with severe manifestations of 2009 pandemic influenza A (H1N1) infection in China: a case--control study. *Virol J* **10**(1), 149.

229. Kwong JC, Campitelli MA, Rosella LC (2011) Obesity and respiratory hospitalizations during influenza seasons in Ontario, Canada: a cohort study. *Clin Infect Dis* **53**(5), 413-421.

230. Campitelli M, Rosella L, Kwong J (2013) The association between obesity and outpatient visits for acute respiratory infections in Ontario, Canada. *Int J Obes* .

231. Smith AG, Sheridan PA, Tseng RJ, Sheridan JF, Beck MA (2009) Selective impairment in dendritic cell function and altered antigen-specific CD8 T-cell responses in diet-induced obese mice infected with influenza virus. *Immunology* **126**(2), 268-279.

232. Wang Y, Li JV, Saric J, Keiser J, Wu J, Utzinger J, Holmes E (2010) Advances in metabolic profiling of experimental nematode and trematode infections. *Adv Parasitol* **73**, 373-404.

233. Wang Y, Utzinger J, Saric J, Li JV, Burckhardt J, Dirnhofer S, Nicholson JK, Singer BH, Brun R, Holmes E (2008) Global metabolic responses of mice to Trypanosoma brucei brucei infection. *Proc Natl Acad Sci U S A* **105**(16), 6127-6132.

234. Saric J, Li JV, Wang Y, Keiser J, Bundy JG, Holmes E, Utzinger J (2008) Metabolic profiling of an Echinostoma caproni infection in the mouse for biomarker discovery. *PLoS Negl Trop Dis* **2**(7), e254.

235. Shearer J, Duggan G, Weljie A, Hittel D, Wasserman D, Vogel H (2008) Metabolomic profiling of dietary-induced insulin resistance in the high fat–fed C57BL/6J mouse. *Diabetes Obes Metab* **10**(10), 950-958.

236. Jung JY, Kim YN, Shin JH, Lee HS, Seong JK (2012) 1H NMR-based metabolite profiling of diet-induced obesity in a mouse mode. *BMB Rep* **45**(7), 419-424.

237. Saric J, Li JV, Utzinger J, Wang Y, Keiser J, Dirnhofer S, Beckonert O, Sharabiani MT, Fonville JM, Nicholson JK (2010) Systems parasitology: effects of Fasciola hepatica on the neurochemical profile in the rat brain. *Mol Syst Biol* **6**(1).

238. Saric J, Li JV, Swann JR, Utzinger J, Calvert G, Nicholson JK, Dirnhofer S, Dallman MJ, Bictash M, Holmes E (2010) Integrated cytokine and metabolic analysis of pathological responses to parasite exposure in rodents. *J Proteome Res* **9**(5), 2255-2264.

239. Beckonert O, Keun HC, Ebbels TM, Bundy J, Holmes E, Lindon JC, Nicholson JK (2007) Metabolic profiling, metabolomic and metabonomic procedures for NMR spectroscopy of urine, plasma, serum and tissue extracts. *Nat Protoc* **2**(11), 2692-2703.

240. Veselkov KA, Vingara LK, Masson P, Robinette SL, Want E, Li JV, Barton RH, Boursier-Neyret C, Walther B, Ebbels TM (2011) Optimized preprocessing of ultra-performance liquid chromatography/mass spectrometry urinary metabolic profiles for improved information recovery. *Anal Chem* **83**(15), 5864-5872.

241. Trygg J, Holmes E, Lundstedt T (2007) Chemometrics in metabonomics. *J Proteome Res* **6**(2), 469-479.

242. Eriksson L, Antti H, Gottfries J, Holmes E, Johansson E, Lindgren F, Long I, Lundstedt T, Trygg J, Wold S (2004) Using chemometrics for navigating in the large data sets of genomics, proteomics, and metabonomics (gpm). *Anal Bioanal Chem* **380**(3), 419-429.

243. Cloarec O, Dumas ME, Trygg J, Craig A, Barton RH, Lindon JC, Nicholson JK, Holmes E (2005) Evaluation of the orthogonal projection on latent structure model limitations caused by chemical shift variability and improved visualization of biomarker changes in 1H NMR spectroscopic metabonomic studies. *Anal Chem* **77**(2), 517-526.

244. Saric J, Wang Y, Li J, Coen M, Utzinger J, Marchesi JR, Keiser J, Veselkov K, Lindon JC, Nicholson JK (2007) Species variation in the fecal metabolome gives insight into differential gastrointestinal function. *J Proteome Res* **7**(01), 352-360.

245. Li JV, Holmes E, Saric J, Keiser J, Dirnhofer S, Utzinger J, Wang Y (2009) Metabolic profiling of a< i> Schistosoma mansoni</i> infection in mouse tissues using magic angle spinning-nuclear magnetic resonance spectroscopy. *Int J Parasitol* **39**(5), 547-558.

246. Karasawa H, Nagata-Goto S, Takaishi K, Kumagae Y (2009) A novel model of type 2 diabetes mellitus based on obesity induced by high-fat diet in BDF1 mice. *Metab Clin Exp* **58**(3), 296-303.

247. Ferrannini E (2011) Learning from glycosuria. *Diabetes* **60**(3), 695-696.

248. Saric J (2010) Interactions between immunity and metabolism–contributions from the metabolic profiling of parasite-rodent models. *Parasitology* **137**(9), 1451.

249. Bindels L, Porporato P, Dewulf E, Verrax J, Neyrinck A, Martin J, Scott K, Calderon PB, Feron O, Muccioli G (2012) Gut microbiota-derived propionate reduces cancer cell proliferation in the liver. *Br J Cancer* **107**(8), 1337-1344.

250. Harrison FE, Best JL, Meredith ME, Gamlin CR, Borza D, May JM (2012) Increased expression of SVCT2 in a new mouse model raises ascorbic acid in tissues and protects against paraquat-induced oxidative damage in lung. *PloS one* **7**(4), e35623.

251. Corpe CP, Tu H, Eck P, Wang J, Faulhaber-Walter R, Schnermann J, Margolis S, Padayatty S, Sun H, Wang Y (2010) Vitamin C transporter Slc23a1 links renal reabsorption, vitamin C tissue accumulation, and perinatal survival in mice. *J Clin Invest* **120**(4), 1069-1083.

252. Nishikimi M, Fukuyama R, Minoshima S, Shimizu N, Yagi K (1994) Cloning and chromosomal mapping of the human nonfunctional gene for L-gulono-gamma-lactone oxidase, the enzyme for L-ascorbic acid biosynthesis missing in man. *J Biol Chem* **269**(18), 13685-13688.

253. Li W, Maeda N, Beck MA (2006) Vitamin C Deficiency Increases the Lung Pathology of Influenza Virus–Infected Gulo−/− Mice. *J Nutr* **136**(10), 2611-2616.

254. Jackson JA, Wong K, Chad Krier N, Riordan HD (2005) Screening for Vitamin C in the Urine: Is it Clinically Significant? *J Orthomol Med* **20**(4), 259-261.

255. De Tullio MC (2012) Beyond the antioxidant: The double life of vitamin C. Subcell Biochem **56**, 49-65.

256. Kim Y, Kim H, Bae S, Choi J, Lim SY, Lee N, Kong JM, Hwang Y, Kang JS, Lee WJ (2013) Vitamin C Is an Essential Factor on the Anti-viral Immune Responses through the Production of Interferon-α/β at the Initial Stage of Influenza A Virus (H3N2) Infection. *Immune Netw* **13**(2), 70-74.

257. Choi A, Knobil K, Otterbein SL, Eastman DA, Jacoby DB (1996) Oxidant stress responses in influenza virus pneumonia: gene expression and transcription factor activation. *Am J Phsiol* **271**(3), L383-L391.

258. Erickson JC, Hollopeter G, Palmiter RD (1996) Attenuation of the obesity syndrome of ob/ob mice by the loss of neuropeptide Y. *Science* **274**(5293), 1704-1707.

259. Sheetz MJ & King GL (2002) Molecular understanding of hyperglycemia's adverse effects for diabetic complications. *JAMA* **288**(20), 2579-2588.

260. Pearce EL & Pearce EJ (2013) Metabolic pathways in immune cell activation and quiescence. *Immunity* **38**(4), 633-643.

261. Fanos V, Locci E, Noto A, Lazzarotto T, Manzoni P, Atzori L, Lanari M (2013) Urinary metabolomics in newborns infected by human cytomegalovirus: a preliminary investigation. *Early Hum Dev* **89**, S58-S61.

262. Wang X, Zhang A, Han Y, Wang P, Sun H, Song G, Dong T, Yuan Y, Yuan X, Zhang M (2012) Urine metabolomics analysis for biomarker discovery and detection of jaundice syndrome in patients with liver disease. *Mol Cell Proteomics* **11**(8), 370-380.

263. Scarpace PJ & Zhang Y (2009) Leptin resistance: a prediposing factor for diet-induced obesity. *American Journal of Physiology-Regulatory, Integrative and Comparative Physiology* **296**(3), R493-R500.

264. Knight ZA, Hannan KS, Greenberg ML, Friedman JM (2010) Hyperleptinemia is required for the development of leptin resistance. *PLoS One* **5**(6), e11376.

265. Papathanassoglou E, El-Haschimi K, Li XC, Matarese G, Strom T, Mantzoros C (2006) Leptin receptor expression and signaling in lymphocytes: kinetics during lymphocyte activation, role in lymphocyte survival, and response to high fat diet in mice. *J Immunol* **176**(12), 7745-7752.

266. Nave H, Mueller G, Siegmund B, Jacobs R, Stroh T, Schueler U, Hopfe M, Behrendt P, Buchenauer T, Pabst R (2008) Resistance of Janus kinase-2 dependent leptin signaling in natural killer (NK) cells: a novel mechanism of NK cell dysfunction in diet-induced obesity. *Endocrinology* **149**(7), 3370-3378.

267. Johnston RA, Theman TA, Lu FL, Terry RD, Williams ES, Shore SA (2008) Diet-induced obesity causes innate airway hyperresponsiveness to methacholine and enhances ozone-induced pulmonary inflammation. *J Appl Physiol (1985)* **104**(6), 1727-1735.

268. Kim HY, Lee HJ, Chang Y, Pichavant M, Shore SA, Fitzgerald KA, Iwakura Y, Israel E, Bolger K, Faul J (2013) Interleukin-17-producing innate lymphoid cells and the NLRP3 inflammasome facilitate obesity-associated airway hyperreactivity. *Nat Med* .